Doctorado en Empresa, Internet y Tecnologías de las Comunicaciones
Universidad de las Palmas de Gran Canaria

VLC systems for smart cities: mobility management scheme for vehicular networks

Edmundo Torres Zapata

Supervisor: Rafael Pérez Jiménez

Co-Supervisor: Jóse Rabadan Borges

Febrery 2022

Doctorado en Empresa, Internet y Tecnologías de las Comunicaciones
Universidad de las Palmas de Gran Canaria

VLC systems for smart cities: mobility management scheme for vehicular networks

Edmundo Torres Zapata

Supervisor: Rafael Pérez Jiménez

Co-Supervisor: Jóse Rabadan Borges

Febrery 2022

Contents

Dr. JOSÉ RABADAN BORGES COORDINADOR/A DEL PROGRAMA DE DOCTORADO EMPRESA, INTERNET Y TECNOLOGÍAS DE LAS COMUNICACIONES DE LA UNIVERSIDAD DE LAS PALMAS DE GRAN CANARIA

INFORMA,

De que la Comisión Académica del Programa de Doctorado, en su sesión de fecha ..... tomó el acuerdo de dar el consentimiento para su tramitación, a la tesis doctoral titulada "VLC systems for smart cities: mobility management scheme for vehicular networks" presentada por el doctorando D. Edmundo Torres Zapata y dirigida por los Doctores Rafael Pérez Jiménez y José Rabadan Borges

Y para que así conste, y a efectos de lo previsto en el Artº 11 del Reglamento de Estudios de Doctorado (BOULPGC 04/03/2019) de la Universidad de Las Palmas de Gran Canaria, firmo la presente en Las Palmas de Gran Canaria, a.....de.....de dos mil ventidos

UNIVERSIDAD DE LAS PALMAS DE GRAN CANARIA
ESCUELA DE DOCTORADO

Programa de doctorado Empresa, Internet y Tecnologías de las Comunicaciones.

Título de la Tesis: VLC systems for smart cities: mobility management scheme for vehicular networks

Tesis Doctoral presentada por D. Edmundo Torres Zapata

Dirigida por el Dr. Rafael Pérez Jiménez

Codirigida por el Dr. José Rabadan Borges

Las Palmas de Gran Canaria, a de de 2022

El/la Director/a, El/la Codirector/a El/la Doctorando/a,

(firma) (firma) (firma)

Dedication

Quiero dedicar este trabajo de tesis a mis padres que me han apoyado durante todos estos años y que sin ellos no hubiese a llegado a ser quien hoy soy. Ellos han tenido la paciencia para verme intentar este gran meta, y jamás me han fallado.

También a mis diversos mentores que he tenido como son Martín Luna, Rafa, José Rabadan y Víctor que me han sabido guía en mi labor de investigación. Espero haber mejorado un poco en estos años gracias a su dedicación.

A Vicente que me ayudo a llegar a un país nuevo para mi.

Y finalmente todos los amigos que me han apoyado, de los cuales quiero destacar los diversos compañeros de piso que he tenido (Alisa, Alexa, Lena, Sara, Fede, Leandro,Ste, Marcelo, Ludo y Cleofe)

Acknowledgement

Funding

This work has received funding from European Union's Horizon 2020 Marie Skłodowska-Curie Actions, under Grant Agreement no. 764461 (Project VisIoN).

I would like to express my sincere gratitude to:

- My supervisor : Rafael Pérez Jimenez
- My co-supervisor: Jóse Rabadan Borges
- Academic staff:
  - José Martín Luna Rivera
  - Víctor Guerra Yanez
  - Julio Rufo
  - Vicente Matus
- Academic Staff from other departments:
  - Prof. Ali Khalighi
  - Prof. Zabih Ghassemlooy
- Other Institutions:
  - Universidad Autónoma de San Luis Potosí
  - ECM-Marseille
  - Northumbria University

List of Figures

List of Tables

Resumen

In the last years, the use of the Internet has been expanded to any possible area since telephony until home automation thanks to the benefits that the Internet of Things(IoT) provides. It enables the possibility to intercommunicate multiple processes to bring them additional information and optimize their operation. The sum of multiple IoT solutions with the purpose to improve the health, transportation, governance, and environmental services in an urban area converge in the smart cities concept. In a smart city environment, the operation of these sectors can be monitored in real-time to make clever decisions and they operate efficiently. Additionally, IoT brings them the capabilities to offer new services. The sum of all these benefits provokes the great acceptance and massive expansion of IoT in the last years. Moreover, recently the number of Internet users has grown until reach two-thirds of the global population, each one using three devices approximately. As consequence, the demand for a higher number of wireless connections has grown exponentially until reaching 18.4 billion wireless connections in 2018. And, some regions of the radio frequency spectrum are almost saturated especially commercial RF bands such as 2.5 and 5 GHz bands. For this reason, it is necessary to look for alternative communication technologies.

One potential option to solve this demand is Visible Light Communications (VLC), an emergent technology that uses LED-based devices to transmit data. This technology differs from traditional RF because their bands are allocated in the Visible Light spectrum (430 THz to 790 THz) bringing a huge bandwidth. The data transmission is possible to modulate the light intensity emitted by LED devices in short periods to be perceived by humans. While the reception utilizes photodiode-based receivers and commercial cameras to sense the light variations. VLC bands are far from RF bands permitting to operate both technologies in the same place without interference, and they can complement each other.

The integration of the transportation sector in smart cities environments has rise the interest from the scientific community and industrial parties. Especially, the

development of Intelligent Transport System (ITS) which brings to the vehicles the capability to operate some process autonomously improving the driver's experience and preventing accidents. This technology needs a high number of sensors to recognize potential hazards in the area. Although, there are a lot of threats that can not be detected by the car's sensors. Thus, ITS needs the possibility to get information from other vehicles or even local authorities to guarantee the driver's security. For this reason, these systems must incorporate a communication system. Dedicated Short-Range Communications (DSRC) has been adopted as the main option to support the communication. This is an RF technology developed over years. So, it is a trustworthy and mature solution. However, the vehicle is exposed to a large variety of environments and meteorological conditions that can compromise the transmissions. Due to the fundamental of this information is to keep the driver's security, the ITS communication must be reliable in any possible situation. Therefore, ITS needs an auxiliary communication system to prevent any outage in DSRC.

VLC appears as a viable backup technology option because of the low implementation cost. It converts the tail and headlamps to transmitters without excessive additional charge. Similarly, the street and traffic lights can be adapted to provide communication services to a determinate area without great complications. Furthermore, VLC presents desirable features in vehicular scenarios such as Doppler shift immunity and low fading. In the last decade, several research groups have characterized the communication link in vehicular scenarios for vehicle-to-vehicle (V2V), vehicle-to-infrastructure(V2I), and infrastructure-to-vehicle(I2V) schemes where the channel presents ideal conditions. Additionally, some experimental proof of concepts has validated its good performance in these surroundings. In spite, there are many open issues to resolve before the incorporation of this technology in vehicular safety applications. One pending task to resolve is how the vehicular node will deal with the limited communication range of a VLC Access Point (AP). This is a major threat because a vehicular node using the I2V scheme changes several times of AP connection in a short period. Every new connection takes some seconds to resolve which limits the vehicular node's connection in case of an emergency. Accordingly, the network requires a set of protocols to transfer the user's session minimizing its

access time to the next cell.

The set of mechanisms where two AP exchange the user information to accelerate its ingress is known as handover. Currently, there are not many handover schemes developed for VLC. Due to the low latency requirement in ITS scenarios, handover solutions for home and office are impractical. For this reason, it is necessary to develop an appropriate solution for these environments.

This research work studied mobility problems in a VLC network considering vehicular scenarios. The main goal is to develop a handover scheme that can support seamless communication. This work was done using the following methodology, first study the communication channel in these environments, then analyze the channel data to propose a solution and corroborate the solution through a simulation approach. The first step is a study of the communication link in vehicular scenarios through statistical methods such as Monte-Carlo simulation with Ray-tracing. The simulations give the Channel Input Response (CIR) at different moments when the vehicle circulates the tunnel. The sum of CIRs results helps us to understand the system limitations and the main problems that the handover scheme needs to deal with. Additionally, the CIR analysis corroborates the V2I and I2V high performance permitting high-speed communication. Moreover, these results reveal one challenge to confront which is the abrupt disconnection of the V2I link. Considering this information a solution was proposed that is composed of a detection algorithm, handover protocols, and a novel network topology. The handover protocol which fits better to the network necessity is Hierarchical Mobile IPv6 (HMIPv6) because it has a reduced resolution time. As well, the handover can be supported by a new network topology defined as "2.5 layer topology" which provides redundancy to the uplink.

The solutions were validated through system-level simulations using the OMNET++ platform. This approach evaluates the execution of MAC layer protocols with realistic channel models allowing a truthful representation of the network. The simulator recreates the exact conditions of vehicles moving through the tunnel and receiving vital information. The validation was done in a demanding situation where the

vehicular node is receiving a data rate of 450 kbps, exceeding the minimum requirements for safety application. The results demonstrate that the proposed handover solution presents high efficiency providing a low packet loss and a steady connection, where its disconnection time is below 1 %. Finally, the solution operates adequately when there is a large number of users in the network without jeopardizing the communication.

Resumen

Recientemente el uso de Internet se ha expandido en muchas áreas que van desde la telefonía y llegando a áreas mas rutinarias como la domótica. Esto gracias a los enormes beneficios del Internet (IoT por sus siglas en Inglés) de las Cosas les ha provisto. IoT ha abierto la posibilidad de intercomunicar muchos procesos para que estos sean capas de obtener información que les permita mejorar su desempeño. Cuando múltiples soluciones asistidas por IoT son encaminadas a mejorar sectores como salud (sanidad), transporte, procesos burocráticos o gestión ambiental de manera conjunta estas conforman el concepto de Ciudades Inteligentes. En los entornos de ciudades inteligentes los procesos de dichos sectores pueden ser monitoreados en tiempo real, y en base a esta información ellos pueden operar de manera más eficiente. Además de que IoT les permite acceder a nuevos tipos de servicios que antes no hubiese sido posible. Debido a los grandes beneficios provistos por esta tecnología, han provocado una gran expansión de IoT en muchas áreas en años recientes. Además de este factor, el numero de usuarios de Internet ha continuado incrementando hasta llegar a dos tercios de la población mundial, con una media de 3 dispositivos per usuario. Dado estos dos factores, la demanda de redes inalámbricas a crecido estipulando que existen 18.4 billones de conexiones a Internet en el año 2018. Esto ha hecho que regiones del espectro electromagnético se estén saturando en ambientes urbanos, especialmente las bandas comerciales de 2.5 y 5 GHz. Por esta razón es necesario buscar tecnologías de comunicación alternas que no utilicen dicha región.

Las Comunicaciones por Luz Visible (VLC por sus siglas en Inglés) aparecen como una potencial solución a este problema. Estas habilitan lamparas LED para poder ser utilizadas con una doble función iluminar y comunicar. La mayor diferencia de VLC con respecto a otras tecnologías inalámbricas es que transmite información usando las bandas de luz visible del espectro (430 THz a 790 THz) que pueden proveer de un gran ancho de banda. Para poder transmitir los transmisores VLC modulan la intensidad de la luz emitida por un dispositivo LED, dichos cambios de intensidad son tan breves que no pueden ser percibidos por el ojo humano. A su vez,

VLC utiliza como receptores dispositivos electrónicos que cuentan con un receptor fotoeléctrico o en su vez cámara integradas en diversos dispositivos como los teléfonos móviles. Una ventaja de esta tecnología es que las bandas VLC y las de cualquier tecnología de radiofrecuencia están muy distantes para poder generar interferencia, y además se pueden utilizar de manera conjunta para mejorar la comunicación.

Un sector donde ha surgido el interés de incorporar los beneficios de IoT por la comunidad científica y diversas empresas es el sector de transporte. Entre las potenciales incorporaciones en dicho sector, se encuentra los sistemas de Transporte Inteligente (ITS por sus siglas en Inglés). Los cuales proveen a los vehículos de poder operar algunas de sus funciones de manera autónoma para poder mejorar su desempeño, y prever accidentes viales. Para poder realizar estas funciones el vehículo debe contar con una gran variedad de sensores que le permitan reconocer peligros en el entorno. A pesar de que se cuenta con un numero basto de sensores, existen amenazas que no pueden ser vistas por ellos. Debido a esto es necesario que ITS puedan obtener dicha información mediante otros medios, como puede ser que vehículos en el área le informen de ellos, o incluso este gubernamentales como el Departamento de Tráfico. Esto crea la necesidad que ITS cuenten con un sistema de comunicación. Las Comunicaciones Dedicadas de Corto Alcance (DSRC por sus siglas en Inglés) emergen como una opción solida y altamente comprobada que provee los servicios de comunicación. A pesar de esto, el vehículo es expuesto a diversos biomas, y efectos meteorológicos que pueden perjudicar el desempeño de dichos sistemas poniendo en riesgo la comunicación. Dicha información es necesario para poder garantizar la seguridad del piloto, por lo que la comunicación de ITS necesita ser robusta ante cualquier situación.

Bajo este contexto, VLC emerge como una posible solución para tener una tecnología de respaldo debido a bajo costo de implementación reutilizando hardware existente en el vehículo. Esta tecnología adapta las lámparas delanteras y traseras como transmisores sin conste adicionales. De la misma manera, el alumbrado publico puede ser utilizado por la tecnología cumpliendo una función similar. Aparte de los bajos costos de implementación, esta tecnología presenta una serie de ventajas para

entornos vehiculares como puede ser que la comunicación es inmune a efectos Doppler y presenta bajo desvanecimiento. Durante la pasada década, diversos investigadores han trabajado en estudiar el desempeño de los sistemas VLC tomando en cuenta entornos vehiculares. Dentro de los trabajos de interés se encuentra el caracterizar el canal para los diversos enlaces de comunicación que puede ocurrir en este escenario. Que son los siguientes esquemas de comunicación: Vehículo a vehículo (V2V por sus siglas en Inglés), vehículo a infraestructura (V2I por sus siglas en Inglés) y I2V (por sus siglas en Inglés). En complemento se han realizado validaciones experimentales como pruebas de concepto para validar las diversas características de los enlaces estudiadas previamente. A pesar de la gran cantidad de esfuerzos que diversos equipos de trabajo han invertido en desarrollar la tecnología, aun hay una gran cantidad de problemáticas relacionadas sin ser estudiadas. Un problema que no ha sido estudiado a profundidad es como solventar en limitado rango de comunicación de los Punto de Acceso (AP por sus siglas en Inglés) de dicha tecnología. Este es un problema fundamental por combatir debidos a que el nodo vehicular se mueve contantemente cambiando de AP varias veces en un lapso pequeño. Debido a que cada nueva conexión tiene un tiempo de latencia antes de poder recibir y transmitir información esto reduce el tiempo total de comunicación de ITS dejándolo expuesto a no recibir un mensaje de emergencia. Por lo tanto, es necesario el proveer a la red una serie de protocolos conocidos como handover que puedan transferir la sesión del usuario entre puntos de acceso y así disminuir la latencia para restaurar la comunicación. En la actualidad no se tiene alguna solución concisa para los problemas de movilidad en una red VLC por lo que es un problema abierto. Además, las redes diseñadas para ITS tienen requerimientos adicionales como es una baja, por lo que no se puede utilizar estrategias de handover diseñada para redes en casa y oficinas. Este trabajo de tesis doctoral busca poder diseñar una solución para los problemas de movilidad señalados.

Para poder cumplir con la meta propuesta se trabajo con la siguiente metodología. Primero se realizaron estudios del canal VLC tomando en cuenta las características del entorno de interés. Una vez concluidos, se analizo la información de la respuesta al impulso de Canal, la información fue utilizada para planear una estrategia ade-

cuada. Finalmente, la solución propuesta fue validada mediante simulaciones. El estudio de canal se realizó usando métodos estadísticos como son las simulaciones Monte-Carlo con trazado de rayos. Para poder realizar dicho estudio se acoto el escenario de estudio a un túnel vehicular. La información del canal en diversos puntos del túnel los conocimientos necesarios para entender la problemática y corroboro la factibilidad de desarrollar dicho sistema de comunicación. Además, estos estudios nos enseñaron un problema a tratar, el cual es una abrupta desconexión en el canal de subida. Finalmente, toda esta información fue tomada en cuenta durante la planeación de la estrategia de handover.

En este trabajo se propone una solución conjunta formada por un algoritmo de detección, un protocolo de handover y una nueva topología de red. Dentro de la revisión literaria, el protocolo que mejor se adapta a nuestras necesidades fue " Hierarchical Mobile IPv6 (HMIPv6)" el cual tiene poca latencia. Otra adición fue el elaborar una topología de red nombrada "topología de capa 2.5", la cual añade redundancia en el enlace de subida y ayuda que los puntos de acceso tengan una mayor cobertura. Las propuestas fueron validadas con simulaciones de sistema elaboradas con la plataforma OMNET++. Este método permite el validad los diversos protocolos de capa MAC considerando modelos realistas de canal, lo que da una representación fidedigna de la red. Adicionalmente, las simulaciones recrean las condiciones del entorno considerando la estructura del túnel y su impacto en la comunicación. Los resultados reflejan que el nodo vehicular con la propuesta es capas de mantener una comunicación estable y una taza baja de tramas perdidas, donde este nodo solamente pierde conexión el 1 % del tiempo total de comunicación. Finalmente, la solución no presenta fallos, ni merma su desempeño de manera alarmante cuando un numero grande de nodos vehiculares comparten la red.

Objetivos

La meta global de este trabajo de investigación es poder integrar la tecnología VLC a entornos de ciudades inteligentes. Diversos objetivos fueron planteados teniendo esto en mente.

Objetivo Primario

1. El desarrollar un mecanismo de handover que permita a una red basada en tecnología VLC, el poder proveer comunicación estable a sus usuarios. Aun en situaciones cuando los usuarios presentan patrones de movilidad a alta velocidad.

Objetivos secundarios

La elaboración de estos objetivos fue orientada a que en conjunto ellos ayudaran en el desarrollo de la estrategia de movilidad.

1. Estudiar el canal de comunicación de una red VLC desplegada en el entorno de un túnel vehicular. Dicho análisis se realizará mediante simulaciones Monte-Carlo con trazado de rayos

2. Desarrollar una plataforma de simulación de una red VLC que permita validar los esquemas de movilidad propuestos. Dicha plataforma debe considerar modelos de canal realistas y una evaluación detallada de los protocolos que se ejecutan en la capa MAC.

3. Diseñar mecanismos de handover de baja latencia. Este es un pilar del cual dependerá si la red puede proporcionar comunicación continua a los nodos.

4. Desarrollar algoritmos de detección que inicien el proceso de handover. Estos deben activar de manera oportuna cuando el nodo este por dejar el área de cobertura de un punto de acceso. Su diseño estará basado en los resultados obtenidos del objetivo 1

5. Validar las diferentes propuestas mediante simulaciones ejecutadas a través de la plataforma OMNET++. Estas tienen como premisa el poder garantizar el buen desempeño de la solución actuando en conjunto. Dicha esta conformada por modificaciones a la topología de red, un protocolo de handover y un algoritmo de detección.

Conclusiones

Este trabajo de tesis doctoral se enfoco en los problemas de movilidad dentro de una red VLC. El cual tiene como principal objetivo el estudiar dichos problemas centrándose en un area donde los sistemas VLC aparezcan como una potencial solución y el desarrollar una estrategia para dichos entornos que proporcione una conexión estable. El trabajo de investigación fue acotado a entornos de comunicación vehicular los cuales tienen particulares restricciones como baja tolerancia a desconexiones, por lo que las estrategias deben tener baja latencia en resolver. Además, la propuesta debe ser diseñada considerando como actúan los enlaces VLC en el. Cabe destacar que este es un estudio inicial a dicho problema. Por lo que existen un gran número de problemas por resolver antes de tener una solución que pueda ser implementada en un sistema final. A pesar de esto, este trabajo de tesis ha generado el conocimiento necesario para dar una aportación a futuros trabajos en esta área.

La revisión del estado de arte nos ha demostrado que existe interés por diversos entes académicos e industriales para incorporar la tecnología VLC en diversas aplicaciones vehiculare, en especial las de seguridad para ITS. Esta tecnología aplicada para estos entornos ha progresado mediante el estudio del canal y posteriormente con pruebas de concepto. Por lo que el siguiente paso natural es el estudiar la interoperabilidad de estos sistemas, así como su integración para funcionar como una red. Dentro de las conclusiones obtenidas al revisar el estado del arte son las siguientes. Primero, a pesar de que la gran parte de los sistemas VLC para entornos vehiculares han optado por modulaciones Multiplexación por división de frecuencias ortogonales (OFDM por sus siglas en Inglés), la inclusión de estándares como el IEEE 802.15.7-2018 no ha sido descartada completamente. Como prueba de esto existen diversos trabajos que se han dedicado a estudiar la compatibilidad de este estándar con dichos entornos. Segundo, la tecnología VLC tiene diversas ventajas para ser usada en estos entornos como son inmunidad a efecto Doppler y bajo desvanecimiento. Además, experimentalmente se ha medido la duración media de los enlaces V2V en entornos urbanos teniendo duración suficiente para intercambiar la información necesaria. Entre las principales barreras a sortear es el garantizar que el nodo vehicular cuente

en todo momento con una conexión para poder recibir mensajes en caso de un siniestro. Realizar esto es un proceso complicado, ya que dicho nodo se mueve de manera constante a alta velocidad cambiando de punto de acceso de manera continua debido a poco rango de alcance de ellos. Debido a esto es necesario desarrollar esquemas de soporte a la movilidad dentro de la red que pueda desempeñar con poca latencia. En la literatura, la mayoría de las soluciones de handover se encuentra en etapas tempranas. De estos trabajos, la mayoría de ellos están enfocados para ayudar en entornos como oficinas y hogares que no pueden ser utilizados en entornos vehiculares sin adaptarlos de manera debida. Como tercera conclusión del estado del arte podemos inferir que el problema a tratar de movilidad en entornos vehiculares para una red VLC es un tema novedoso con gran potencial. Una vez estudiadas las propuestas para tecnologías basadas en radiofrecuencia podemos concluir que el retraso mayor dentro de los esquemas de handover es durante la fase de ejecución. Por lo que la solución propuesta debe considerarlos de manera integral las diversas etapas de proceso de handover como son la detención, ejecución y el recolectar la información.

En el capítulo 4 introdujimos la metodología que utilizamos para poder realizar la investigación. Esta fue realizada mediante simulaciones de sistemas, las cuales tienen gran flexibilidad para evaluar una red con diversos parámetros como el cambiar número de usuarios, su ubicación, entre otros parámetros en comparación con métodos analíticos como son las cadenas de Markov por citar un ejemplo. Para esto se desarrolló módulos de simulación donde se incluía los aspectos mas relevantes de un sistema VLC tomando como base las especificaciones del estándar IEEE 802.15.7 cumpliendo el Objetivo 2. El simulador desarrollado destaca por evaluar de manera conjunta la capa PHY y MAC junto a un modelo de canal realista. Este es capas de poder ver el impacto de nodos que no cuentan con línea de vista con respecto otros nodos de la red. Esto se logra gracias a la inclusión de un simulador Monte-Carlo con trazado de rayos dentro del simulador de red, para tener resultados mas precisos. Normalmente en gran parte de la literatura evalúan estos sistemas ignorando las contribuciones que no son de línea de vista. En el capítulo 5 realizamos una serie de experimentos para poder resaltar la importancia de incluir una canal realista.

Dichos experimentos acomodan a los nodos a evaluar de manera que ellos tengan la misma componente de línea de vista en cada configuración, pero difiriendo sus componentes de no línea de vista por configuración. Una vez realizados los experimentos se pudo corroborar la importancia de incluir las componentes multi trayecto de la luz al momento de evaluar protocolos de capa MAC en sistemas VLC. Ya que las reflexiones de la señal óptica en el escenario pueden cambiar el desempeño de dichos protocolos.

El trabajo de tesis se centró en estudiar la movilidad en túneles vehiculares, y en el capítulo 6 presenta el análisis del canal VLC para una red implementada en este recinto. Esta evaluación se realiza mediante simulaciones Monte-Carlo con trazado de rayos modelando un túnel vehicular de dos carriles para obtener la respuesta de canal para los enlaces de bajada y subida. Este proceso completa el Objetivo 1. Los resultados fueron positivos donde la evaluación de los enlaces demostró que ellos posean un ancho de banda considerable y una ganancia DC del canal aceptable. La información recabada ayudo a planar una estrategia de handover. Entre las conclusiones obtenidas a partir de estos estudios de canal se encuentra las siguientes. Primero es que los sistemas VLC en estos recintos deben adaptarse a los sistemas de iluminación existentes, esto debido a que ellos tienen estrictas restricciones. También las lamparas utilizadas en estos lugares las del vehículo y las de iluminación publica tienen patrones de radiaciones peculiares que no deben ser modeladas como un emisor Lambertiano. En la propuesta de red presentada separamos la localización del receptor de los demás elementos de Punto de Acceso, colocándolo cerca de arroyo vehicular. Esta configuración permite que el punto de acceso obtenga un enlace directo desde la lampara del vehículo mejorando la comunicación. Este es solución no explorada para mejorar los enlaces V2I y I2V, ya que todos los modelos presentados en la literatura el receptor esta adjunto al transmisor. Esto es respaldado por los buenos resultados obtenidos donde dicho enlace presenta baja dispersión del retardo. Lo cual valida la Hipótesis 1. Parte del análisis fue él estudiar el comportamiento temporal del enlace de comunicación. Para esto múltiples respuestas al impulso del canal fueron congregadas, y asumiendo que el vehículo se mueve a una velocidad de 100 km/h, se pudo recrear la variación temporal de cana para un vehículo que

transita en este lugar. Esto permitió calcular los tiempos de coherencia del canal el cual supera los cientos de milisegundos, lo cual permite transmitir tramas de gran tamaño sin complicaciones. La suma de todos estos resultados positivos en el estudio de canal permite concluir que el canal VLC en estos entornos cuenta con condiciones ideales para poder sostener la comunicación sin problemas. Otro resultado de estos estudios es el entender en comportamiento del canal de subida. Este refleja un incremento continuo de ganancia DC del canal, por lo tanto, de potencia recibida. Y repentinamente sufre una caída abrupta poniendo en riesgo la comunicación. Debido a esto es necesario establecer un esquema de redundancia en dicho enlace. Esto ha llevado a generar una solución mediante la propuesta de una nueva topología de red llamada "topología de capa 2.5". La solución propuesta habilita a los diversos receptores de la red para poder recibir una trama de manera conjunta y luego enviar dicha a su respectivo destino, extendiendo el rango del punto de acceso. Una ver realizada la validación del esquema propuesto en 7 demostrando un superior desempeño podemos concluir que un diseño inteligente de red mejora las capacidades de una red VLC. El capítulo 7 mostro la solución de handover, una vez realizado las pruebas de validación, esta demostró una eficiente operación al poder proveer comunicación solida a los vehículos en el recinto. Los resultados demostraron que la estrategia seleccionada brindaba a los nodos vehiculares una conexión el 99.9% del tiempo en que ellos se movían en la red. Esto sumado a una taza de error de $5e^{-4}$ lo cual puede ser considerado como una conexión constante. Esto tomando en cuenta que el nodo vehicular estaba demandando una taza de datos de 450 kbps, la cual esta muy por encima de los requerimientos para aplicaciones de seguridad en ITS. Por lo que se concluye que una red VLC puede solventar las comunicaciones vehiculares.

Chapter 1

Introduction

1.1 Background

In the last decade, the Internet of Things (IoT) has improved, simplified, and enabled new services to many economy sectors. IoT constitutes a network of embedded devices that incorporates sensors and communication functions. Within the Machine-to-Machine (M2M) connections category, there will be 14.7 billion connections by 2023 using 2.5 and 5 GHz bands [5]. At the same time, the number of users of mobile communication is still growing. At the end of the first part of 2020, there were 5.43 billion LTE subscriptions, representing 59.2% of mobile subscriptions globally using 800, 1800, and 2600 MHz bands [6]. Each year, the users demand a higher data rate per device. For example, the average mobile connection speed was 13.2 Mbps in 2018, and there is a forecast to reach 43.9 Mbps by 2023 [5]. Therefore, the occupation of commercial radio-frequency bands has increased exponentially, making it necessary to implement new strategies for addressing the spectrum scarcity. In urban environments, when the number of devices per area is high, and the communication systems require complex channel access schemes for coexisting. This problem raises communication latency that can be crucial in some applications. For this reason, it is necessary to find alternative technologies that offer increasingly efficient use of this scarce resource.

Visible Light Communication (VLC) is an emerging wireless optical technology that alleviates the spectrum shortage. This wireless communication system operates in the license-free spectrum from 400 to 790 THz. However, the slow rise-time of commercial lighting lamps is a factor that limits their throughput. Typically, VLC transmitters are embedded in the White Light Emitting Diode (WLED) lamps or LCD screens to re-use the hardware and power source. Thus, these transmitters allow the dual functionality of the VLC system, which is illumination and data communication. The most feasible transmission technique uses Intensity Modulation/Direct Detection (IM/DD), where the optical power is modulated to transmit the information. Meanwhile, the light intensity waveform emitted by the WLEDs is demodulated using a photodiode or image sensor receiver, integrated into commercial cameras. These receivers convert the optical power into a current signal.

Currently, this technology is capable of providing downlink speeds up to a few hundred Mbps [7] in indoor scenarios. VLC has experienced a steep growth since the first proofs of concept developed by Nakagawa *et al.* in the early 2000's [8], and there are currently two consolidated standards (IEEE 802.15.7r1 [9], and ITU G.9991 [10]) and some task groups working on Optical Wireless Communication (OWC). As well, some Industrial companies have started to invest in VLC developments. Some emergent companies such as Oledcomm and pureLIFI have manufactured their own Hi-speed VLC / Infrared (IR) systems for Office and Home applications with the commercial name of "LI-FI"; also, some of the big electronic companies have increased their portfolio with VLC solutions. Phillips has created trueLIFI, a light bulb capable of transmitting up to 250 Mbps [11]. However, this technology is still in the early stages, and there are many open issues to solve. During the last years, the research on VLC has been focused on demonstrating the limits of the technology in terms of achievable data rates [12] and channel modeling [13] [14]. Nonetheless, the scientific community has not put sufficient effort into solving problems on upper communication layers to ensure the integration as an operating network.

On the other hand,Intelligent Transport System (ITS), promoted by the vehicles industry, is one of the potential areas of application for VLC technology. ITS aims to improve driving experiences, optimize vehicle resources and prevent accidents. This type of system includes a set of sensors to obtain real-time information from the vehicles' surroundings. However, the data captured is not enough to avoid all possible risks. Therefore, the vehicles must possess a communication system to acquire information from external agents known as Road-Side Unit (RSU) and near vehicles. In particular, Dedicated Short Range Communications (DSRC) at 5.9 GHz offers the potential to support wireless data communications between vehicle-based devices and infrastructure [15]. The Vehicle Safety Communications (VSC) project has been developed to ensure that the proposed DSRC communication protocols meet the needs of vehicle safety applications [16]. ITS communication needs to be redundant when DSCR can not guarantee a secure transmission with low latency. Therefore, there is necessary to appeal an alternative option where VLC arises as a promising emergent candidate. VLC implementation reduces hardware and operation costs using vehicles and existing street infrastructure illumination devices. In addition, the power LEDs serve a double function communicating and illuminating. More importantly, VLC does not interfere with RF devices, and consequently, with DSRC systems, the external agents that affect DSCR do not impact VLC communication and vice-versa. Thus, the connected vehicle application could be operated in most situations by one of these two technologies.

1.2 Research Problem and Hypotheses

The incorporation of VLC into vehicular environments requires solving different issues. A primary challenge of VLC is the limited coverage area of the VLC Access Point (VLC-AP). This problem will increase with the high mobility of vehicles, especially when they move out of the coverage of the serving cell. Due to the vehicle's high speed movement, they stays briefly in each cell. For this reason, one of the

main challenges currently faced by the research community is the lack of handover strategies to provide seamless communication when the vehicular node is moving at high speed. Handover schemes for VLC systems have not been widely studied yet. So far, most of these works have been conducted for indoor environments. We especially remark on the different paradigms used to solve the VLC mobility challenge between indoor and outdoor scenarios. On the one hand, indoor VLC networks focus on using handover schemes that avoid unnecessary handovers to decrease the usage of networks resources. The user in these environments stays long periods in a single AP. So, the handover strategies in these situations prioritize holding a session to avoid wasting resources when the conditions are not clear to make a decision. On the other hand, outdoor VLC networks need sensitive handover schemes to avoid suffering abrupt interruptions. In the literature, a large number of studies on handover have been carried out, but mainly for RF technologies. Handover strategies for VLC can use RF approaches as a model, but they need to be adapted to the specific characteristics of this technology. E.G. VLC links could be asymmetrical (uplink and downlink) with a narrow radiation pattern presenting limitations on the communication [17]. Despite the existing RF solutions, VLC represents a promising technology that may be used to effectively alleviate the load of the RF wireless networks.

Problem Statement

This thesis addresses the open research problem of designing handover strategies for a vehicular VLC network in urban areas. More specifically, it focuses on the communication problem for safety services within the road tunnel scenarios. The value that this study brings is the potential exploitation of the existing tunnel's lighting infrastructure for reliable communication services. The core contribution involves exploring the critical issues and key features of designing a comprehensive handover mechanism within PHY and MAC layers for high-speed vehicles using a VLC network.

This dissertation formulates the following hypotheses:

Hypothesis 1: *The use of VLC as a backup communication technology for some urban applications alleviates the burden on already saturated RF-based networks and minimizes the risk of communication failure of primary networks.*

Smart-city environments have vital processes that require reliable communications to prevent risks to people or damage to the city's infrastructure. For instance, the safety messages in the ITS application have the objective of avoiding possible vehicular accidents. Due to the spectrum allocation of the wireless optical signals, the VLC channels do not suffer the same interference and atmospheric effects that other RF-based technologies allocated on 2.5 and 5 GHz bands. For this reason, safety applications can increase their redundancy and robustness by adding a VLC link.

Hypothesis 2: *A VLC network can sustain seamless communication even in a high mobility scenario.*

One of the main constraints of using VLC systems is that they provide coverage areas spatially limited. This problem increases when the user remains briefly in an AP because the time spent in the handover resolution reduces the communication time slot. Most locations have multiple light sources to have a soft illumination and in the VLC system's network scheme each lamp is considered as an access point. Therefore, a deployed VLC network in these scenarios has enough APs to extend its service in the entire enclosure, and the network can provide continuous communication when the user moves to a different room's area. To avoid an interruption it is necessary to perform efficient session migration from one AP to another AP providing a transparent handover for the user. The handover problem for the VLC indoor environment has been studied before in the literature. But, the handover mechanism for VLC networks enabling vehicular application is a recent open research subject that has been barely studied in the literature. Such scenarios demand low latency protocols and efficient detection schemes to minimize the node's unconnected period. Also, these mechanisms need to be sensitive to prioritize cell exchange. This thesis work shows that a VLC network with a proper Handover strategy can provide an steady communication in these scenarios.

Hypothesis 3: *VLC network services can fulfill the specifications and requirements of safety messages in ITS.*

Services provided by a VLC network need to fulfill the requirements of the primary technology that is backing up. VLC has attractive capabilities in bandwidth and low latency. Additionally, it has multiple PHY modes that enable the configuration of the data rate, the particular bit error rate performance, or the link range needed for the application. For this thesis, the study cases demand those requirements of a low data-rate network with low latency, regardless of the number of users in the network.

Hypothesis 4

The uplink limitations in a VLC network can be coped with a novel design of the network topology.

One of the main constraints of VLC systems is that the transmitter of the mobile node needs to point out in the AP direction. It makes VLC systems susceptible to the variations of the transmitter and receiver positions and orientations, limiting the coverage area. An effective network design can extend the AP coverage area to allow a soft transition. It is possible when the APs share resources such as the receiver hardware. It allows them to receive the user's communication reducing the effects of its position and transmitter orientation. This receivers share scheme requires to add an intermediate communication layer to manage the frame distribution, we have defined this modifications as "2.5 layer"

1.3 Aim and Objectives

The global aim of this thesis is to contribute to the integration of VLC technology in smart cities' environments. One of the main problems to solve consists of developing

a handover mechanism for a VLC network with seamless communication for a high mobility scenario in a Smart Cities environment; thus, this thesis will focus on it. As a first approach, a particularly complex and relevant scenario, as the vehicle to infrastructure communication in road tunnels, has been selected for testing our proposals. Nevertheless, other scenarios or use cases can be studied in a similar way and the obtained results can be easily generalized to them. Additionally, a powerful simulation tool is needed to validate the different designs properly. Since available alternatives do not fulfill this work's accuracy requirements, the design and implementation of this type of simulation platform will be another global objective for this thesis. A more detailed description of the work objectives are the following:

These objectives are oriented to develop a handover strategy. Also, to validate the proposed hypothesis.

1. To study the communication channel of the road tunnel scenario using Ray-Tracing Monte-Carlo Simulations. The results test the feasibility of the VLC network in this scenario and help to explore the system limitations and performance.

2. To develop a simulation platform of a VLC network that permits the validation of the handover schemes. The simulator includes a realistic channel model and a detailed emulation of the protocols. It brings a trustful representation of the MAC and PHY layer of the VLC network.

3. To design a handover mechanism that reduces the latency on the handshake process. The solution needs to provide seamless communication to the vehicular nodes in the area. In addition, this solution will be assisted by a new reception scheme to guarantee the vehicles are always connected.

4. To develop a detection algorithm able to identify opportunely when the vehicular node left the AP coverage area. This algorithm is based on the channel result from objective 1 to make a specific solution for this scenario.

5. To validate any proposed handover solution through an OMNeT++ based simulator developed in objective 2. The main goal of this validation is to ensure the good performance of the complete solution, which includes modifications on the network topology, handover protocol, and the detection algorithm. The simulation considers the characteristics of the road tunnel scenarios from objective 1.

1.4 Justification and Methodology

There is a growing interest from the Industrial and Academic sectors to explore the application of VLC in many different areas. Moreover, ongoing research projects are supporting this growth, as the Eliot project from H2020 [18] or the COST Action NEW FOCUS[19], among many others. Of particular interest is the European project *Visible light-based Interoperability and Networking* (VisIoN) funded by the

European Union's Horizon 2020 research and innovation program under the Marie Skłodowska-Curie grant agreement n° 764461 [20]. The project goal is to make significant contributions to the fundamental scientific understanding and technical know-how of VLC. VisIoN is divided into three main application areas: VLC for Smart Cities (Home and Office), VLC for Smart Transportation and, VLC for Manufacturing and Medical. The background areas are photonics, wireless communications, modulation, and physical and upper-layer protocols. VisIoN is held by eight public research institutions and three industrial sector parties in seven countries, which aims to train a new generation of Early-Stage Researchers (ESRs) in the emerging area of VLC. This initiative has achieved important progress on VLC that includes research works on a wide range of topics such as novel equalization, modulation, and channel access techniques to improve the data rate and the number of users held by a VLC network. Additionally, new possible transmitters, such as Organic LED screens, are studied and characterized. Other research works include the integration of VLC in applications such as Intelligent Transport Systems, localization, health monitoring, or automation processes in the industry.

The University of Las Palmas de Gran Canaria (ULPGC) is participating in the VisIoN project with two ESR projects under the supervision of Professor Rafael Perez Jimenez at the Institute for Technological Development and Innovation in Communications (IDeTIC). As part of these efforts, this dissertation has been driven by the VisIoN program, under project ESR 5 - VLC for Smart Cities. The goal is to enable the integration of VLC into heterogeneous networks (HetNets) by an improvement of MAC and upper-layer protocols. One of the flaws of the VLC system is the scarcity of mechanisms to coordinate the operation of multiple AP in the area, especially in smart cities ecosystems where network structure changes dynamically. Therefore, instruments to manage these changes without interrupting the node operation are necessary. Additionally, all the proposals, need to consider the unique characteristics of the VLC communication adding its channel model in their design.

The work presented in this thesis is a comprehensive research of the problem comprising multiple layers of the OSI model. The study began with an analysis of the channel model in this scenario to design a practical solution. It originates a handover strategy working PHY and MAC layers. This strategy is composed of a system topology that increases the communication range and redundancy, a low latency handover protocol, and a detection algorithm. As result, the network can provide a stable communication service without strong interruption in this scenario.

The research methodology used comprises six main parts with the corresponding activities. Figure 1 shows the implemented roadmap to achieve the goal of this research work. First, we designed an initial communication system considering the VLC infrastructure characteristics of the scenario of interest. This design followed the regulation of the European normative for the illumination system in road tunnels. Then, we used this setup to study the communication channel to analyze the feasibility of the proposed mechanism. The results also show the time-variant channel behavior to plan a handover strategy. The next step was to develop a VLC

Physical and MAC layers simulator to validate the proposed solution. It consists of a system-level simulator programmed in the OMNET++ platform. In the next stage, we proposed a handover mechanism considering the channel information of the vehicular tunnel scenario. So, it was necessary to integrate this solution into our simulator. Finally, we evaluated the solution and analyzed the performance results.

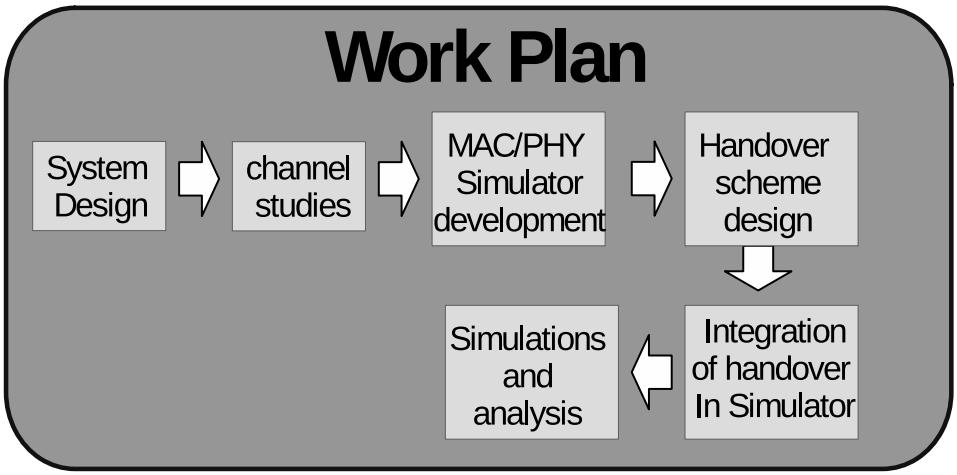

Figure 1: The research methodology proposed in this thesis work.

1.5 Outline of the Thesis

The remainder of this thesis is organized as follows.

Chapter 2 gives an overview of the background knowledge about VLC technology and how it has been integrated into vehicular scenarios. Then, it presents a review of handover schemes and their incorporation into VLC systems.

Chapter 3 describes the theoretical frame of the PHY and MAC layers in the IEEE 802.15.7 standard. It is a vital piece for understanding the rest of this research work since it has been chosen as the reference for the works development and ensure its compatibility with other networks.

Chapter 4 introduces the VLC simulator that needs to integrate the PHY and MAC layers. Here, the components of the simulator are described and validated.

Chapter 5 presents the validation of the developed simulator, and highlights the inclusion of realistic channel models during the MAC layer assessments.

Chapter 6 investigates the application of VLC in the vehicular tunnel scenario. This part of the thesis is fundamental because it formulates the proposed strategy and its limitations. Finally, Monte Carlo simulations are included to evaluate the performance results of the proposed mechanism. These simulations consider the elements present in the vehicular tunnel scenario and the characteristic of the illumination infrastructure.

Chapter 7 itemizes the steps on the proposed solution. It reports the methodology used to evaluate its performance.

Chapter 8 concludes the thesis. It gives a summary of the main findings, and some suggestions for future research works.

Chapter 2

State of Art

This chapter presents the background information related to the handover research problem on VLC-based vehicular communications. The content of this chapter is divided into four sections. Firstly, it describes how VLC has evolved in the last decade. Then, it gives a brief introduction to the incorporation of VLC in vehicular networks. After that, it presents an overview of the handover problem that has been widely studied using radio technologies. Finally, some of the most representative research studies on the handover problem in VLC are described. Surprisingly, despite the low number of research works addressing the handover problem using VLC, a significant number of them covers vehicular scenarios.

2.1 VLC Evolution

The recent path of LED lighting technology has caused that most illumination systems are migrating to this technology. The significant additional energy savings and the long life span of the hardware are some of the main reasons. Another advantage of LED lighting is the fast transitions between the On and Off states. The latter opens the possibility of flicking the light in a microsecond enabling the dual purpose of illumination and data communication [21]. More than two decades have passed since the initial works based on LED lights. During this time, two different VLC standards have been published so far related to this technology, the IEEE 802.15.7 and ITU.9991, and one additional is on the process (IEEE 802.11bb). The first and most referenced standard is the IEEE 802.15.7, released in 2011 [22]. Initially, this standard considered only the modulations for photodiode-based receivers. It included three basic Physical layers (PHY) operation modes: a low data rate for outdoors (in the hundreds of kbps), a high-speed configuration for indoor environments (in the tens of Mbps), and a high-speed environment with multiple light sources that consider color shift-keying transmission schemes (in the tens of Mbps). All these layer types consider only the usage of photodiode-based receivers. However, the IEEE 802.15.7 standard has been recently updated in 2019, adding cameras as receivers with the Optical Camera Communication (OCC) concept. The updated version extended the standard with three more PHY operation modes [9].

The following modulation schemes are only considered in the IEEE 802.15.7 standard with photodiode-based receivers: Variable pulse position modulation (VPPM), On-Off Keying(OOK), and Color Shift Keying(CSK). It did not include the Orthogonal Frequency Division Multiplexing (OFDM) based technique yet, which is a modulation resilient to the multipath effects on the channel. Contrary to this, the ITU.9991 has adopted the OFDM modulation scheme [10]. Since VLC works using IM/DD, OFDM-based modulation schemes cannot transmit complex constellations or negative values. Therefore, the OFDM modulator needs to adapt to these restrictions. An example is the DC-biased optical OFDM (DCO-OFDM) scheme, which uses Hermitian symmetry to transmit only real values on the Fourier Transformation [23]. Then, the signal is mounted on a DC level using an optical bias-T.

One of the fundamental parts of a communication system is knowing the signal propagation behaviour due to the channel characteristics. In this area, VLC has been benefited from the previous studies in the field of Infrared (IR). VLC uses the same methodologies to obtain the channel models. For example, the works of Gfeller [24] and Barry [25] have been used as the reference due to their high accuracy. However, there are complex scenarios, such as an office with many reflecting surfaces, where these approaches become unfeasible because of the impractical computational load. Lopez-Hernandez et. al. in [26] mitigated this problem by proposing a much faster statistical approach based on a Monte Carlo ray-tracing algorithm. Nguyen et al. introduced later on one of the first channel simulators for VLC [27]. Furthermore, the authors in [13] and [14] used ray-tracing with realistic 3D CAD models of the scenario to get an accurate channel impulse response (CIR).

In recent years, VLC has explored potential application areas that include positioning, healthcare environments, vehicle-to-vehicle communication, informative panels, advertising displays, underwater communications, etc. Positioning based on VLC, known as Visible Light Positioning (VLP), aims to obtain the position of a user by utilizing visible light signals with several advantages compared with traditional RF-based localization. It can achieve higher positioning accuracy than GPS in indoor environments with no electromagnetic interference. All the relevant positioning techniques for indoor positioning can be adopted for the VLC based indoor positioning. The healthcare sector is also a promising area. The patients' vital signs need monitoring, but wired sensors solutions impede mobility. Moreover, hospitals have strict restrictions on the use of RF equipment. Thus, VLC emerges as an option to support wireless communication between the body sensors and the monitoring equipment allowing the patients to walk freely [28, 29, 30]. In addition, the use of VLC technology in industrial environments has grown the interest of the research community. The reason is that VLC is immune to electromagnetic interference caused by the high-power engines used in industrial warehouses and factories. This technology allows providing real-time information to the robots used in automatized production lines [31, 32, 33]. In addition, VLC can assist IoT applications in offices and homes to obtain information from a sensors network. It takes advantage of buildings infrastructure where the surveillance cameras can be adopted as receivers using OCC schemes and transport information to a central processor. It is possible to deploy communication solutions without increasing considerably the implemen-

tation and operation cost [34, 35]. The usage of the VLC technology in automotive applications is also another field of study in the existing literature. This potential area, of particular interest in this thesis work, will be analyzed deeply in the next section.

2.2 VLC in vehicular Networks

The inclusion of VLC as a communication option for ITS has been explored since 2005 when Tanimoto et al. proposed the use of traffic lights to provide data to vehicles [36]. This first work considered a high-speed camera to sense the traffic lights and compared consecutive images to eliminate the background information. The initial step to incorporate VLC technology for ITS application is channel characterization. It provides knowledge about the main challenges to deal with and the feasibility of the implementation. In 2009, Rui L. et al. presented in [37] the first VLC channel model for the infrastructure-to-vehicle(I2V) link. The model considers only Line-of-Sign (LOS) contribution. In [38], Lee et al. presented complementary studies by considering a whole urban area. They explore the impact of multi-path components from surrounded buildings and near vehicles for Vehicle-to-Infrastructure (V2I) communication links and vehicle-to-vehicle (V2V). They conclude that V2V links show purely LoS components and lower delay spread regarding V2I scenarios. On the other hand, the V2I transmission scheme shows poor performance. Wu et al. [39], addressed the duration of VLC links for the V2V scheme. A vehicle circulating over different urban scenarios was characterized using a video database. The study reflects that the duration of V2V links is conditioned to the type of street (number of lanes) and if the vehicles are moving in an urban or rural area. The average link duration in an urban scenario is 6.72 seconds. Cui et al. [40], determined the stationarity nature of the VLC-based vehicular channel using a similar procedure. The results showed higher coherence time regarding DSRC with values in tens of milliseconds. Luo et al. [41, 42], presented an exhaustive analysis of the V2V channel, including the impact of the road reflections in the communication. Another relevant problem in VLC V2V communication is to ensure the system can operate full-duplex data communication. The main limiter is the differences between light emitted from headlamps and taillamps [1]. They provide distinct radiation patterns and power so that the communication range varies as can be seen in Figure 2. Since 2015 the influence of meteorological conditions on VLC channels has been studied for outdoor VLC and OCC systems. The VLC channel is affected by fog [43], rain [44], and other weather conditions. For example, Matus et al. [34], recently measured the impact of sandstorms for OCC links. In [43], they measure the channel impact adding different fog conditions to a VLC link of 1 meter. They conclude the use of Fresnel lens improves the signal reception and mitigates fog effects. Otherwise, [44] performed experimental measures adding rain conditions. The measured signal presents erratic fluctuation with suddenly peaks increments and abrupt decrements. The results show that rain could decrease the Signal-to-Noise Ratio (SNR) level until 60%.

In addition to the VLC channel-based vehicular studies, some proof of concept

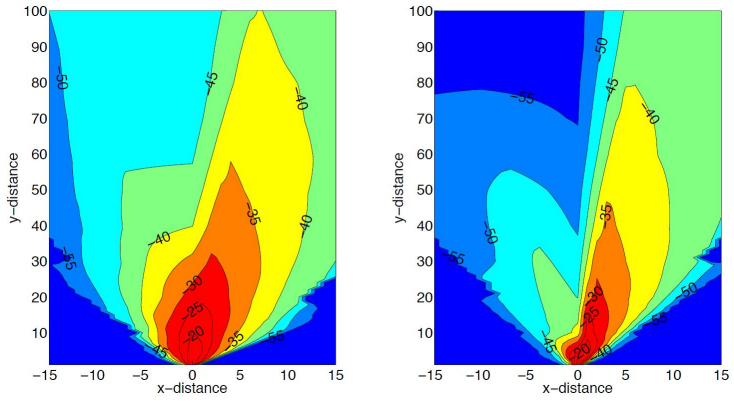

Figure 2: The headlamp radiation pattern obtained from experimental measurements in [1]

has been performed during the last decade. Alin-Mihai Cailean and Mihai Dimian [45, 46], designed a hardware architecture for Vehicular VLC systems. They also established the minimum requirements that the VLC system needs to cover safety applications for ITS. The safety messages in ITS applications have a frame size between 208 to 904 bits with a transmission frequency of 10 Hz. Additionally, the VLC network needs to provide a constant data rate of 27 kbps per user. Furthermore, emergency transmissions do not tolerate a delay over 20 ms. Yoo and Lee [47], developed a proof of concept prototype using a headlamp with a communication range of 20 meters. Yu et al. [48], incorporated a VLC prototype into the scooter hardware. The authors performed a practical validation of the channel using a modified transmitter jointly with a Lidar to increase the accuracy of the measures. At the same time, Bellè et al. [49], built a prototype that comprised IEEE802.15.7 standard-compliant MAC and PHY communication layers. The results show low latency to process and decode the optical signal by the hardware in almost all the configurations of the PHY layer. Unfortunately, when the system uses Reed-Salomon Codification to reduce the error rate, the decode time increases to 268 ms. Therefore, it will be necessary to look for an alternative codification option or not use it. Murat et al. [50], validated the performance of the PHY layer of standard IEEE 802.15.7 in vehicular scenarios. It measured the Bit-error-Rate (BER) of optical transmission using a fog light to a vehicle. The authors evaluated multiple transmission schemes of PHY I mode. In this validation, the PHY configurations based in On-Off Keying modulations present a better performance, with lower Bit-Error Rate and lower process time to decode the optical signal. Cailean and Dimian [51], discussed the issues that need to be addressed to incorporate the IEEE 802.15.7 standard in vehicular applications. Moreover, Turan et. al. [52], studied the problems of using multi-hop transmission, validating with hardware probes. More recently, the Fraunhofer Heinrich Hertz Institute (HHI) tested a vehicular platoon assisted with a LiFi communication system in a real-world scenario [53].

The presented overview summarizes the most relevant works of VLC in vehicular communications. The research of VLC for vehicular communication has been centered to study and resolve physical layer problems. Although, there is a lot of open

issues on MAC layer because the protocols in this layer were design to assist an indoor network. For example, there is a lack of mechanism that support the user's mobility. In an home/office network, this is not a mayor problem since the user nodes remains in a semi-static position. Oppositely, the nodes in a vehicular network changes repeatedly of AP. Unfortunately, there are a small number of works in the literature that deal with this problem. Therefore, the mechanism to support mobility remains an open issue. Due to the few publications about handover for VLC networks, the analysis of the state of the art about handover is split into two sections. First, section 2.3 explains a general panorama of handover. While section 2.4 covers the works of handover for VLC networks.

2.3 Handover

VLC technology is still in an early stage with several open problems. The VLC incorporation in the ITS environment formulates the necessity of a handover procedure as the user moves in-between cells without interrupting the communication service. The handover process consists of three main phases: information gathering, handover decision, and handover execution. Information gathering is the sub-process of collecting the input signal to determine when to start a handover. The second phase is detection which is the set of algorithms to predict the user movement and trigger the handover execution. The last phase is the handover execution that is the steps on the protocol to resolve the handshake successfully. These protocols involve message exchange between the node, the current AP, and the target AP to update the authorizations.

The signals gathered for the handover are defined by the nature of the communication system and user destination. A user can be moved from a current AP to a new AP by employing the same technology (horizontal handover) or changing its connection type to access an alternative infrastructure (vertical handover) when current communication may present low or outage probability. Vertical handover requires transmitting an independent signal from a different technology, commonly associated with Quality-of-Service (QoS). For example, protocols like Multipath TCP senses end-to-end latency [54, 55]. Another option is to compute the bandwidth resources between each available option [56]. The resources, or even a specific technology, can prioritize using this calculation. Thus, the number of possible cost functions is wide [57, 58, 59]. Hass et al. [60], proposed a dynamic balancing algorithm that uses the Channel State Information for hybrid network VLC and WLAN. Although, this work was centered only on horizontal handovers. The signals used in horizontal handover estimation must depend on the user position. A Physical indicator commonly chosen in the VLC system is the Received Signal Strength (RSS) [2, 61]. This indicator has been considered in most horizontal schemes since the initial work in [62]. In a complementary way, the Signal-to-Noise Ratio (SNR) and Signal-to-Interference ratio (SIR) can execute the same function of locating user's position. Furthermore, there are link-layer indicators that have not been explored in VLC systems, such as Bit-Error-Rate and Frame-error-Rate [63, 64, 65].

The second phase comprises the signal detection that triggers the handover execu-

tion. One of the main issues in this phase is the temporal anomalies of the measured signal generated by shadowing effects. These phenomena can incorrectly initialize the handover process. Initially, the VLC system considers a fixed threshold and two decisions modes, Instant or Dwell handover. The latter operation mode resolves after a second delayed measure corroborates a failure [66, 67]. The time between two measurements is defined as Time-to-Trigger (TTT). Later, dynamically dwell was proposed to adapt to the different user behavior. For example, if a user often moves, the waiting time needs to be shorter and the delay between decision changes. The result shown in[66] compares these three detection schemes bearing in mind four common mobility patterns. In them, Instant Dwell presents poor performance where the node is connected less than 40% of the total simulation time. Oppositely, dynamic dwell demonstrates better efficiency where the user is connected since 47 % in the worst case until 71 % of the time. Another typical problem is to have a sensitive trigger to start the handover. When the signal difference between the APs is relatively small, the system decision oscillates, executing a handover continuously between both APs. Costa Da Silva et al. [63], studied this problem and proposed an algorithm with Handover Margin (HOM) to avoid the ping-pong effect. In this algorithm, the signal to the target AP needs to surpass at least the current AP HOM signal. When the user has changed the service provider, it cannot return to the previous AP until more robust return conditions have been accomplished. Additionally, Wu et al. [68], proposed the Skipping algorithm, which is a more resilient version. Skipping algorithm reduce 26 % of the average requested handover regarding Costa Da Silva proposal, when the user is moving at 10 m/s. It is pertinent to mention that these techniques are adaptations from RAN algorithms, recently studied in VLC systems. Therefore, the conclusion is that the handover problem has been scarcely explored.

There is a wide range of handover protocols that enables the mobility of a user. Only those protocols compatible with Internet Protocol (IP) will be of interest here as they are universally extended. Since these protocols are independent of the transmission technology, they can be adapted easily. Mobile IPv6 protocol (MIPv6) is a highly accepted mobility solution developed since 1996 [69]. However, it takes several seconds to resolve, becoming unviable for many applications [70, 71]. Other alternative protocols have emerged based on MIPv6. Fast Handover Mobile IPv6 (FMIPv6) is another early solution proposed by Dommety in 2003 [72]. In this proposal, the Mobile Node (MN) detects in advance the next AP. Then, it requests the entering authorization to minimize the interruption time [73].

The Hierarchical Mobile IPv6 (HMIPv6) is a Layer 2 protocol introduced in [74]. HMIPv6 splits the network into two domains, where the inter-domain is coordinated by a module called Mobility Anchor Point (MAP) [75]. MAP manages the traffic inside the network and redirects the packet to the user location. A further discussion of this model will be presented in section 6.5. A different approach is to redirect the traffic to the new target AP during the handover execution. Proxy Mobile IPv6(PMIPv6) [76], is a protocol based on this technique. Under this protocol, when the packets are delivered to the previous AP, it buffers them using a tunneling session until the handover has been resolved [77, 78, 79, 80, 81]. One of the most common

tunneling protocols used jointly with this technique is MultiProtocol Label Switching (MPLS). Additionally, studies have shown that the protocol combining FMIPv6 and PMIPv6 can provide faster handover performance. The authors in [82, 83], proposed the Fast handover Proxy Mobile IPv6 (FPMIPv6) to support Radio Access Networks (RAN) for cell phones. This proposal showed good performance with low latency, where an average handover process can resolve in 100 ms [84].

Complementary to these protocols, there are some additional mechanisms to increase the redundancy during the transition. An example of such schemes is the Coordinated MultiPoint transmission (CoMP) studied for VLC applications [2]. It provides a soft handover with almost null packet loss during this transition. This scheme operates once the handover protocol has been initialize until its resolution has ended. During this time interval, both APs (current and target) transmits the optical signal simultaneously to provide redundancy. It guarantees that no matter if the user has left the coverage area of the current AP, it will not lose a packet. However, it requires several modifications to the system architecture to prevent symbol interference [85]. They validate this transmission scheme considering the conditions of a VLC network deployed in a office environment. CoMP shows superior data rate performance regarding hard handover scheme. Figure 3 displays the validation scenario representation on the right side, and the data rate result on the left side from [85] An additional option to execute a soft handover is presented in [86] that is compatible with Orthogonal Frequency division Multiplexing (OFDM). In this case, there is not necessary to synchronize the AP. The packets are transmitted by both AP using different bands during the handover resolution.

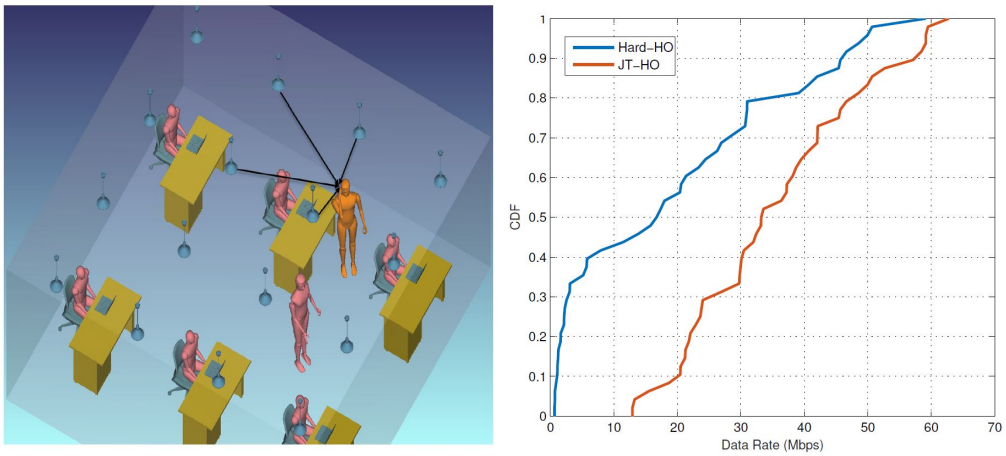

Figure 3: Data rate of a moving user where the AP uses CoMP scheme for a soft handover, and a hard handover case from [2]

2.4 Handover for VLC

In VLC, the handover problem is a topic barely explored. Only a few studies have been carried out on covering indoor environments and vertical schemes in heterogeneous networks. Therefore, the most relevant research works in the area are

described in this section. Most of these works have been published in the last five years.

In [87, 88], the authors proposed a prediction handover scheme for VLC heterogeneous network. The developed algorithm considers the drawbacks and penalties to execute a handover decision. Dinic et. al. [89], presented a horizontal handover scheme for a VLC network with Orthogonal Frequency-Division Multiplexing (OFDM). This scheme establishes the handover process using assigned channels that provides redundant communication to soft the transition. This frequency-based soft handover increase the datarate retransmitting the information at different OFDM bands. A similar arrangement is presented in [90].

Katz et al. [91], studied the integration of VLC/WLAN, which allows executing the handover process from the network layer. The handover scheme changes the packet's path when there is an interruption to restore the service immediately. It requires at least two connection cycles previously [3, 92]. They test this proposal sending a constant data rate of 3 Mbps during 10 seconds, and provoking an outage during this time. The handover scheme lose 9.36 % of the downlink packets before to detect the failure. However, in a stand-alone VLC-only network is not possible to guarantee this last condition, limiting the potential applications. Figure 4 shows the testbed used in [3] to measure the handover latency. Murat et al. [93] proposed a detection algorithm that is triggered when the network configuration changes. When a user ingresses/egresses to/from the network, the algorithm evaluates the need of reallocating any user. It helps to reduce the resources needed by the signaling messages. The same authors also studied the channel for indoor scenarios using Jointly Transmission COMP (JT-CoMP) in the two APs [2]. The results showed an improvement in the link data rate. Also, they evaluated the original CoMP scheme in vehicular scenarios. But the results reflected some problems with its execution. For that reason, they adapted the CoMP scheme to decrease the impact of the vehicle speed variations incorporating an algorithm with dynamic HOM and TTT values [94]. In [95], the authors optimize the HOM and TTT parameters using a Q-Learning approach. Moreover, Quang-Hien et al. [96], presented a hierarchical VLC system that integrates a set of RSU with the road luminaries using OCC-based communications links. The lamps were grouped in sections to extend the cell coverage area. The handover was triggered using the image information. This approach requires high-speed frame rate cameras with 1000 frames-per-second, which is a drawback.

Jarchlo et al. [97, 98], presented an alternative solution. They created a handover scheme named "Flight" based on link aggregation using Multipath TCP protocol (MPTCP). In this scheme, the vehicle can support two VLC links working simultaneously. One VLC link provides communication while the other serves as a backup. The protocol patrols the link status using the Address Resolution Protocol (ARP) message. When the system cannot provide a round trip communication, it faces a link failure, triggering the use of the auxiliary link. The route modifications are performed in the Transport layer, where the packet's destination address is changed. It minimizes the disconnection time. During this period, the vehicle nodes can detect a new AP to establish another backup link [97, 98]. The outage time depends on the

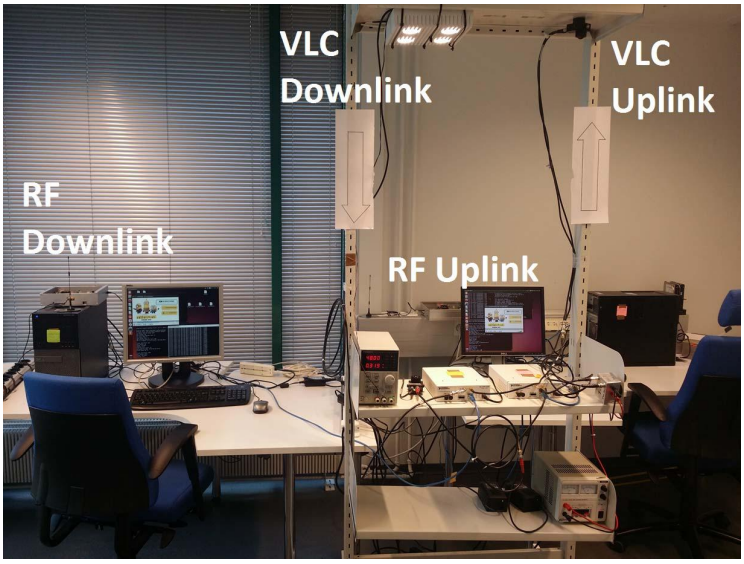

Figure 4: Testbend of vertical handover RF / VLC done by Muhammad et al [3]

ARP frequency. For this scheme, the user requires two receivers and two transmitters to hold, simultaneously, the communication in both links. Finally, the solution was integrated with an RF communication system to increase the redundancy and presented as LI WI in [4], the system architecture is shown in Figure 5. The result from the figure shows a latency of 30 ms which is enough small to be considered seamless communication. However, the hardware requirements of having three receivers working in parallel can not be ideal for all the applications and increases cost.

In [99], the authors studied a platooning system with a hybrid communication system. This system requires a quick vertical handover to RF when the VLC system fails. A detection scheme named prediction-based vertical handover(PVHO) is proposed that considers tracking the packet sequence, vehicles positions, and variations on the frame size to sense any failure on the VLC link. System-level simulations were performed to evaluate the proposal using the Simulation of Urban MObility (SUMO) tool that allows multi-modal traffic simulation in urban scenarios. These evaluations included the cases when the vehicles' caravan turned some corners and possible blockage of external vehicles between the caravan members.

A system-level simulation tool provides a common way to validate new handover schemes. Due to the relative novelty of VLC, there are not many software libraries of this technology for this kind of simulator. While some research groups have created some ns3-based modules to evaluate VLC links[100, 101], none of them provide official support. However, these modules mostly consider only the link physical layer properties ignoring protocols from the link and upper layers. Some additional research works include evaluations of the multiple access scheme on the standard IEEE 802.15.7 under diverse conditions without evaluating the VLC link [102, 103, 104]. As can be seen, mobility protocols for VLC are an open issue to solve. Finding a universal solution for any scenario is complicated, so we limited

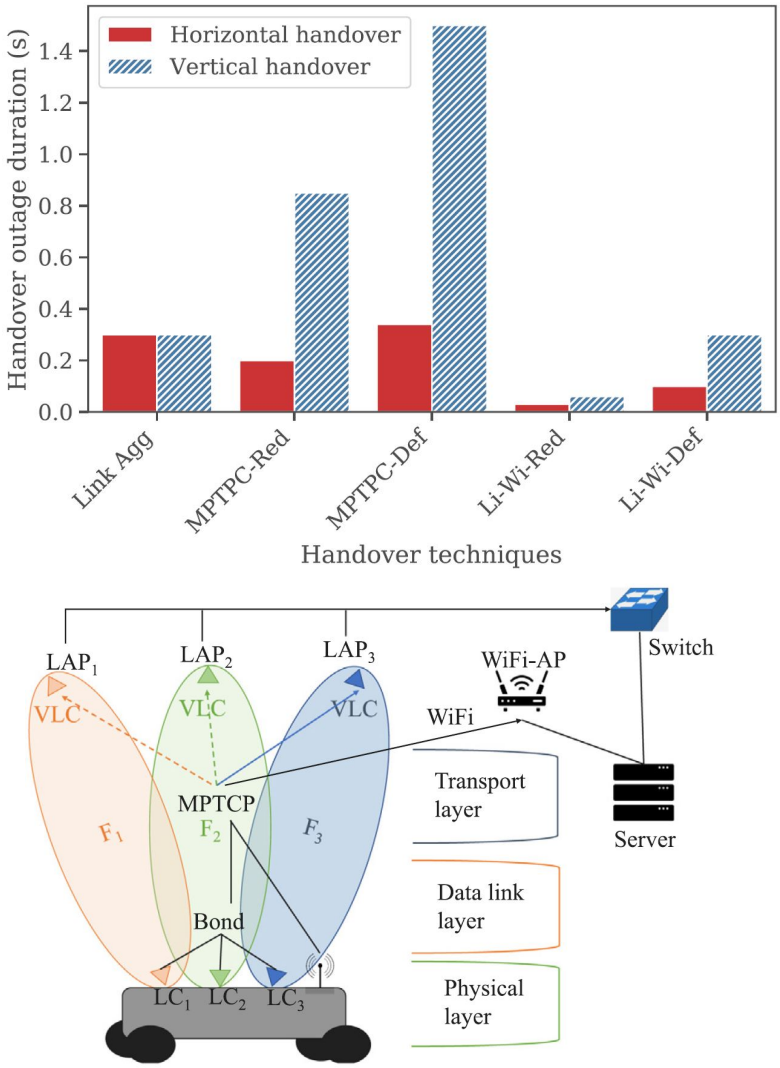

Figure 5: On the bottom, system diagram of LI WI. On the top, comparative of outage duration between some handover scheme including LI WI [4].

this study to vehicular tunnels.

Chapter 3

Theoretical Framework

This chapter presents the framework used in this thesis to address the problem of designing the handover mechanism that enables fully interoperable vehicular VLC networks. It focuses on the protocols and most relevant aspects within the physical (PHY) and Medium Access Control (MAC) layers defined in the current version of the IEEE 802.15.7 standardization published in 2018. This standard allows optical wireless communications using image sensors (cameras), high-speed photodiodes (PD), or low-speed PD as a receiver offering data rates to support audio and video multimedia services. It defines the mechanisms to secure the network and guarantee a harmonious coexistence of multiple users, ensures a steady illumination of the LED lamps while transmitting data, and several other procedures to maintain operating the network. However, as networks continue to grow and diversify, the interoperability role increases its importance to provide end-to-end communication. Therefore, this chapter will cover the network topologies defined in the standard IEEE 802.15.7-2018 and the main aspects of the PHY and MAC specifications.

3.1 Network Topologies

The IEEE 802.15.7-2018 standard supports three network topologies: star, peer-to-peer, and broadcast. These topologies are shown in Figure 6. The star topology is one of the most common network setups. In this configuration, every node connects to one central network device or coordinator, preventing direct communication among them. The communication between a node and coordinator uses a half-duplex VLC link. If they need to send a message to other nodes inside the network, they ask the coordinator to act as an intermediary. Thus, the central connection allows the network to continue functioning even if a single node fails. The centralized network device acts as a server, and the peripheral nodes act as clients. This configuration requires all the mechanisms in the MAC layer because multiple nodes share the medium. It also performs procedures to verify the identity of any incoming user. The peer-to-peer configuration needs two or more endpoints to establish communication to share information without requiring a separate network device. One of the devices assumes the coordinator role to guide the communication. Finally, the

broadcasting topology describes a one-to-all communication mode. For node identification, in all these configurations the coordinator assigns a 64-bits address to each node.

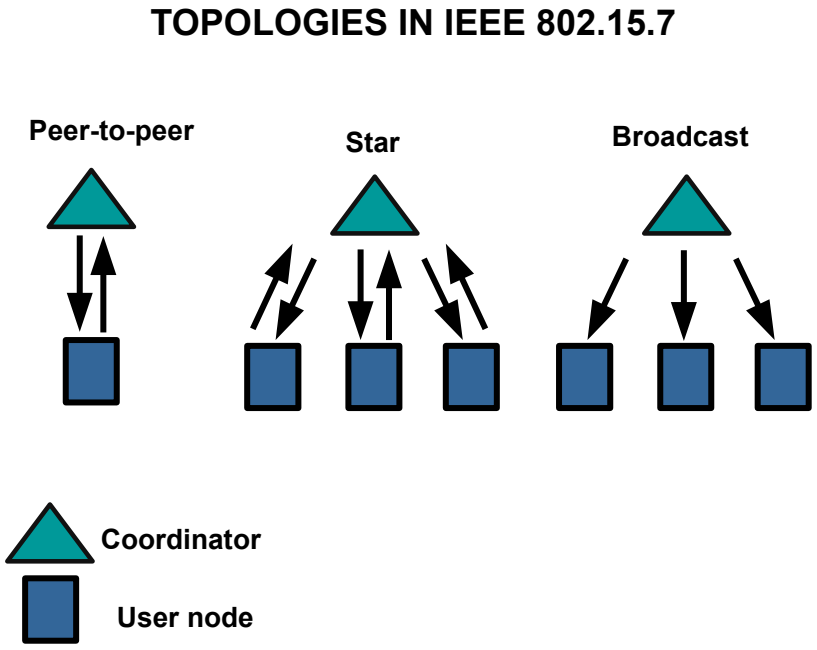

Figure 6: Network topologies supported in the standard IEEE 802.15.7.

Alternatively, the nodes can be classified according to their properties instead of their function on the network. This classification includes three types of nodes: mobile, infrastructure, and vehicular nodes. The mobile node comprises any portable gadget that requires high-speed communication. They have power supply limitations, so the uplink uses low power transmission with short-range. The infrastructure nodes have an unlimited power source since they are fixed in a particular location. It allows them to manage high-power luminaries to extend the communication range in a wide area. Finally, vehicular nodes that they have enough energy and computing power to support intense luminaries without the necessity to be fixed. Thus, they can accomplish long-range communication too. Generally, the applications do not demand high-speed communication. The three topologies explained at the beginning are shaped by these node types. For example, peer-to-peer communication is commonly used when two mobiles node needs to exchange information. Another typical case of this configuration is when two vehicular nodes send safety notifications to avoid accidents. On the other hand, the star topology and broadcast often use an infrastructure node to serve as a coordinator because of its properties and the vehicular and mobile nodes as the user node.

3.2 Physical Layer (PHY)

This section presents a general description of the IEEE 802.15.7-2018 PHY layer that supports VLC communications. Although Optical Camera Communications (OCC) is also considered within the framework of the OWC standardization, the discussions here will focus on the traditional PD as a receiver to simplify the interpretation of the framework. The IEEE 802.15.7-2018 PHY layer supports the following six operation modes:

- PHY I: This operation type is intended for outdoor use in low data rate applications. This mode uses OOK modulation (on-off keying) and Variable Pulse Position Modulation (V-PPM) reaching data rates in the hundreds of kbps. It has two codification stages to reduce the bit error rate caused by outdoor agents.

- PHY II: This operation mode is designed for indoor high-speed applications. It uses the same modulation as PHY I with data rates in the tens of Mbps. However, it operates with higher optical clock frequencies using only one codification stage to reduce errors and improve the speed.

- PHY III: This operation mode benefits from the different bands of RGB LEDs and requires a set of three receivers with the corresponding filter. This mode aims for applications using Color Shift Keying modulation with data rates in tens of Mbps.

- PHY IV: It is a camera-based operation mode for low data rate applications. This PHY mode comprises five modulations schemes: Undersampled Frequency Shift ON-OFF Keying (UFSOOK), Twinkle VPPM, spatial-2-phase-shift-keying (S2-PSK), Hybrid-Spatial-PSK, and Offset-Variable Pulse Wavelength Modulation. They have a maximum data rate of 22 Kbps, but averagely they present a performance in the order of some bits per second.

- PHY V: This PHY mode consists of four different modulation techniques for camera receivers: Rolling Shutter FSK (RSFSK), Camera-OOK(C-OOK), Camera M-ary FSK (CM-FSK), and Mirror Pulse Modulation(MPM). The operation mode PHY V presents a higher data rate comparing PHY IV. But, the modulation techniques only support data rates in the order of kbps.

- PHY VI: This mode joins different screen-to-camera communication schemes. In these modulations, the screen segments its surface to have a high number of individual transmitters. This PHY mode includes six transmission schemes: Asynchronous Quick Link(A-QL), Hidden A-QL(HA-QL), Variable Transparent Amplitude-Shape-Color (VTASC), Sequential Scalable Two-Dimensional Color (SS2DC), Invisible Data Embedding-MPFSK-blend (IDE-MPFSK-blend), and IDE-watermark. The capacity of this operation mode extends up to some kbps.

Specifically, the operation modes PHY I and II are discussed here. The physical layer of a VLC system takes care of the transmission and reception processes of the optical signal. This layer needs to perform the following tasks:

1. To activate/deactivate the transceiver.
2. To calculate the Wavelength Quality Indicator (WQI).
3. To perform channel selection (whenever is possible).
4. To perform Error detection.
5. To synchronize transmission.

PHY I and II are of particular interest because they can currently provide higher data rates and lower latency, which fit under the requirements of the vehicular application. Tables 1 and 2 show the configuration options for the PHY operation modes I and II. The major differences between these two configurations are the use of a slower Optical Clock and a two-stage forward error correction (FEC) coding in PHY I which makes the communication more reliable. In comparison, PHY II has only one-stage FEC coding and higher optical clocks that increase the data rate.

Table 1: Configurations options for PHY I mode.

Modulation	RLL code	Optical Clock rate (kHz)	FEC		Datarate (kbps)
			Outer code	Inner code	
OOK	Manchester	200	(15,7)	1 / 4	11.67
			(15,11)	1 / 3	22.44
			(15,11)	2 / 3	48.89
			(15,11)	none	73.3
			none	none	100
VPPM	4B6B	400	(15,2)	none	35.56
			(15,4)	none	71.11
			(15,7)	none	124.4
			none	none	266.6

The modulations formats developed in the PHY I and II are on-off keying (OOK) and variable pulse position modulation (VPPM). OOK is a simple IM/DD modulation scheme where a rectangular pulse represents the logical value of 1 (led ON) and 0 the absence of the pulse (led OFF). The simpleness of OOK allows faster communication, but the brightness of illumination is greatly affected by the input ratio of 0 and 1 bits. If a long sequence of OFF states appears in a data frame, OOK modulation with Manchester coding avoids flickering effects. The transmission process with Manchester coding extends to two optical-clock (OC) intervals to balance the illumination level. Figure 7 illustrates the use of OOK with Manchester coding. During the first OC interval (led ON), the Machester code outputs a rectangular pulse when the node transmits a value of 1, and if the node sends a value of 0, then a pulse is output in the second OC interval.

Table 2: Configurations options for PHY II mode.

Modulation	RLL code	Optical Clock Rate (MHz)	FEC	Data rate (Mbps)
VPPM	4B6B	3.75	RS (64,32)	1.25
			RS (160,128)	2
		7.5	RS (64,32)	2.5
			RS (160,128)	4
			none	5
OOK	8B10B	15	RS (64,32)	6
			RS (160,128)	9.6
		30	RS (64,32)	12
			RS (160,128)	19.2
		60	RS (64,32)	24
			RS (160,128)	38.4
		120	RS (64,32)	48
			RS (160,128)	76.8
			none	96

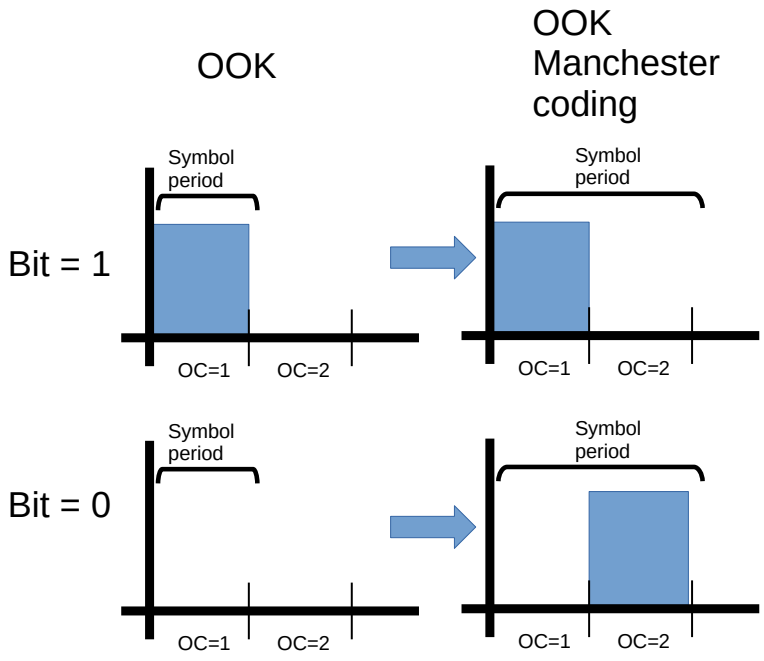

Figure 7: OOK madulation with Manchester coding.

VPPM is a modulation scheme that provides pulse width-based dimming control and offers protection against intra-frame flicker. The amplitude of the pulse in VPPM is always constant, and therefore the attenuation control is carried out using the pulse width and not with the amplitude. In comparison, the transmitted data based

on OOK requires adding extra fields on the data frame to control the illumination level. In VPPM, the information is in a single OC interval, where the bit 0 is mapped using a positive pulse at the beginning of the period, and the bit 1 is mapped using a positive pulse at the end of the OC interval. Figure 8 illustrates examples of VPPM modulation using two different duty cycle configurations.

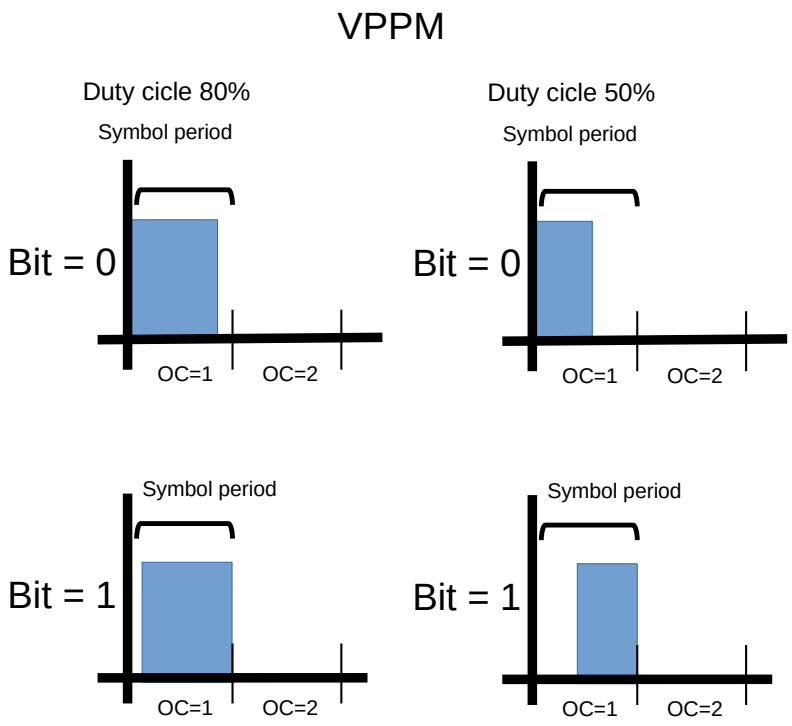

Figure 8: VPP modulation for two duty cycle configuration.

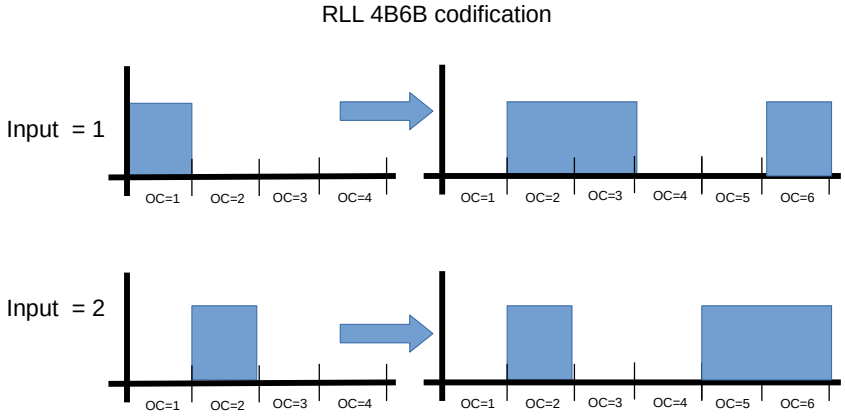

Figure 9: Examples of RLL 4B6B.

Additionally, these modulations with Run-Length Limited (RLL) line codes (such as Manchester code) can overcome the flickering effects of the sequence of 1s and 0s. However, these mechanisms increase the number of optical clock intervals used in the data transmission process, limiting the data rate of the system. A list of predefined RLL codes can be consulted in [9]. Figure 9 shows the example of a 4B6B block code. This codification scheme of rate 4/6 has an input of 4 bits (1000) and outputs an encoded-word of 6 bits with the same number of ON and OFF states (011001). Moreover, PHY II uses an extra codification stage with Reed-Salomon codes to reduce the errors on the transmissions. These codes require more resources to be processed [49]. The maximum data rate in PHY I and II can only be supported when the network is working with a peer-to-peer communication scheme, where there is not necessarily a channel access scheme. If a network has a star topology with multiple users, the data rate strongly reduces.

The standard allows a data frame structure defined for the PHY layer. This data frame is used to transfer the data in all operation modes. This VLC data frame includes a Physical Protocol Data Unit (PPDU). The structure of PPDU specifies the PHY Service Data Unit (PSDU), the Physical Header (PHR), and the Synchronization Header (SHR). The general structure of PPDU can be seen in Figure 10. SHR is the preamble to detect and synchronize the beginning of frame transmission. PHR is the PHY layer header, and they incorporate the necessary information to adjust minor reception configurations such as the channel selection, the size of the frame, etc. Figure 11 shows the PHR format. On the other hand, PSDU is the payload of the PPDU that processes in subsequent layers, such as the MAC layer. Nevertheless, PSDU possesses its frame format composed of MAC header(MHR), payload, and MAC Footer(MFR). The most relevant fields of the MHR are analyzed in more detail later.

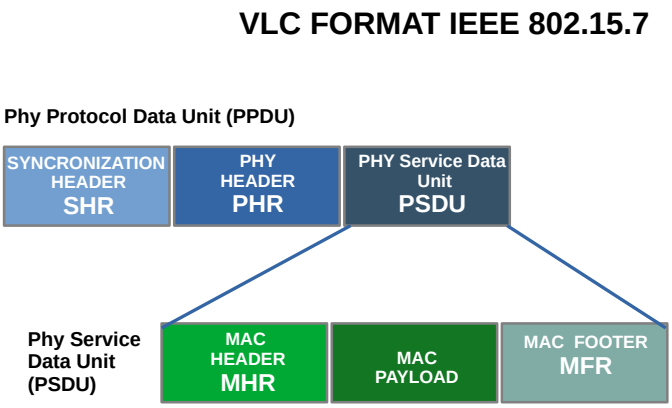

Figure 10: Frame format in IEEE 802.15.7 standard of PPDU.

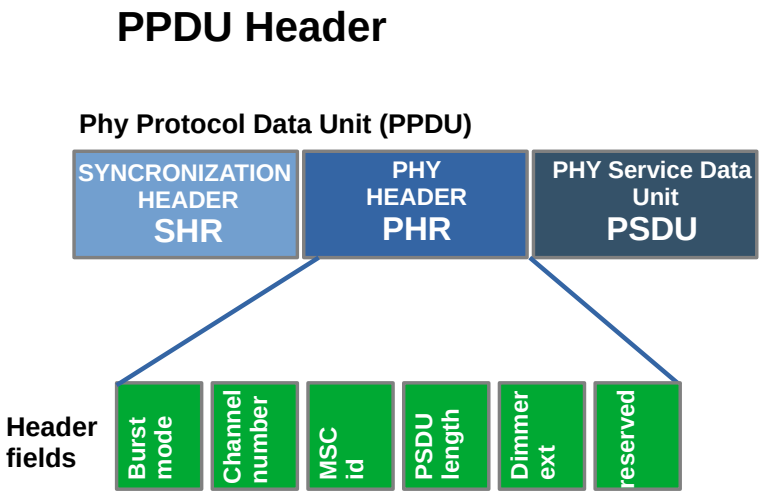

Figure 11: PPDU header fields.

3.3 MAC layer

IEEE 802.15.7 MAC layer presents a set of rules and procedures to ensure the user security. Additionally, it allows the the fair coexistence of multiple nodes operating in the network. To ensure this, it assigns a coordinator node to manage a portion of the network which dictate the appropriated time to transmit. Finally, the standard provides the frame formats to communicate between nodes. The MAC protocol is primarily responsible for coordinating the channel access of the user nodes (devices). Some of the tasks performed by the MAC layer are:

- Node Synchronization.
- Node association and disassociation to the network.
- Manage the resources of the network.
- Security mechanism.

The IEEE 802.15.7-2018 standard can operate using an optional Superframe mode to achieve low latency and facilitate synchronization to the user nodes. The format of this Superframe defines the time distribution that starts when a dedicated coordinator sends a beacon frame in predetermined intervals and ends when the next beacon arrives. This time difference is called Beacon Interval (BI). Besides the implicit time synchronization of the beacon frames, they also provide information about the channel distribution. Figure 12 describes the Superframe structure that consists of Active and Inactive periods. During the Active period, the user nodes are allowed to communicate. Otherwise, they are in an idle mode to prevent

struggling with possible neighbor VLC networks. The active period of the Superframes is called Superframe Duration (SD). At the same time, SD is composed of two parts, Contention Access Period (CAP) and Contention-Free Period (CFP). Under this network operation, SD has a fixed size. Hence, when CFP increases, CAP has to decrease. During the CAP, the user nodes access the channel randomly using a back-off mechanism established on the standard, while in CFP, they assign fixed-size time windows known as Guaranteed Time slots (GTS). When a user node requires extra time to transmit, it needs to request to the coordinator additional time slots. Furthermore, the assigned time slots for each user are continuous, and the coordinator dynamically allocates GTS taking this requirement into account.

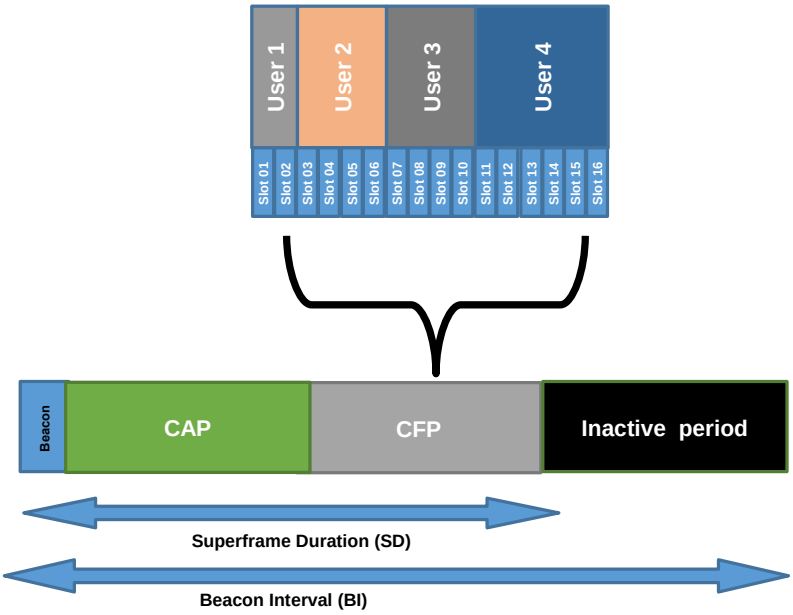

Figure 12: Superframe structure of the IEEE 802.15.7-2018 standard.

Moreover, the ratio between SD and BI (percentage of network activity) can be modified at the beginning of the network operation by setting both Super Order (SO) and Beacon Order (BO) parameters. The maximum value of BO and SO is 14, and SO cannot be higher than BO. The parameter SO increases the number of optical clocks per time slot, taking as initial value the base time *aBaseSlotDuration*. Since SD has a fixed number of time slots (*aNumSuperframeSlots*), the difference between BO and SO will determine the percentage of network activity aforementioned. Equations (3.1) and (3.2) define the amount of optical clocks assigned to SD and BI.

$$SD = aBaseSlotDuration \times aNumSuperframeSlots \times 2^{SO} \tag{3.1}$$

$$BI = aBaseSlotDuration \times aNumSuperframeSlots \times 2^{BO} \tag{3.2}$$

It is worth mentioning that all the processes in the MAC layer rely upon the number of optical clocks. The relation between optical clocks and bits depends on the PHY configuration (modulation and encoding). Finally, if the communication requires a specific ratio η_{MAC} of channel utilization, it is straightforward to demonstrate from the previous equations that the difference between BO and SO should follow Equation (3.3).

$$BO - SO = -\log_2 \eta_{MAC} \tag{3.3}$$

During CAP, the access method is random. Thus, it requires a back-off mechanism to alleviate collision likelihood and decrease latency. The IEEE 802.15.7-2018 standard uses CSMA/CA, where the transmitter node needs to sense the channel before beginning transmission to ensure that it is idle. Figure 13 shows a block diagram of the random access mechanism. It consists of the following steps:

1. An initial waiting time *backOffPeriod* is chosen randomly following a uniform distribution as shown in Equation (3.4).

$$backOffPeriod = aUnitBackoffPeriod \cdot U(2^{BE}) \tag{3.4}$$

   aUnitBackoffPeriod defines the minimum back-off period while the Back-off Exponent (BE) determines the width of the uniform distribution $U(\cdot)$, which ranges from 1 to 2^{BE}.

2. After waiting for *backOffPeriod* optical clocks, the user node senses the channel before transmitting as CSMA/CA suggests. In case of being unable to transmit, a failure is assumed, and a re-transmission is scheduled.

3. If the channel is free, it will transmit and wait for an ACK response to assess that the packet has been correctly delivered.

4. When an unsuccessful transmission happens (ACK not received, or channel occupied, e.g.), a counter named Number of Backoffs (NB) is increased. NB is used for limiting the number of transmission attempts. Furthermore, the BE also increases (up to an upper boundary named *macMaxBE*), rising the maximum possible waiting time.

The back-off mechanism is the most studied part of the MAC layer because it limits the data rate and improves the network reliability. Nonetheless, it is fundamental to evaluate the association process and back-off algorithms during the same network simulation with high node mobility. The association process begins when an unassociated node detects a beacon. After a random period, it sends an association

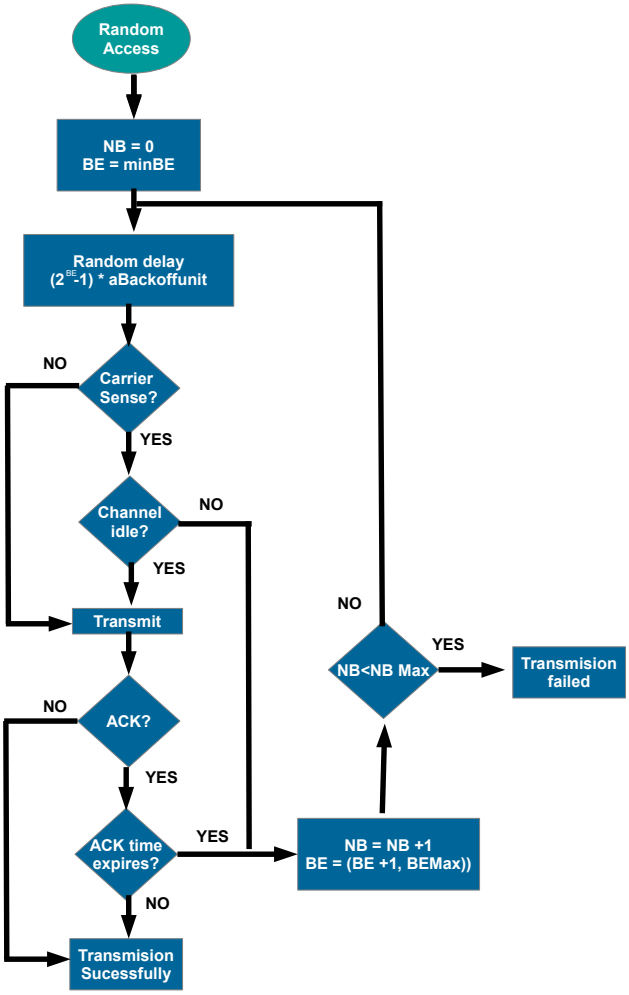

Figure 13: The back-off algorithm during CAP of standard IEEE 802.15.7.

request during CAP. The coordinator immediately sends an ACK frame to inform that the request has successfully arrived. At the same time, the coordinator sends a request to higher layers to determine source availability. When the ACK frame arrives at the node, the *macResponseWaitTime* counter is initialized. This time is longer than the ACK time because the resolution of the association request depends on several aspects, such as scheduling algorithms or even the availability of network-related task time. When the request is resolved, a response arrives at the coordinator. It adds the new node's address to its associated nodes' table and sends the corresponding association response command to the node. The node stores its address and starts to use the network. Figure 14 describes the association process of a new node in the network. The coordinator can expel users using a disassociation notification. This situation happens when the network cannot provide communication to the users anymore or there is a notification from an upper-layer. The standard does not define how the coordinator must physically communicate with

upper layers or the specific frame formats.

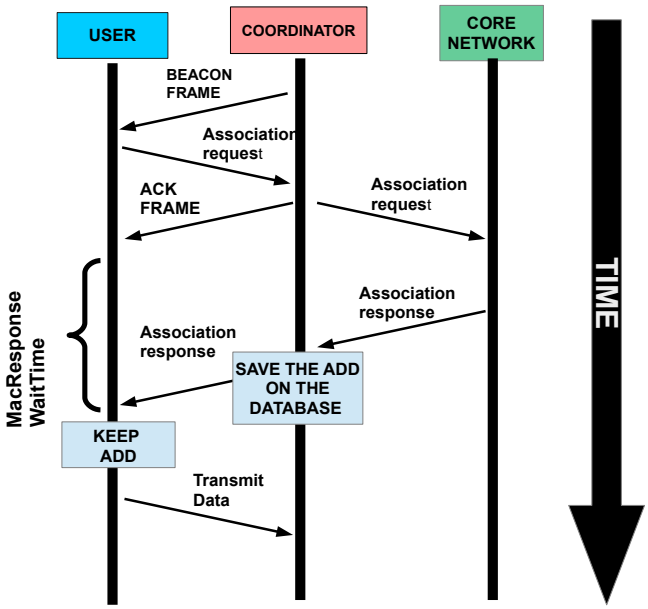

Figure 14: Association process of a new node in a VLC network.

As mentioned before, the frame format of the MAC layer is PSDU. It is located inside the PPDU frame format as its payload. PSDU provides information to the node about the MAC detains and contains the information to be delivered in upper layers. Figure 15 shows the relation between PSDU and PPDU. Additionally, it shows some of the most relevant fields on the PSDU header known as MAC Header (MHR). The frames in the MAC layer are classified according to their purpose. There are five types of MAC frames: Beacon, Data, Acknowledgment(ACK), Command, and Color Visibility Dimming (CVD). Each type of frame presents slight variations on the PSDU format. A brief description of each type of frames is provided next:

1. A Beacon is a specific frame transmitted only by the coordinator. It synchronizes the start of the superframe and provides information about the frame distribution.

2. The data frame is used to transfer the data in all modes. This frame originates from the upper layers.

3. The ACK frame communicates a successful transmission to stop the back-off mechanism.

4. The command frame executes any protocol or requests any permission. It is also a way to provide extra information for decision-making.

5. The CDV frame compensates for the sensation of color when the communication uses a CSK modulation scheme. It only contains a pattern to control the illumination as a payload.

Figure 15 shows the general frame format that is compatible with all these types of frames. This MAC frame is then passed to the PHY as the PHY service data unit (PSDU). One of the relevant fields is frame control which specifies the type of frame and some communication parameters. Between the parameters established by Frame Control fields we can mention the type of frame, the length of destination and source address(16 bits/64 bits), and the need of acknowledge response, among others. Another relevant piece of information is the sequence number used to match ACK frames with their respective Command/Data frame. Meanwhile, the Address Fields determine the destination and provide the retailer information.

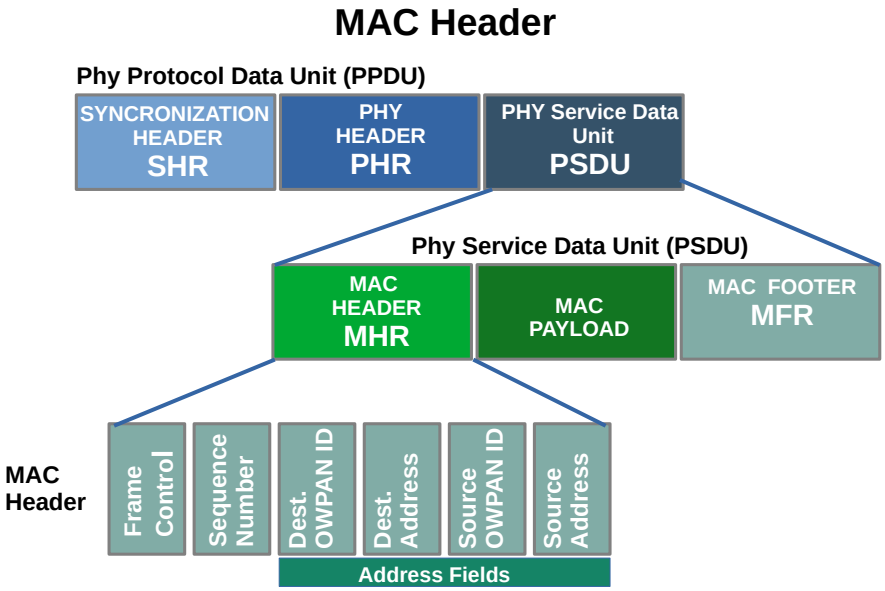

Figure 15: General IEEE 802.15.7 MAC frame format (PSDU)

Chapter 4

Realistic VLC MAC simulations

The analysis of the previous chapter shows that the IEEE 802.15.7 MAC layer provides the tools and procedures to support the VLC network operation. A crucial part of this wireless network is to achieve a steady connection when the user moves over a large area with multiple APs. The mobility of the user raises a fundamental problem in a VLC network due to the small size of the AP coverage area. The mechanism that supports the user's mobility is known as handover. However, the ongoing standard does not provide a concrete solution for handover, but it just gives a few suggestions without shaping a complete procedure. Therefore, designing a solid handover strategy for a mobile VLC network is an open research problem.

4.1 Fundamentals

The challenge of a handover scheme is to elaborate a comprehensive solution (PHY and MAC layer) that provides the network with the capacity to transfer a user session from one AP to another when it changes its position avoiding abrupt disconnections. This solution needs to recognize the user movement and execute the necessary procedures in advance for enabling the connection to the adjacent site, minimizing the time of the entering process. Therefore, it becomes elemental to understand the system requirements and design a solution that fits the network properties. As described in Chapter 2, the handover stages include the detection phase, which is fundamental to trigger the handover process. The RSS indicator is a typical signal used for this decision due to the low latency and less complex process. A functional detection algorithm that estimates when a user is leaving the AP covering area requires the characterization of the time-varying communication link. After that, it is necessary to evaluate the operation of the handover strategy by considering the scenario description, the properties, and the limitations of VLC technology. In addition, the execution of the handover protocol can be affected and interrupted when multiple users share the network resources. Moreover, in dynamic scenarios such as vehicular environments, the conditions of the communication channel may change during the execution of the protocol. Therefore, it becomes necessary to test the protocol in a deployed network.

In the literature, several works have studied and validated some mechanisms in the MAC layer of the VLC IEEE 802.15.7 standard using an analytical methodology, such as Markov chains with queue models. The scientific community interest has been mainly focused on channel access mechanisms to quantify the average latency and collision probability. These methods divide the Markov chain structure into the different states of the transmission scheme, such as back-off, transmission, Carrier Sense, Ack states, and so on, [105, 102]. Unfortunately, the complexity of this methodology grows with the number of users and makes it unlikely for large-size networks. The problem worsens when re-transmission schemes require an additional dimension [106]. Another drawback is that this methodology considers a lossless channel ignoring the link degradation during the transmission. Thus, it can not provide precise results in dynamic scenarios when the communication channel changes continuously.

System-level simulations platforms, known as event-driven simulations, represent a viable option to validate a handover protocol. They perform trustful validation by emulating the interactions and decisions during the protocol's executions. At this early stage, it is more plausible to start the evaluation of the handover protocol using a simulator tool rather than an experimental approach. However, this methodology needs to develop the simulation tools to carry out these evaluations. Furthermore, it is possible to incorporate a realistic channel model to improve the results. This flexible tool can assess different network features (latency, frame-error rate, collision rate, the average number of transmissions, among others). The procedure of Monte Carlo simulation with Ray Tracing (MCRT) is used to incorporate the channel model into the handover protocol. It is a well-known methodology adopted by the scientific community to characterize optical wireless channels. The fusion of MCRT and the network evaluation improves the accuracy of the results. Additionally, MCRT working in standalone mode provide the essential information to design a functional detection algorithm based on RSS. This chapter presents a detailed description of these simulations tools.

4.2 Network Simulation

A system-level simulation platform for vehicular VLC can be built using the network simulators OMNET++, NS-2, OPNET, Prowler, and others. The main advantage of these simulators over C++ language-based platforms is that they provide tools to simulate the events execution time of the protocols. These tools organize the execution time sequence of the programmed object that represents the nodes during the emulation of the protocol. The simulation platform manages the time that each node executes an action, allowing the evaluation of interference situations and other possible problems in the communication. This network simulator can also provide interfaces to scale the number of nodes and layers. Thanks to this, the simulator can reproduce complex networks.

The challenge of the handover process for vehicular VLC networks comes from the limited understanding of the VLC technology applied in mobile networks. As a result of the relative novelty of VLC technology, traditional network simulators are a

limited resource because of the lack of software libraries. Moreover, existing VLC network simulators use either MAC-layer elements [101], or physical channel elements [107]. Therefore, as part of this thesis, we introduce our software libraries for the procedures of both MAC and Physical layers. This framework provides the easiness to adopt the simulations to the proposed handover solution during the system design process. A comprehensive VLC network simulator evaluates the transmission process by considering the MAC-layer of the IEEE 802.15.7r1 standard and an accurate and dynamic channel impulse response. The MAC-layer mechanisms have been developed with OMNET++ while the optical wireless channel impulse response has been calculated using the MCRT algorithm [108]. The resulting simulation platform allows to accurately evaluate the performance of VLC networks, taking into account both LOS and NLOS contributions on each node.

Figure 16 illustrates the structure of the developed VLC network simulator. It comprises two main modules that reflect both the coordinator and the nodes. Each of these modules consists of two parts. The physical layer submodule evaluates the communication performance according to the link's characteristics (accurately obtained using the MCRT algorithm). Meanwhile, the MAC control submodule applies the logical procedures of IEEE 802.15.7r1 and considers time synchronization.

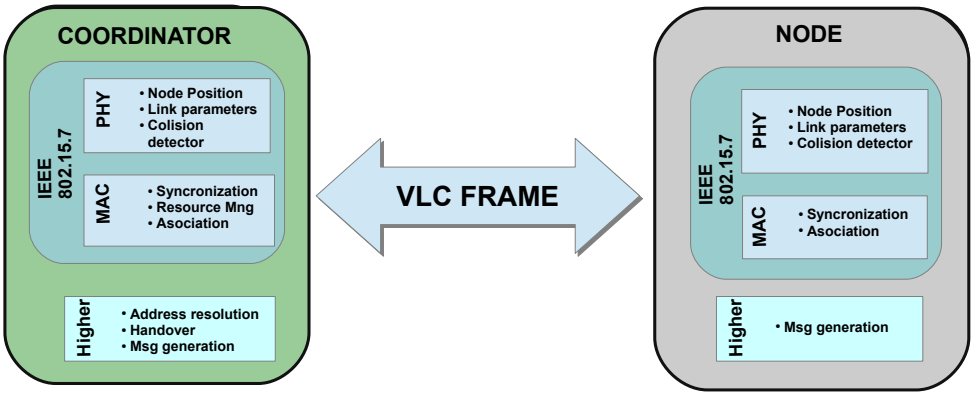

Figure 16: Structure of the developed simulation platform.

An OMNET++ model consists of a hierarchical organization of modules that performs some tasks of the communication nodes. The main modules representing the entire nodes are split into smaller modules with simple tasks. The small modules are associated with a C++ file, and a NED file, while the complex modules only have a NED file. The C++ file contains the behavioral description of each node. On the other hand, the NED file describes its organization and allows simulation parametrization without modifying the C++ file. Specifically, a complex module for the coordinator and another for the user node have been developed in this work. The setup of these two modules includes the MAC and PHY parameters such as BO, SO, the optical clock, the node location, and the transmitted power, among others. These values are modified in the parameters section of each node's NED file. Furthermore, the network organization is described in a separate NED file where the nodes (coordinators and users) are included and connected. At the same time,

the nodes exchange information using a developed special object-oriented program called "Message" that symbolizes the frame transmission. The simulator includes a customized "message" object that adds the most relevant fields of the headers from the PSDU frame format, as defined in the IEEE 802.15.7 standard. Figure 17 shows the format used in the simulations. Additionally, this message has extra information that provides more realistic simulations.

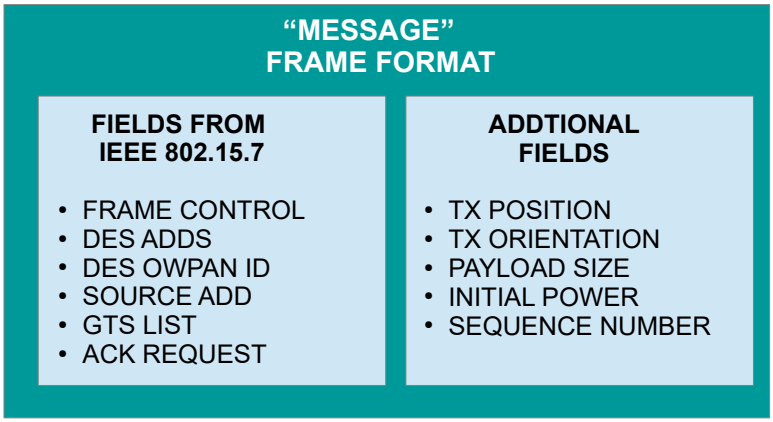

Figure 17: "Message" structure of the frame format in the simulation.

4.2.1 Physical Layer sub-module

Figure 18 describes the structure of the PHY layer sub-module. This sub-module evaluates the communication link using the MCRT algorithm, which considers the spatial distribution of the Tx and RX. Every time the Network simulator requires the CIR, it communicates to the MCRT throughout a communication socket. Then, it updates the nodes' spatial information to proceed with the channel simulation of a single communication link. A description of the MCRT algorithm is presented in Section 4.3. After finishing the channel evaluation, the MCRT calculates the bandwidth restriction and DC channel gain and communicates this information. DC channel gain is used to get the frame's received power. Then, this value is compared to the endpoint sensitivity. If the power is lower than this threshold, the module marks the packet as lost. After that, the bit error rate (BER) and frame error rate are computed using the frame length, the received power, and the modulation scheme information. The BER can be easily calculated using the Signal-to-Noise Ratio (SNR), which depends on the configuration of the VLC PHY transmission mode. For a given packet length N_{packet}, the number of errors N_e in the frame follows a Binomial distribution (Equation 4.1).

$$N_e \sim B(N_{packet}, BER) \tag{4.1}$$

Depending on the error-correction scheme used in the transmission mode, the packet would be marked as correctly received or not, informing the upper layer. The PHY

layer decides when a frame was successfully transmitted using the probability models. Finally, the collision detection block retains the packet to ensure that the communication is not interrupted. This block holds the frame during its transmission period. If another packet arrives during this time, a collision occurs, and both packets are discarded. Then, a new waiting time is estimated considering the end time of the latest transmission. This period depends on the frame size, the optical clock duration, and the used modulation scheme. The frame is delivered to the MAC layer sub-module when the waiting time expires without a collision. The PHY sub-module additionally updates the node positioning if necessary. It is important to clarify that this sub-module processes any frame regardless of its source or destination address.

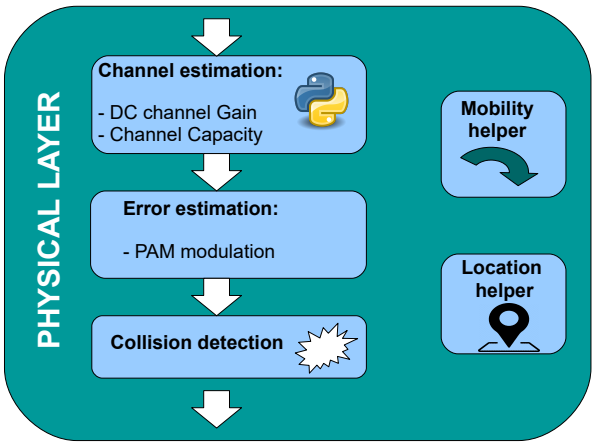

Figure 18: Block diagram of the Physical layer sub-module.

4.2.2 MAC layer sub-module

The MAC layer sub-module is in charge of the logical decisions that the nodes make during the protocol execution. Figure 19 illustrates the organization of this sub-module. Firstly, the MAC layer checks the data frame type when it arrives from the PHY layer. At this stage, the data frame is categorized based on its function (Data, ACK, Command, or Beacon). Then, it is redirected to the corresponding block to be properly processed. The coordinator and user nodes behave differently. One of the most relevant discrepancies is in the synchronization block. The coordinator's sync block transmits a beacon frame continuously to provide a time reference to the users, while the user's sync block receives these beacon frames and operates accordingly. The sub-module stays idle when a beacon is not received (due to collisions or poor channel performance). After that, the command frames are dispatched to the MAC control block. The actions performed by this block depend on the message, which is related to different mechanisms of the standard described in Section 3.3. On the other hand, data frames are handled simultaneously by the temporal Filter block and the ID control block. The temporal Filter block verifies that the user packets are in the correct superframe window. The sub-module discards the packets when they arrive outside the superframe window. The ID control block verifies the

destination and source addresses to check if the node will process the information. Additionally, the coordinator's block checks if the recipient is associated with it, in these cases, the AP serves as an intermediary. This frame is either sent using the VLC channel or passed to upper layers. At this point, the statistics generated during the packet transmission are collected. Finally, the Output Control block handles the data transmission and operates in CAP or CFP mode according to the user's resources. When this block operates in CFP mode, it executes CSMA/CA mechanism, including the random back-off and queues packets.

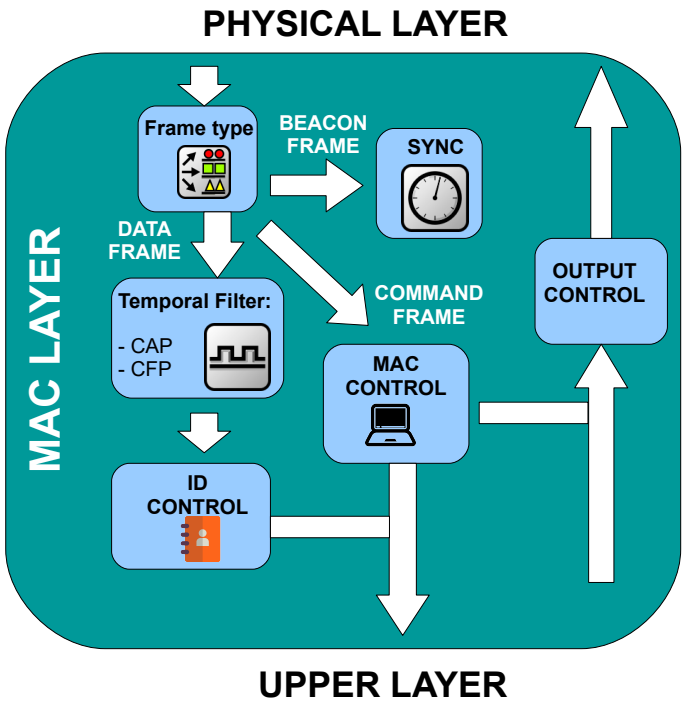

Figure 19: Block Diagram of the MAC layer sub-module.

4.3 VLC Channel

As in any other communication system, realistic channel modelling is a key for VLC system analysis and testing. There are different approaches to approximate the impulse response of an optical wireless channel. As mentioned before, the MCRT approach is used here to evaluate the optical wireless channel of the vehicular VLC network. Using the MCRT method to model the propagation of the optical signals will improve the accuracy of the VLC network simulations. This section gives the necessary background to understand the MCRT technique.

4.3.1 CIR Computation via the MCRT Approach

The optical channel can be modeled as a lineal system described by the Channel Impulse Response (CIR). The CIR is defined as a combination of a direct line-of-

Sigh (LoS) component, $h_{LoS}(t)$, and multiple non-line-of-sight (non-LoS) reflections in each k surface, which can be expressed as

$$h(t) = h_{LoS}(t) + \sum_{k=1}^{\infty} h^k_{non-LoS}(t) \tag{4.2}$$

where $h_{LoS}(t)$ models the LoS contribution of the channel that comes from a direct path of the emitter to the receiver and $h^k_{non-LoS}(t)$ the response of the ongoing reflections from the k-th surface. The LoS response of the channel is defined as

$$h_{LoS}(t) = \frac{R_E}{d^2} A_{eff} \delta\left(t - \frac{d}{c}\right) \tag{4.3}$$

the term R_E denotes the model of the far-field radiation pattern of the emitter, A_{eff} the effective area of the receiver, $\delta\left(t - \frac{d}{c}\right)$ is the time shifted Dirac delta function with d as the distance between transmitter and receiver and c the speed of propagation of the signal. The total effective area of the receiver, A_{eff}, is given by

$$A_{eff}(\theta) = A_R cos(\theta) rect\left[\frac{\theta}{FOV}\right] \tag{4.4}$$

where A_R is the receiver area, θ the incidence angle and FOV the Field of View. The incidence angle is obtained from the light source position and the receiver surface's norm vector. Finally, $rect$ is a function that is unity inside the FOV range and zero outside this range.

The components $h^k_{non-LoS}(t)$ in equation (4.2) are given by the statistical Monte-Carlo model with ray-tracing as was commented before proposed by Lopez-Hernandez [109]. This approach assumes any optical source emits its light similarly to particles with random linear trajectories as the rays. The total power's source is distributed in the number of rays. When these rays impact a scenario surface, it generates a new light source. To reduce the computer resources needed to do a precise estimation of CIR, the simulator uses a variant of the model proposed by Lopez-Hernandez known as modified MCRT algorithm [110]. In this variant, each new light source adds a deterministic LoS contribution. The impulse response detected by the receiver due to the reflection of order k can be approximated by Equation (4.5). This model present a better approximation of the real CIR when there is a high number of N rays and K rebounds. Each rebound generates a reflection pattern $R_{K(i)}$ of the i-th ray's last rebound $K(i)$ at the corresponding angle, while ρ_j is the reflectivity of the j-th surface. It is important to mention that A_{eff} depends on the income angle from the k reflection point.

$$\sum_{k=1}^{\infty} h^k_{non-LoS}(t) \approx \sum_{i=1}^{N} \sum_{k=1}^{K} \frac{1}{N} \left(R_{K(i)} \prod_{j}^{k} \rho_j\right) A_{eff}(\theta_{k,R}) \frac{1}{(d_{k,R})^2} \times \delta(t - t_k) \tag{4.5}$$

The trajectory time is the sum of the traveled distance of the optical signal over the propagation speed c, as can be seen in Equation (4.6). The calculation considers the distance between each reflection point $d_{j-1,j}$ and the last bound with the receiver $d_{k,R}$

$$t_k = \frac{d_{k,R}}{c} + \sum_{j=1}^{k} \frac{d_{j-1,j}}{c} \tag{4.6}$$

For simplicity, $R_{K(i)}$ models a Lambertian emitter, *i.e.*

$$R_{K(i)} = \frac{n+1}{2\pi} P_E cos^n(\phi), \quad 0 \leq \phi \leq \frac{\pi}{2} \tag{4.7}$$

where n is the order of Lambertian emission that determines the lobe distribution, P_E is the emitter's power and ϕ is the emission angle.

The simulator has been divided into three main parts: pre-processing, MCRT calculation, and post-processing. During the pre-processing stage, an OCTREE (octal tree) structure is inflated using a triangularized mesh file of the scenario (.obj file) to render the scenarios surfaces on the simulator. Additionally, a table with the surface's material description is added with the reflection coefficient and reflection pattern. The use of this structure enhances impact calculation performance since it implements a logarithmic-complexity search algorithm. Figures 20 and 21 show the channel propagation model for the MCRT and the algorithm adopted for its implementation.

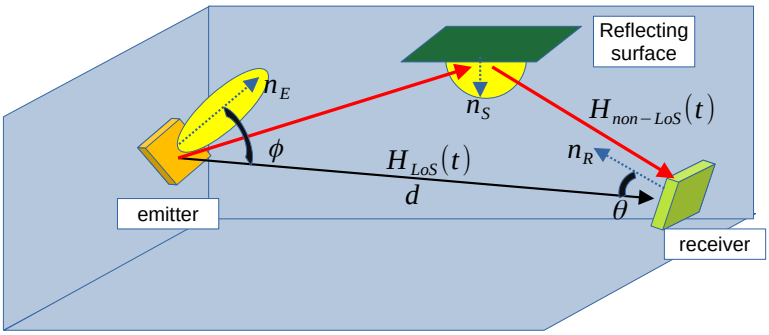

Figure 20: MCRT propagation model.

The next step after calculating the CIR is the post-processing stage to translate the results into metrics and estimate the communication performance. A useful metric is the Signal-to-Noise Ratio (SNR) which can be formulated at the output of a PIN photodiode as follows

$$SNR = \frac{(P_{tx} H(0) R_\lambda)^2}{\sigma_{th}^2 + 2q(P_{tx} H(0) R_\lambda + i_d + i_b)B}. \tag{4.8}$$

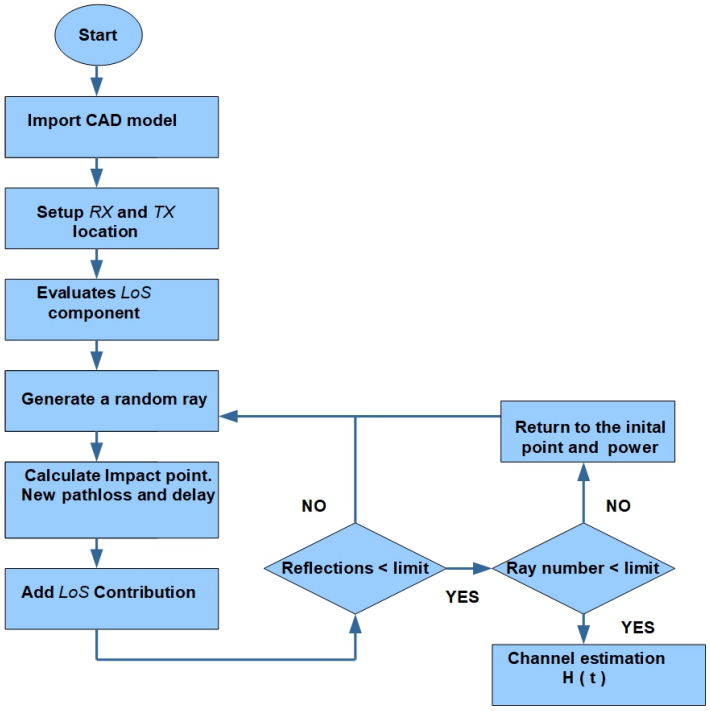

Figure 21: MCRT algorithm.

The above metric depends on the received power P_r described as

$$P_r = P_t * H(0) \tag{4.9}$$

where the DC channel gain of CIR $H(0)$ can be obtained as

$$H(0) = \int_0^\infty h(t)\,\mathrm{d}t. \tag{4.10}$$

In equation (4.8), R_λ is the responsivity of the receiver, σ_{th}^2 is Johnson noise, q is the electron charge, i_d is the receiver's dark current, i_b is the background-induced current, and B is the noise bandwidth of the receiver. In this case, the Johnson noise value is calculated as

$$\sigma_{th}^2 = \frac{8\pi k T_k}{G}\eta A I_2 B^2 + \frac{16\pi^2 k T_K \Gamma}{g_m}\eta^2 A^2 I_3 B^3 \tag{4.11}$$

where η is the fixed capacitance, G the open-loop voltage gain, Γ the FET transistor noise factor, T_k the environment temperature, k the Boltzmann's Constant, and I_2 and I_3 are the Noise Bandwidth Factors. The parameters and noise model were based on [107], where the model was experimentally validated. The table 3 presents the parameters values used in this work for the SNR estimation.

Parameter	Value	Parameter	Value
R_λ Resposivity	0.2 A/W	q electron charge	$1.60217e^{-19}$ C
i_d receiver dark current	0.562	I_B background current	$1.13e^{-6}$ A
B Noise Bandwidth	300000 b/s	i_d dark current	10 nA
G Open Loop Voltage Gain	10	η Fixed capacitance	112 pF / cm2
T_k Temperature absolute	298	Γ FET channel noise factor	1.5
I_3 Noise Bandwidth Factor	0.0868	g_m FET transconductance	30 mS
I_2 Noise Bandwidth Factor	0.562	k Boltzmann's Constant	$1.3806e^{23}$ J/K

Table 3: Parameters for the SNR calculation

Another important restriction on the VLC system is the bandwidth limitations, the wall reflections can cause some critical points where the bandwidth can diminish. Bandwidth is closely related to the delay spread τ_{rms} which is a parameter based on the power delay profile. The delay spread τ_{rms} represents the minimum time between symbols to avoid Inter Symbol Interference (ISI), and the calculation is given by

$$\tau_{rms} = \left(M_2 - M_1^2\right)^{1/2} \tag{4.12}$$

where

$$M_i = \frac{1}{H(0)} \int_0^\infty t^i h(t)\, \mathrm{d}t \qquad \text{for } i = 1, 2. \tag{4.13}$$

Therefore, an approximation of the channel bandwidth B is obtained as follows

$$B \approx \frac{1}{5\tau_{rms}}. \tag{4.14}$$

4.3.2 Integration of MCRT in the Network Simulator

This section describes the incorporation of the MCRT approach into the network simulator. Every time a simulated node receives a new "message", it needs to calculate the channel impact during the transmission. This task is performed by the Channel Estimation Block of the PHY submodule. However, it is necessary some changes regarding the basic scheme of MCRT which are described next.

Channel estimation is a process that consumes a large part of computer resources. If the channel conditions do not change, then it will not be necessary to perform the MCRT simulation every time a new frame arrives at the node. For this reason, the channel estimation block must store the DC channel gain and bandwidth restrictions for each network user regarding the node's link. The database is updated periodically with a programmable refresh time. The flexibility of this time allows evaluating the network according to its nature. For example, since the channel of an indoor network does not change significantly, it is not necessary to update it. Oppositely, the communication channel of a vehicular network is constantly changing, which

means that it needs updating (about every 1 ms). When the information does not need to be updated, the channel estimation block will check on a stored value and attach it to the frame representation. The BER is estimated in a subsequent block.

Figure 22 shows the modifications required in the MCRT as compared to Figure 21. Observe that the red blocks in the diagram represent the pre-processing stage. They render the scenario surfaces and initialize the simulator. The first two blocks in green indicate that the network simulator updates the node position. After that, the blocks in light blue denote the evaluation of the classical MCRT. Finally, the last two blocks in green correspond to the post-processing stage. After the channel evaluation, the MCRT calculates the bandwidth restriction and DC channel gain. Once the PHY submodule database has been renovated, the rest of the simulations proceed normally.

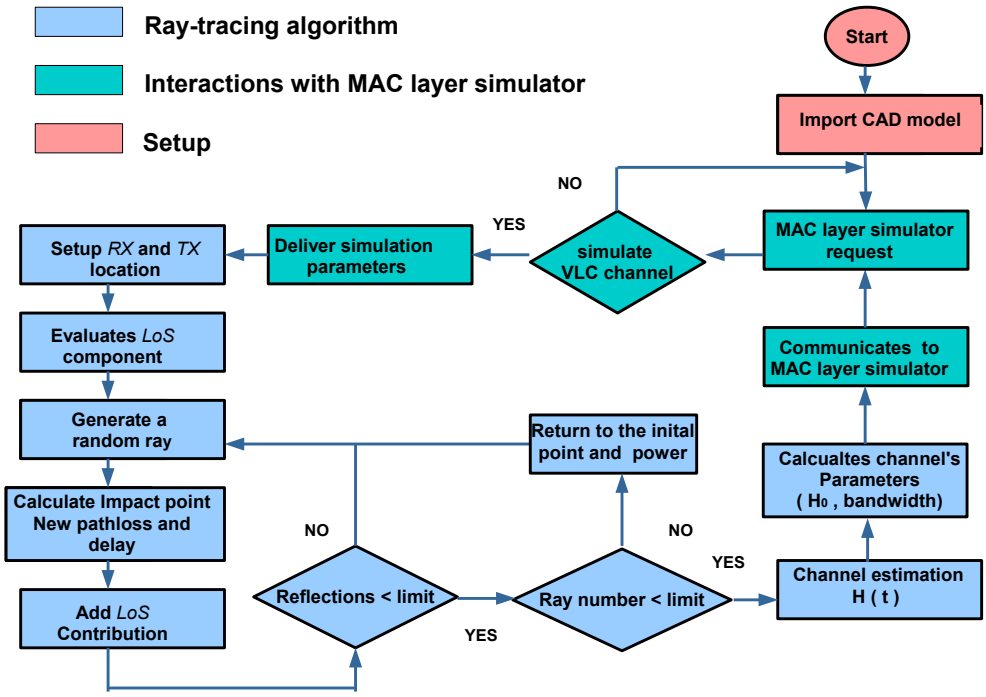

Figure 22: Flow diagram of the Monte Carlo Ray Tracing algorithm for physical layer simulation.

Chapter 5

Experimental Validation of Network Simulation

As discussed above, the development of new libraries specially focused on VLC technology for network simulations platforms, such as the OMNET++ platform used in this thesis, was because most optical network simulators do not consider the effects of the channel on the MAC protocol performance. Indeed, no MAC layer-related work considers the link's $h_{non-LoS}$ contribution during the network evaluation. Consequently, it limits the scenarios that can be properly evaluated with these tools and the accuracy of the obtained results. Additionally, a poor channel model results in incorrect coverage area estimations, influencing the network performance evaluation. This is because there are some cases where communication is possible through the surface's reflections. And this phenomenon can only be considered with a precise VLC link model, including NON-LOS contributions. The channel access scheme is one of the most affected mechanisms by this supposition. The nodes with CSMA/CA schemes scan the channel to see its availability. For example, in a typical indoor VLC network, the coordinator is integrated into a luminary placed in the room's ceiling while the nodes are located below. This situation makes that most of the nodes do not have a FOV contribution. Other VLC network simulators assume that the users can not sense the channel in these circumstances. However, in reality, this result could differ depending on the exact scenario conditions.

The developed simulation tool shows that the integration of MAC and PHY layers provides more insight into the performance of IEEE 802.15.7. This chapter presents a set of experiments that explore situations where a realistic channel model presents different network performance results. Firstly, the chapter explains the setup details, then, the methodology and metric for evaluating the network performance are described, and finally, the results are discussed.

5.1 Experimental setup

To validate the hypothesis that a better network performance estimation is obtained with the proposed simulation strategy, different physical scenarios have been taken into account. They consist of several network configuration, where each network deployment is used for evaluating different situations which are likely to occur in OWC, such as the effect of multipath reflections in the CSMA/CA scheme, or the hidden node problem associated with the receivers' limited FOV. The results were published in [111], this section describes the setup used.

Three different cases have been considered all of them are different configurations of where there is a VLC network composed of 1 coordinator node and 4 user nodes inside a 10 x 10 x 3 m^3 room. All the nodes have a receiver with a 1 cm^2 photodiode and FOV of 60°. The coordinator is at the room's geometrical center (in the XY plane) and the ceiling pointing downwards. The user nodes are set at 1 m height, and their transmitter and receiver are both pointing upwards. These nodes are located at the same radial distance regarding the coordinator's XY center. However, this baseline condition is slightly modified in each case under study. Figure 23 depicts the node distribution of each.

- **Scenario 1:** All the nodes are concentrated in a specific area of the room. This scenario forces a situation in which the user nodes can detect other nodes' transmissions from the optical signals reflected on the ceiling to operate using the CSMA/CA mechanism properly.
- **Scenario 2:** Network nodes are uniformly distributed on a circumference, forming a square. In this case, depending on the radii the user nodes will be aware of other nodes or not, since the distance reduces the received signals power.
- **Scenario 3:** Three nodes are closely located whilst the other one is in the opposite direction. This situation is proposed to see the impact of a single hidden node on the network's performance.

As it was aforementioned, at short distances the reflection allows the correct execution of the MAC mechanisms. Nonetheless, as the nodes increase their distance, the path loss may become too high, lowering the received signal below the endpoint's sensitivity. Figure 24 shows the channel gain for the communications link between two nodes in scenarios 3, using the parameters of Table 4 in the developed simulator.

The number of rays used for the MCRT-based simulation in the channel estimation process determines the results accuracy. One of the strengths of the MCRT scheme is that a contribution to the impulse response is forced after each rebound. Hence, it seemed straightforward that obtaining a relatively accurate estimation of both channel gain and bandwidth could be feasible with a reduced number of rays. To check this assumption, some simulations using the same layout as in Figure 24 were performed. As it can be observed in Figure 25, neither the DC channel gain nor the

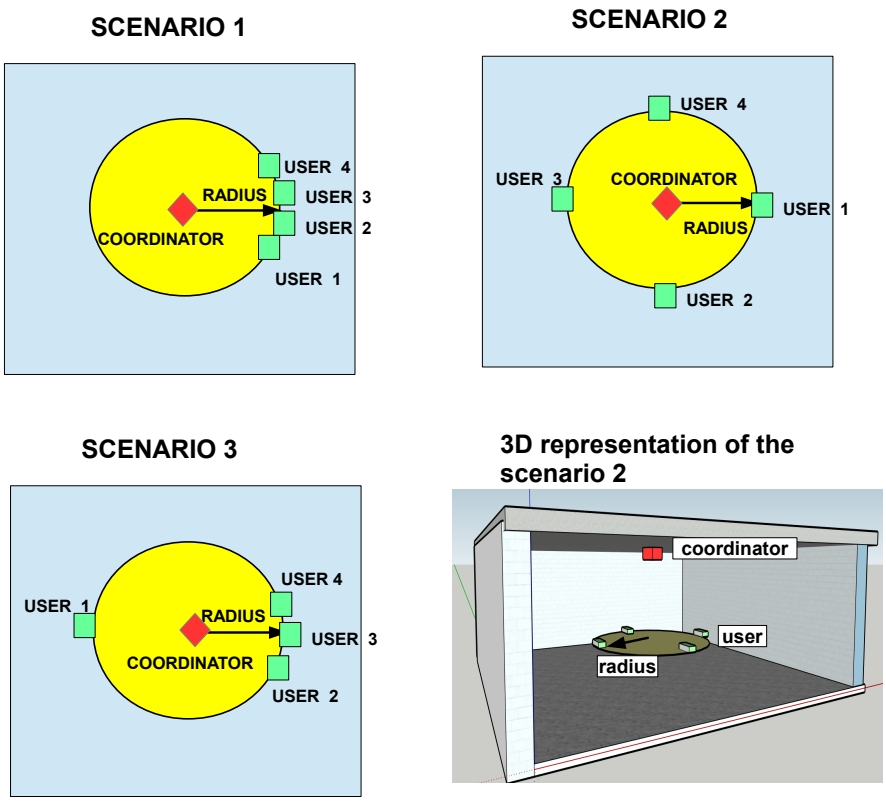

Figure 23: Graphical representation of the scenarios setup.

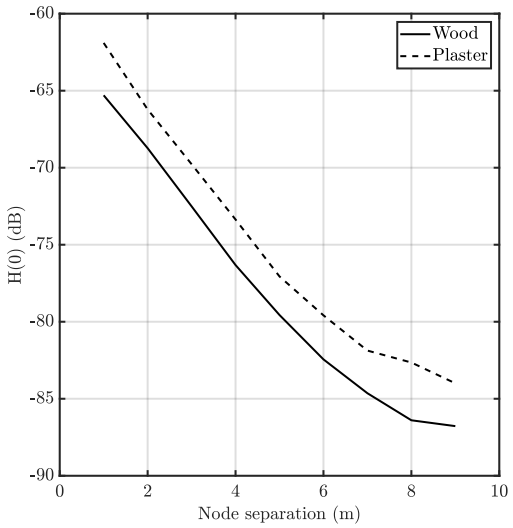

Figure 24: DC channel gain of the NLOS link between nodes at different horizontal distances for different materials in the ceiling (wood and plaster).

bandwidth changed substantially compared to simulations using a higher number of

Parameter	Value	Parameter	Value
Room size	10m x 10m x 3m	ACK length	50 bits
Room's material	Plaster / wood	Optical Clock	60 MHz
Reflection coeficient	0.75 / 0.4	Random time window for an assoaciation request	38 slots
Number of user	4	MAC response wait time	300 ms
Number of AP	1	Backoff Unit	200
Radii	0.5 to 4.5m	MaxBE	3
Number of ray in MMCRT	500	Number of Backoff	5
Reflections per ray	3	Number slots	16
Receiver area	1 cm2	Modulation	OOK
Receiver FOV	60	Code	8B10B
BO	6	Lambertian order (LED)	1
SO	6	Simulation Time	100s
Frame Payload	2000 bits	Coordinator power	200 mW
Frame Header	270 bits	Node power	50 mW

Table 4: Summary of simulation parameters. This table includes information about the scenario and both PHY and MAC layers.

rays (1000 and 5000). The estimated channel gain using 200 or 500 rays is practically indistinguishable from longer simulations. Nonetheless, bandwidth estimation is significantly different for the 200 rays case, whilst acceptable for the 500 rays calculation. Therefore, for the scenarios under consideration, carrying out the channel simulation using 500 rays is a trade-off between calculation speed and accuracy. In addition, despite the slight variation of the bandwidth estimation with respect to more accurate simulations, the presented error is sufficiently small for moderate horizontal node separations, which are the ones at which the CSMA/CA mechanism can physically operate taking into account the sensitivity of the endpoints.

Moreover, in order to properly characterize the network, both saturated and unsaturated traffic conditions have been tested. As it was used in other works [105][112], 70% of the maximum traffic capacity of the network was established as a threshold to determine the saturation condition. For the unsaturated network condition, the frame arrival rate (or frame generation rate) of the nodes corresponded to an exponential distribution with a mean time of 953.6 μs. These frames presented a payload of 2000 bits. Considering the ACK time, header size, and the amount of users, this configuration demands approximately 20.54% of the maximum manageable traffic. On the other hand, the saturated configuration presented a mean time of 100 μs, resulting in beyond-capacity necessities (195% of the maximum traffic). This *a priori* huge value was selected to keep a very demanding situation even when some of the nodes were unable to be associated.

Some parameters of IEEE 802.15.7, concretely the association parameters, were chosen according to other works [113, 114] since there is no guide or reference for them. The association request was sent randomly with a 38 slots window. This

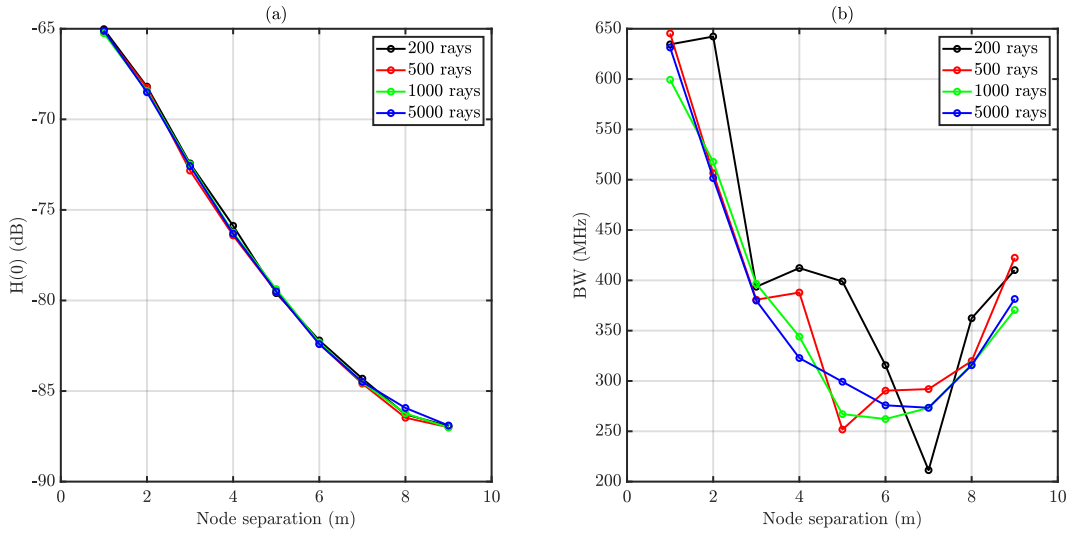

Figure 25: Impact of the amount of rays on the outcomes of the MMCRT simulation. (a) illustrates DC channel gain whilst (b) corresponds to bandwidth.

request must be completed before 300 ms, or the node assumes that it failed and repeats the operation.

5.1.1 Description of the validation procedure

In the three different scenarios evaluations, we have considered. As commented above, three different scenarios targeting, each one was evaluated for a range of radii (geometrical parameter of the scenarios). Furthermore, the analisys include two different ceiling materials, presenting different reflectivity coefficients, and two frame arrival rates (saturated and unsaturated traffic). The simulator was run 15 times in order to obtain statistically significant results, and the extracted metrics were compared to a MAC-only (no path loss) simulation. Considering all the different experimental setups 2,160 simulations were carried out in total. These simulations recreated the behavior of an IEEE 802.15.7 VLC network during 100 seconds, generating between $4{\cdot}10^5$ and $4{\cdot}10^6$ messages per simulation (depending on the simulation parameters). This huge amount of information is enough to obtain consistent statistical conclusions. The simulations were carried out without parallelization in a workstation with an Intel Core i7 (1.99 GHz) and 16 GB of DDR3 RAM. With these computational resources, each simulation was executed in approximately 50 seconds for the non-saturated traffic scenarios, whilst for the saturated traffic ones 170 seconds were spent per execution.

At the beginning of the execution, all the user nodes were marked as un-associated and all the internal variables of the simulation modules were set to their default state. Once the simulation started, the nodes began to perform association requests until they were properly notified by the coordinator node. After a successful association, each node started to generate 2000 bit packets (payload size) at the rate defined by the scenario under evaluation. Each event that occurred during the 100-seconds

simulation was logged into a file, describing the emitter, the receiver, the received power (if applicable), the event type, and a timestamp. All this information was used by the data analysis stage.

5.1.2 Data analysis

From the simulations obtained an elaborated information about the network configurations performances and main characteristic need to be generated. The metrics obtained from the simulation were collected as follows.

- **Throughput**. It is the aggregated traffic that arrives to the coordinator, and it was calculated as the amount of payload bits obtained from data frames divided by the simulation time.
- **Queued Packet Delivery Probability (QPDP)**. This is a measure of the network availability for those packets that have not overflowed the node's frame buffer. It is calculated as the total number of correctly delivered packets divided by the amount of queued packets.
- **End-to-end Packet Delivery Probability (EPDP)**. This measure is analogous to the previous, but it takes into account also the discarded packets due to excess of traffic on each user node. Therefore, EPDP should be strictly lower that QPDP since it is calculated as the total correctly received frames divided by the amount of generated frames.
- **Node active time**. This metric indicates the amount of time that a node has been correctly associated to the network. It is calculated as the difference between the timestamps related to periods in which the user node is correctly associated to the network.
- **Delivery time**. It is the time that the communication system spends to successfully deliver a frame. This measure is calculated as the difference between the timestamps of the first delivery attempt of a message and its correct reception.

5.2 Results

This section presents the results corresponding to the simulated scenarios for discussion and comparisons. The section is subdivided considering each one of the metrics detailed previously. The impact of the evaluated parameters on each metric is presented and in-depth discussed. Moreover, the results of the parametric hypothesis test on the impact of the ceiling material are presented in the final subsection.

5.2.1 Throughput

The network throughput is the result of aggregating all the correctly delivered traffic at the coordinator node. It is expected that situations in which the user nodes are capable of properly sensing the channel, this metric is maximized. On the other hand,

as the CSMA/CA performance gets impaired by an excessive link range between nodes (or even between coordinator and node), it is expected that the throughput decreases. Figure 26 depicts the obtained throughput for the two evaluated traffic conditions.

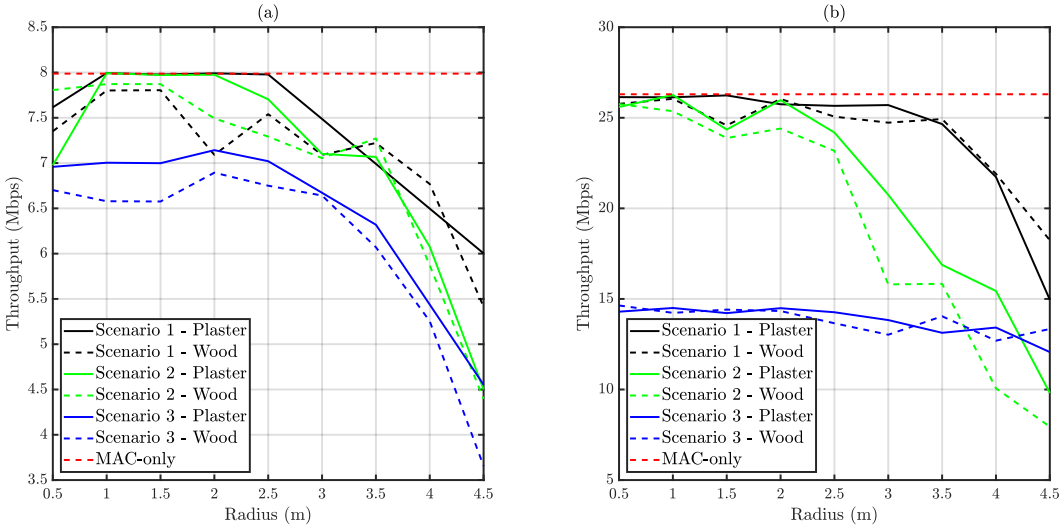

Figure 26: Obtained average throughput versus distance. (a) depicts unsaturated traffic whilst (b) corresponds to saturated traffic.

It can be observed that Scenario 1 presents a performance close to the MAC-only simulation for radius below 2.5 meters. The reduced link range between coordinator and user nodes, and the advantageous location of the nodes in terms of CSMA/CA operation contribute to this result. Scenario 2 presents a similar behavior, but the distance at which throughput starts to diminish respect to the MAC-only simulation is smaller. This occurs because the nodes, which are placed on a regular mesh, loss their mutual visibility before the coordinator-node link is affected by the geometry. Respect to Scenario 3, it is observed that it has the worst performance due to the presence of a hidden node. The commented trends apply to both traffic conditions, but the difference between Scenario 3 and Scenario 1 is sharper for saturated traffic than for reduced traffic necessities. This higher impact on performance is due to the effect of delivery probability, which is presented in the following subsection.

5.2.2 Delivery probability

In this subsection, two different metrics are presented. On the one hand, QPDP takes into account only those messages that were accepted in each node's buffer. On the other hand, EPDP also considers the discarded messages due to traffic overflow. As commented, EPDP must be strictly lower than QPDP. The relation between both metrics provides an estimation of the amount of traffic that is lost because of excessive buffering time. Figure 27 depicts QPDP, whilst Figure 28 illustrates EPDP results.

It can be observed that once a message is queued, the probability of correctly de-

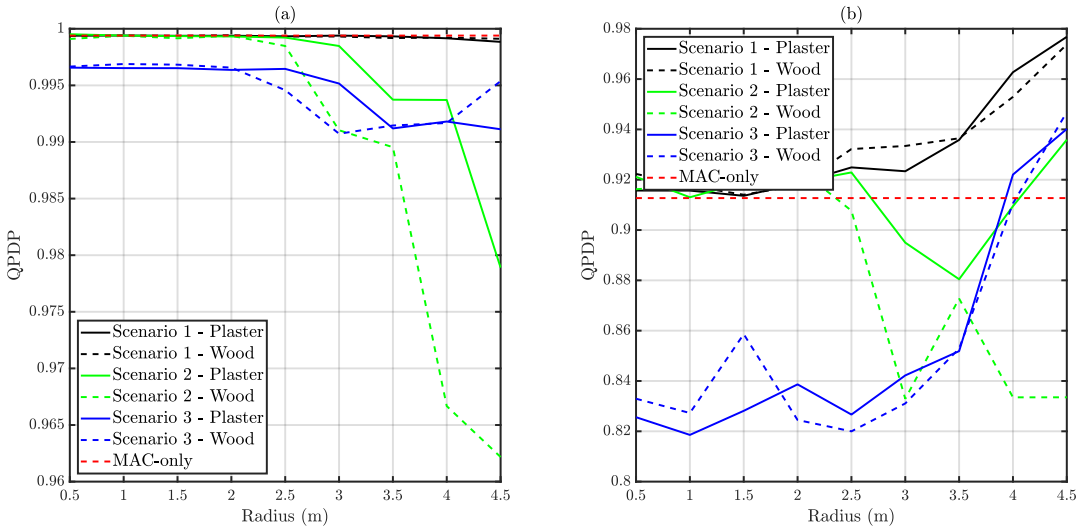

Figure 27: Obtained average QPDP versus distance. (a) depicts unsaturated traffic whilst (b) corresponds to saturated traffic.

livering it is above 82% in all the scenarios. In the case of unsaturated traffic, the impact of distance on this metric is very reduced, due to the number retransmissions. However, as it will be commented below, both delivery time and EPDP increased dramatically with distance. An increment on the delivery time would imply more channel resources per message, which may tend to a buffer overflow. It is also observed in Figure 27 that under saturated traffic conditions the QPDP is significantly higher for Scenario 1 than for the MAC-only situation. This exotic situation is derived from the increased disconnection probability at those distances. During some periods, due to the disconnection, the remaining nodes have more relaxed CAP restrictions.

As commented above, EPDP is smaller than QPDP. For unsaturated traffic, the trend is similar for all the three scenarios, presenting an EPDP around 0.9 at 3 meters. At this distance, the number of required retransmissions starts to be significant, and some traffic is lost at each node due to overflow. On the other hand, traffic-saturated scenarios presented EPDP values below the MAC-only reference simulation in all the cases. As commented during the throughput subsection, there are distances at which collisions may occur with a higher probability at each scenario. Moreover, the shape of throughput and EPDP curves are closely related as expected.

5.2.3 Node active time and delivery time

Node active time measures the time spent by a node in the VLC network, whilst delivery time indicates the time difference between a correct reception and the first try. Node active time is presented normalized respect to the simulation time. Hence, it corresponds to the network availability from the node's viewpoint. It must be taken into account that frame generation does not stop during disconnection periods.

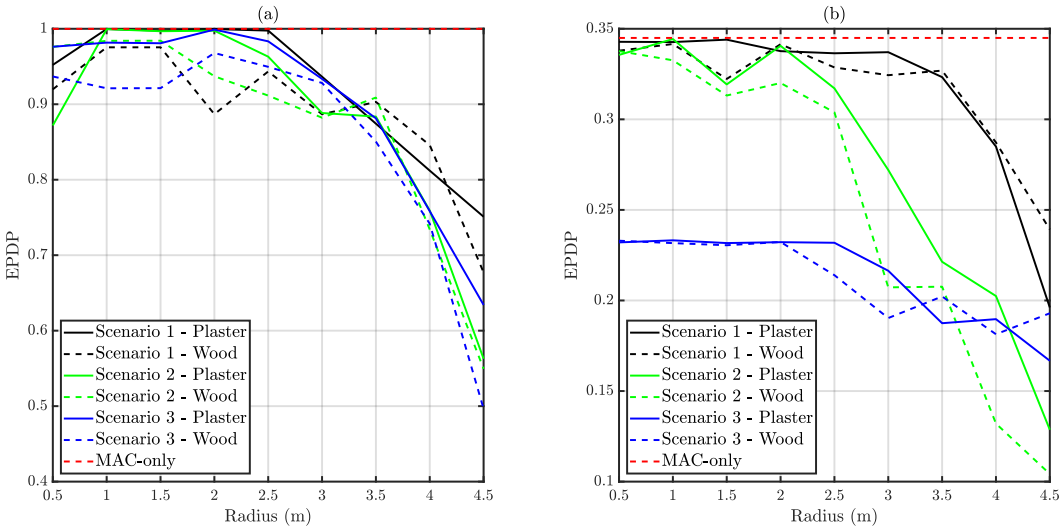

Figure 28: Obtained average EPDP versus distance. (a) depicts unsaturated traffic whilst (b) corresponds to saturated traffic.

Therefore, reduced node active times may incur also into a reduction of the EPDP due to packet losses. Figures 29 and 30 present the normalized node active time and delivery time respectively.

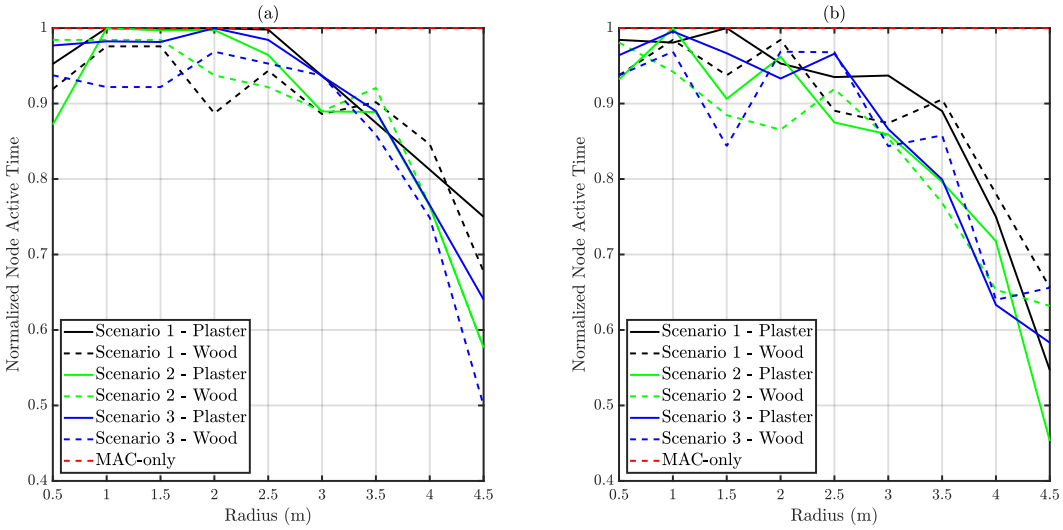

Figure 29: Obtained average Normalized Node Active Time versus distance. (a) depicts unsaturated traffic whilst (b) corresponds to saturated traffic.

Comparing saturated and unsaturated traffic conditions, it is observed that demanding traffic requirements affected node active time, slightly diminishing it. A larger collision probability due to extensive channel occupation led to an increased disconnection probability.

Regarding delivery time, it can be observed in Figure 30 that Scenario 1 conserves a

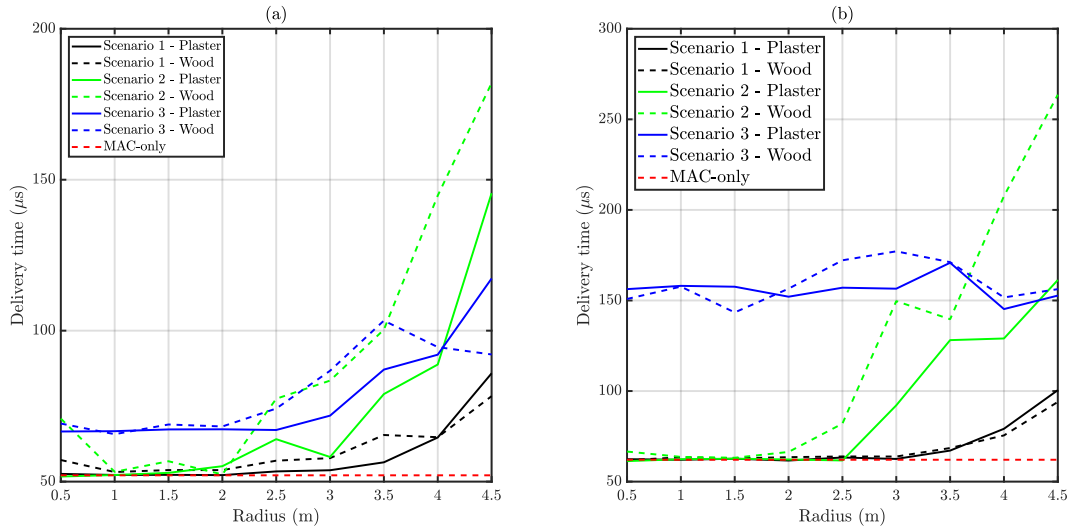

Figure 30: Obtained average Delivery Time versus distance. (a) depicts unsaturated traffic whilst (b) corresponds to saturated traffic.

good performance for all the link ranges, thanks to a proper carrier sensing. However, Scenario 2 loses performance beyond 2.5 meters approximately since the visibility between nodes is lost. This trend is broken in Scenario 3, which only has a single hidden node. In this case delivery time is conserved regardless the link distance. The minimum theoretical time a packet spends in the queue (considering the 50-slots buffer) is approximately 14 ms in this work. Depending on the application, the resulting overall latency (delivery time plus queue time) may be unacceptable, and GTS should be used instead.

5.2.4 Results conclusions

From the presented metrics results, we can deduce that the proposed simulation scheme with MAC and PHY integrated into the network performance evaluation provides more accurate and flexible results. Firstly, depending on the scenario, there are significant differences between our analysis and the obtained by other simulations, which consider only LOS links. And on the other hand, the proposed approach provides different results for each scenario allowing us to evaluate the advantages and drawbacks of each configuration in a precise way.

Chapter 6

VLC for vehicular tunnels

As the analysis of propagation channel characteristics is essential for all wireless communication technologies, a well-understanding of the communication channel is necessary to design an efficient handover strategy for vehicular networks. However, developing a universal handover solution is a challenging task that takes time. Due to time restrictions, this research project only studies the mobility problems of a VLC Network deployed in a vehicular tunnel. The selected scenario provides some desirable conditions in this initial research stage. Firstly, a vehicular tunnel is a controlled environment where a VLC network can operate without external interference, such as ambient light. Secondly, tunnels confine the vehicles' routes making it easier to predict the movement. Thus, estimating the user's destination and the appropriate time to begin the handover is simple. In addition, we note that the performance of the DSRC system is depleted in these scenarios when additional vehicles are moving in the area [115, 116]. As a consequence, ITS requires redundant communication for this type of environment.

This chapter, therefore, describes and analyses the vehicular VLC-based communication network architecture considered in this work. The scenario of application is a vehicular tunnel with two lanes and multiple VLC Road-Side Units (RSU). These units are integrated into the tunnel's luminaries, where the placement and characteristics of the illumination system follow the strict regulations of vehicular tunnels. At the same time, the dimensions of the tunnel's structure delimit the positions of the VLC RSU and vehicular node. Therefore, the channel conditions provide predefined patterns that simplify the studies. Moreover, the RSU Rx position also places a system's design problem due to the multiple options or degrees of freedom available for setting the receiver.

In the first part of the chapter, we are going to introduce the characteristics of the tunnel scenario. The second section presents the network structure. Then, we are going to describe the MCRT set up to evaluate the communication system. The fourth section shows the simulation results and debates their impact on ITS application. The final section discusses the conclusion from these results, and how they influence the network settings.

6.1 Vehicle Application Scenario

The main shapes of road tunnels are circular, rectangular, or horseshoe. In general, the highway's dimensions often remain the same regardless of the tunnel's type, while the walls and ceilings change based on the shape. For convenience, we model a rectangular tunnel scenario using the CAD tool. Figure 31 shows the two-lane tunnel scenario under consideration. We have considered a tunnel length of 15m, a wall-to-wall width range between 9 to 13.2 m, and a sidewalk of 0.5 m per side. The height of the tunnel range is 4.2 to 4.9 m [117]. We use the maximum dimensions in the CAD model to study the more demanding scenario, and the tunnel lighting regulations to define the maximum separation between the lamps, avoiding the flickering effect on the drivers. The distribution of the illumination lamps dictates the location of the AP along the tunnel.

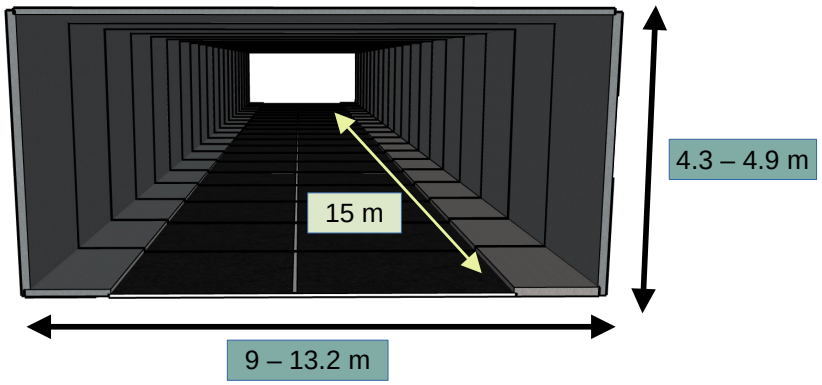

Figure 31: Dimensions of the two-lane tunnel scenario.

In [118], the authors presented some reports about the installation of illumination systems in tunnels. A typical location reported for the lamps is at 4.48m in height and assuming asphalt material for the floor and concrete for the walls. These materials' reflectance has already been studied in [119, 120] by considering the spectral distribution of a vehicle headlamp. For this work, we assume that the asphalt and concrete materials are Lambartian surfaces with reflectivities of 0.07 and 0.17, respectively.

6.2 VLC Network

The proposed VLC network in the tunnel scenario comprises multiple Access Points (AP) distributed along the tunnel. Figure 32 shows the block diagram of the described system. Each AP plays the role of an RSU updating the vital information to vehicular nodes in a specific area. These APs interconnect by an optical backbone, and the module called Aggregation Agent (AA) coordinates them. The VLC

network follows the structure of a star topology using IoT Device Management protocol (IDMP) that includes self-configurable devices [121]. The AA module has to deal with the main actions during the mobility process. Internally it has two virtual submodules named: Mobility Anchor Point (MAP) and Handover Manage Entity (HME). MAP registers the user credential and provides the vehicular node an internal address to locate it, and HME defines when to initialize a handover process.

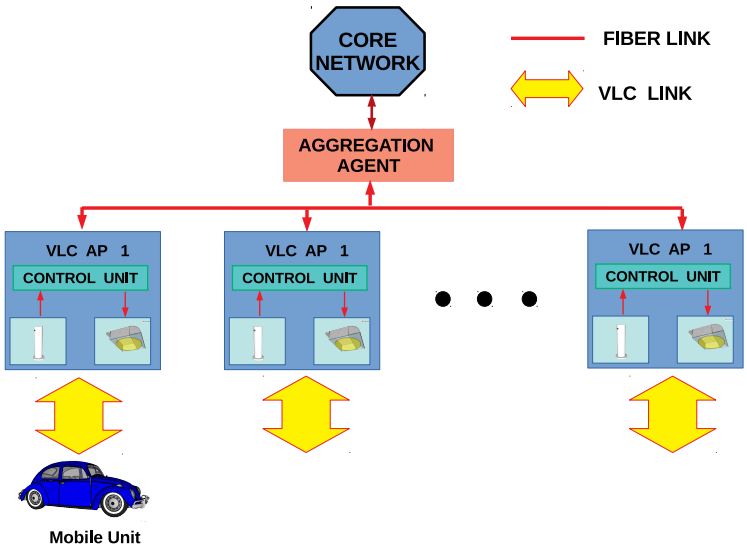

Figure 32: Diagram of the initial VLC network proposal.

On the other hand, ITS can access this network using the Mobile Unit (MU), a VLC module installed on the vehicle. Typically, the APs have their downlink and uplink endpoints in the same spot. In this work, however, we disaggregate these two endpoints. Figure 33 displays a representative image of the communication links. The downlink comprises a tunnel-mounted VLC transmitter (LED lamp) and a vehicle-mounted VLC receiver. The sensor is located on the middle point of the vehicle hood. On the other hand, the uplink consists of the vehicle's headlamp and an RSU close to the tunnel's wall. This receiver is located some distance (cm) over the tunnel floor, but several meters beyond the AP transmitter to get LOS signal from the vehicle lamps.

The luminaries distribution is compliant with the tunnel lighting normative, which conditions the AP coverage area. Moreover, Table 6.2 illustrates the relationship between the average vehicle's speed and the separation between the lamps to prevent flickering effects. The worst possible scenario happens when the spacing between APs is 12m (the largest), where the channel undergoes the highest DC channel gain variations.

The radiation patterns of the lamps (transmitters) in vehicular environments do not follow the typical Lambertian profile, which makes us perform some adaptations. Since a tunnel lamp needs to provide illumination in an extended area, its radiation profile has two main lobes instead of one. Meanwhile, the vehicle's beam headlamps

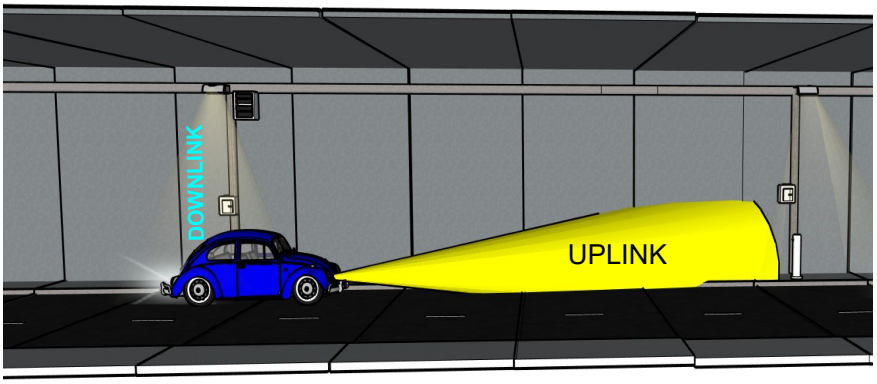

Figure 33: Conceptual image of the communication link of VLC system in vehicular tunnel.

Vehicle speed (km / h)	Max lamp distance (m)
50	5.6
60	6.7
70	7.8
80	8.9
90	10
100	11
110	12

Table 5: Max lamps distance to avoid flickering effects

are designed to cover a long way ahead and avoid affecting other drivers. Thus, these lamps possess some asymmetrical radiation patterns. In this work, we follow a realistic approach by using the characteristics of commercial light LED lamps. For the downlink, the tunnel lamp's profile of this work follows the technical datasheet of the Ariana lamp model used in Altel tunnel (Alicante, Spain) [118]. While the transmitter's profile in the uplink comes after performing some experimental measures using a Toyota Corolla headlamp. Figure 34 shows the resulted radiation patterns included in the simulations of the vehicular VLC network.

6.3 Channel Simulation Setup

This section describes the simulation setup to obtain the CIR of both downlink and uplink. It requires running the MCRT algorithm to yield the CIR when the vehicle is at different positions $h(d, t)$. The MCRT simulation engine launches 40,000 random rays from the optical source, each having a maximum of 3 rebounds.

We use a referenced Cartesian coordinate system to facilitate the comprehension of the distribution of the elements. The origin is the point at the beginning of the tunnel segment, in the right-down corner. The X-axis is the horizontal line along the

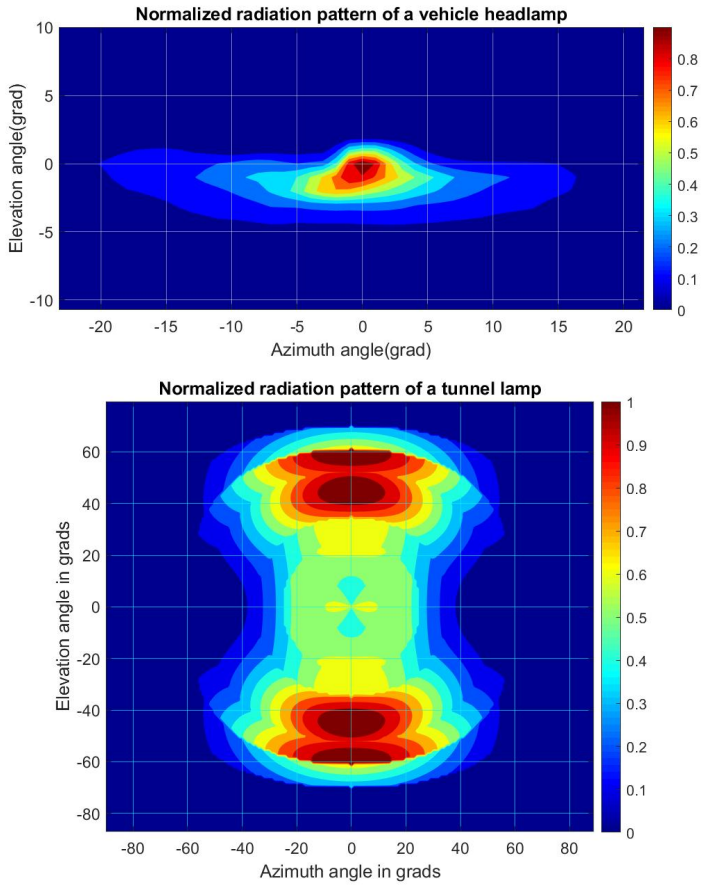

Figure 34: Radiation patterns of the vehicle's headlamp (top) and the tunnel lamp (bottom).

width of the tunnel, Y-axis is the length of the tunnel, and the Z-axis is the height of the tunnel. The system's uplink and downlink are independent channels that require two different simulation configurations. For the downlink simulation, we use two different transmitter configurations: the lamp on the tunnel's center pointing downwards (Case 1) and pointing on the sides with an elevation of 45° (Case 2). Regardless of the case, the lamps are 4.4 meters in height. Figure 35 illustrates the simulated downlink scenario. The CIR is obtained using a photodiode-based receiver of area 7.6 mm^2 and 68° of Field Of View (FOV) pointing upwards in the XY plane, at 1 m height.

Since the uplink communication implies the V2I scenario, the simulation needs to consider the vehicle's movement. We take advantage of the scenario's geometry to place several receivers close to the tunnel's wall. Using this approach, all the CIR values of $h(d,t)$ can be obtained in a single run of the MCRT algorithm. The transmitter points slightly tilted (85° elevation and -5° azimuth) concerning the tunnel's direction at 3 meters from the wall. This configuration represents the maximum distance between the edge of the lane and the closest wall according to [117], which is the worst possible case in the uplink. The orientation of the lamp corresponds to the actual vehicle's headlamp orientation. The receiver points to the

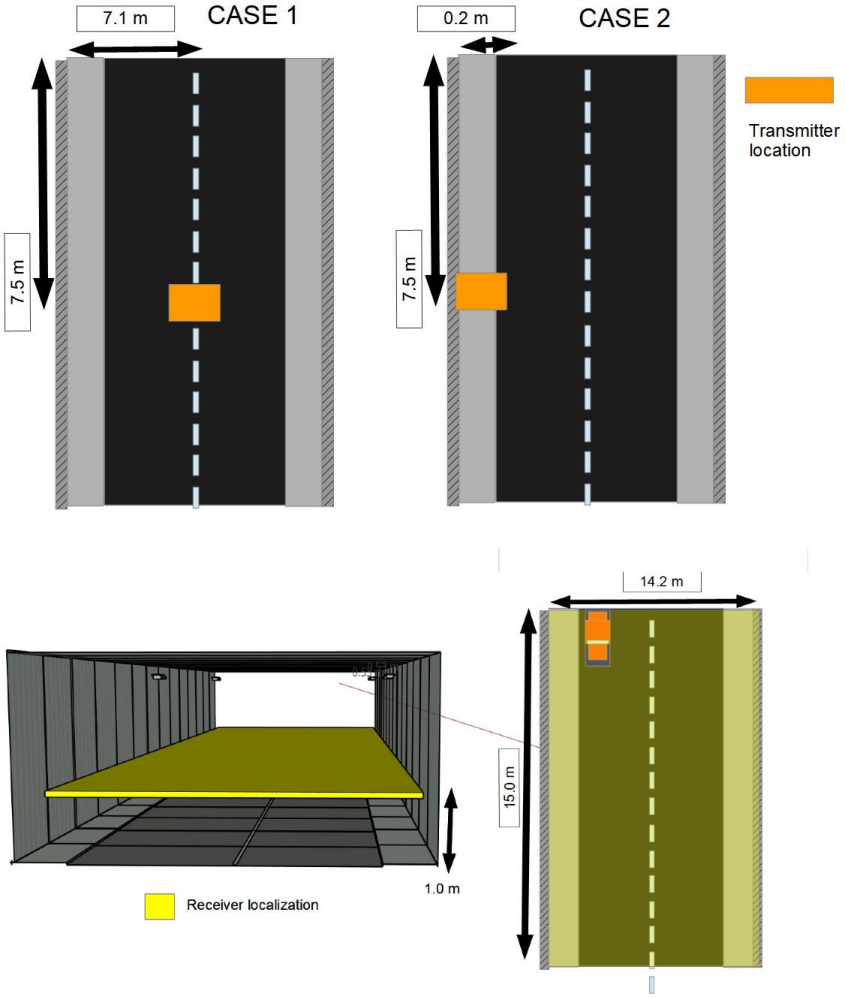

Figure 35: Simulation setup to evaluate the downlink channel.

traffic's opposite direction, placing it from 0 to 1.5 m from the wall. Three different receiver heights are tested to explore the link's behavior with this parameter, which *a priori* will highly impact the channel availability due to the transmitter's orientation and radiation pattern. Figure 36 depicts the uplink scenario.

6.4 VLC Communication channel in the tunnel scenario

The CIR of the channel can be evaluated using the channel simulation setup described in the previous section. It depends on the position of the transmitters and receiver. In V2I and I2V scenarios the RSU's Tx and Rx are fixed while the vehicular node is constantly moving. Additionally, it is assumed that a car travels a rectilinear track parallel to the Y-axis with a speed v. For this reason, it is possible to describe all possible combinations with a single variable. The downlink's an uplink's CIR will change for different points Y Thus, the CIR function depends on the vehicle

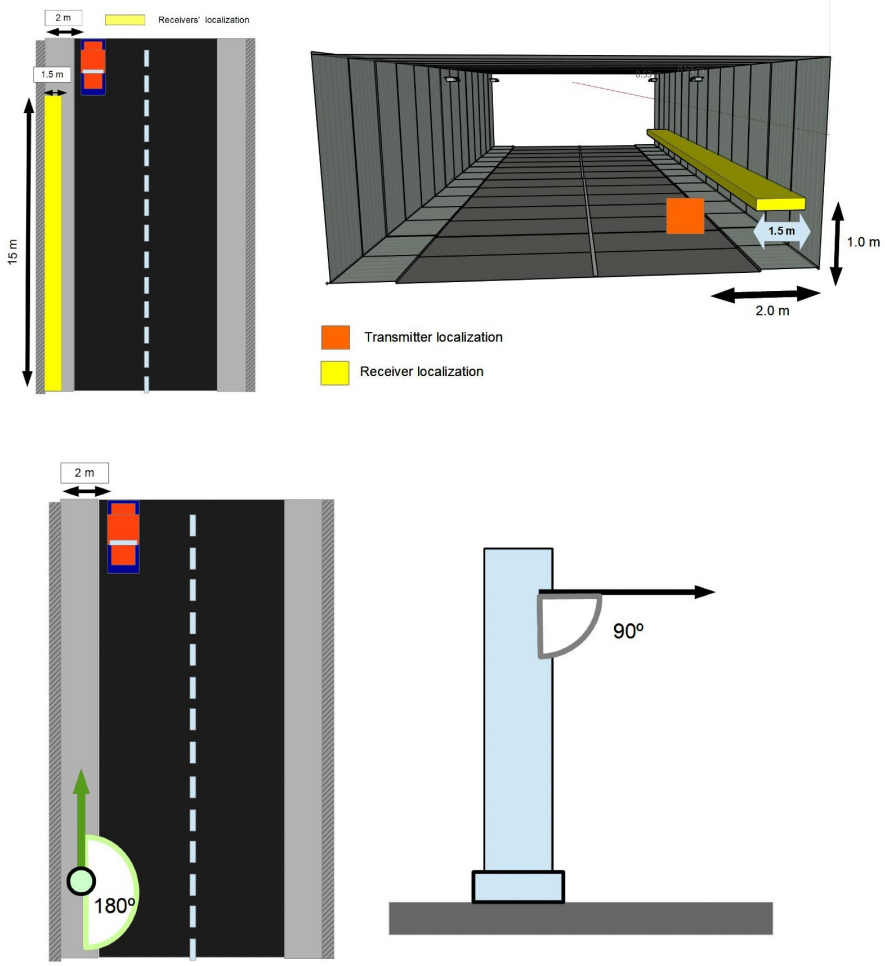

Figure 36: Simulation setup for the uplink evaluation. On the top, the Tx and RX locations. On the bottom Rx schematic orientation.

location expressed as $h(y,t)$. Because the car is moving at a steady speed, the channel response can be transformed into a time-varying impulse response $h(\tau,t)$, where τ is the instant when the channel is measured and depends of the vehicle speed. Then, with $h(\tau,t)$, it is possible to estimate an upper bound system performance in terms of coherence time and bandwidth. The channel characteristic is studied here following the analysis previously explained in Section 4.3. Where the CIR's DC channel gain function $H(\tau,0)$ also depends of the instant τ when the channel is evaluated. The coherence time and the bandwidth of the channel impulse response provide some preliminary insights about the impact of the vehicle's speed on the communication capabilities of the presented V2X scenario.

An approximation of the slow fading can be calculated using the normalized autocorrelation function of $H(\tau,0)$ using equation 6.1. This approximation is valid in a wide sense stationary process with uncorrelated scattering (WSSUS) channels. In this equation, τ' is a time shift to compare the channel condition at different

moments. This metric sense the conditions changes on the channel caused by fading. When the autocorrelation falls below a threshold R_{th}, the resulting lag can be interpreted as coherence time T_c (Equation 6.2). The threshold R_{th} has been set to 50% of the signal's peak (3 dB). So, it can be used to determine the maximum transmission time without failure. As a consequence, the ideal frame size.

$$T_c = E\left[H(\tau', 0)H^*(\tau + \tau', 0)\right] \tag{6.1}$$

$$T_c < R_{th} \tag{6.2}$$

6.4.1 Downlink Channel

Figure 37 presents the simulation results obtained in the evaluation of the downlink CIR when the vehicle crosses the tunnel. We evaluated $h(y, t)$ for Case 1 and Case 2 at three different receiver's Y-axis positions { 0, 3.75, 7.5}, the X-axis position is at 4.5 m and Z-axis position is at 1.0 m. Point 0 corresponds to the vehicle when it is on the edge of the AP area, point 7.5 when the vehicle is at the center of the AP area, and point 3.75 is an intermediate location between these two points. Observe how the channel response $h(y, t)$ changes at a different point in the scenario and how the excess delay contributions on the CIR significantly vary with distance. In the figure, the receiver gets an LoS component, and later there is a long interval to receive non-LoS contributions. It means that these contributions cames after the signal has been reflected at least 2 times suffering a drastic power reduction (2nd order reflections). This situation causes low CIR's delay spread values providing large bandwidth.

Figure 38 shows the time-varying DC channel gain calculated using Equation 4.10, and considering that the vehicles is moving at $100km/h$. These outcomes have a linear relation with the received signal's power. The figure show the channel variation since the vehicular node arrives to the RSU coverage area at instant equals to zero, until it leaves the site after half second. One of the concerns was that the lateral displacement of the car could affect communication. These slight variations can be caused by human error when the driver becomes misaligned to the lane. Therefore, we decided to compare three different tracks with a separation of $\pm$ 1 m from the centrum, the sensed point extends from 4 to 6 meters in the X-axis. These benchmarks are edge situations where the vehicle could stay. In Case 1, the highest values concentrate in a narrow area, while the spatial response for Case 2 is wider. Consequently, the received optical power would not be strongly affected in Case 2 by lateral moves of the vehicle (X-axis). Furthermore, for the wall-mounted luminaires, the channel gain fluctuation in the Y-axis (traffic flow direction) is less sharp than in the top-mounted case. It will probably imply a higher coherence time if a whole time-frequency analysis is carried out.

Figure 39 shows the downlink CIR's DC gain autocorrelation a methodology to measure the changes on the channel conditions with a range from 1 to 0. When

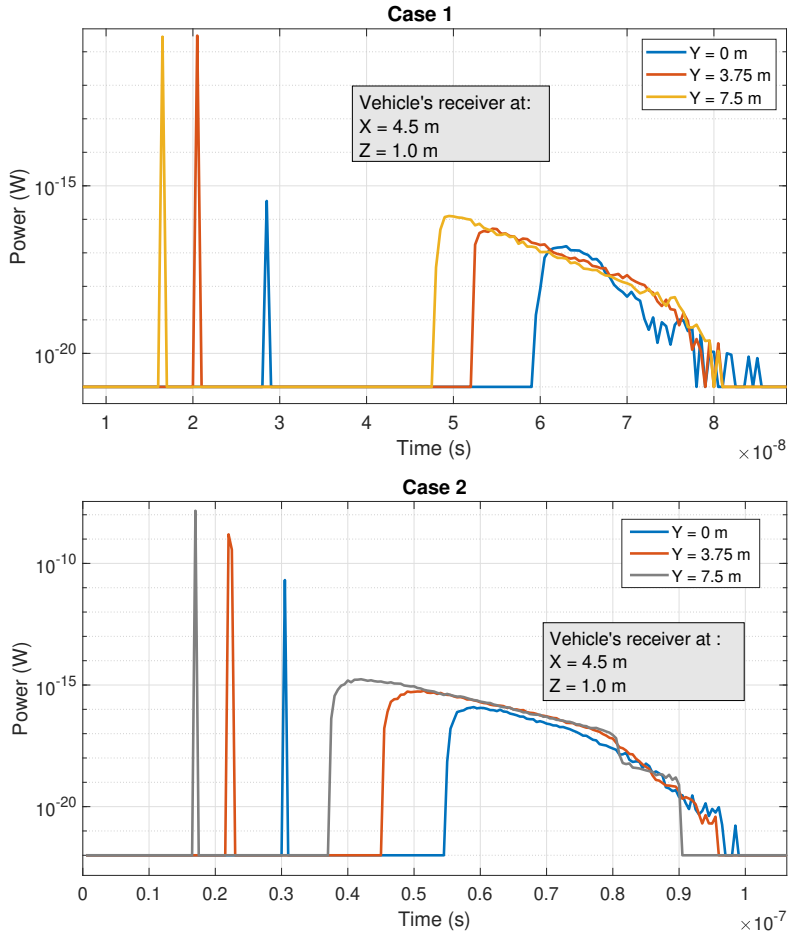

Figure 37: Downlink's CIR $h(y, \tau)$ of a VLC vehicular system in a tunnel scenario. The evaluation considers 2 lamps position (top is case 1 and bottom case 2) and the receiver position $Y = \{7.5, 3.75, 0.0\}$.

the autocorrelation is close to 1, it means the channel conditions are identical in both locations. If the conditions are too different below 0.5, it risks transmission. Similarly, to the previous analysis, the vehicle was placed at three different positions on X-axis for both lamp configurations. The coherence time T_c in all the evaluated cases surpass 100 ms, as can be seen in the figures. It means that the downlink can support the transmission of a 2 Mb long frame when the transmitter is using OOK modulation with an optical clock of 60 Mhz. The results from case 1 are less affected by the receiver's lateral position, but the obtained coherence time values are lower than in case 2. T_c is below 150 ms for case 1 and around 200 ms for case 2. It is important to mention, this metric dictates the maximum size. However, there are other factors to consider such as latency during the channel access to define the final frame size.

Finally, the time-varying downlink's Delay Spread of the downlink channel is also analyzed in Figure 40 for three vehicle's positions. As was mention before, the RMS delay spread is inverse to the channel capacity. So, when the values are almost zero the communication can support high data rate. The results exhibits values below

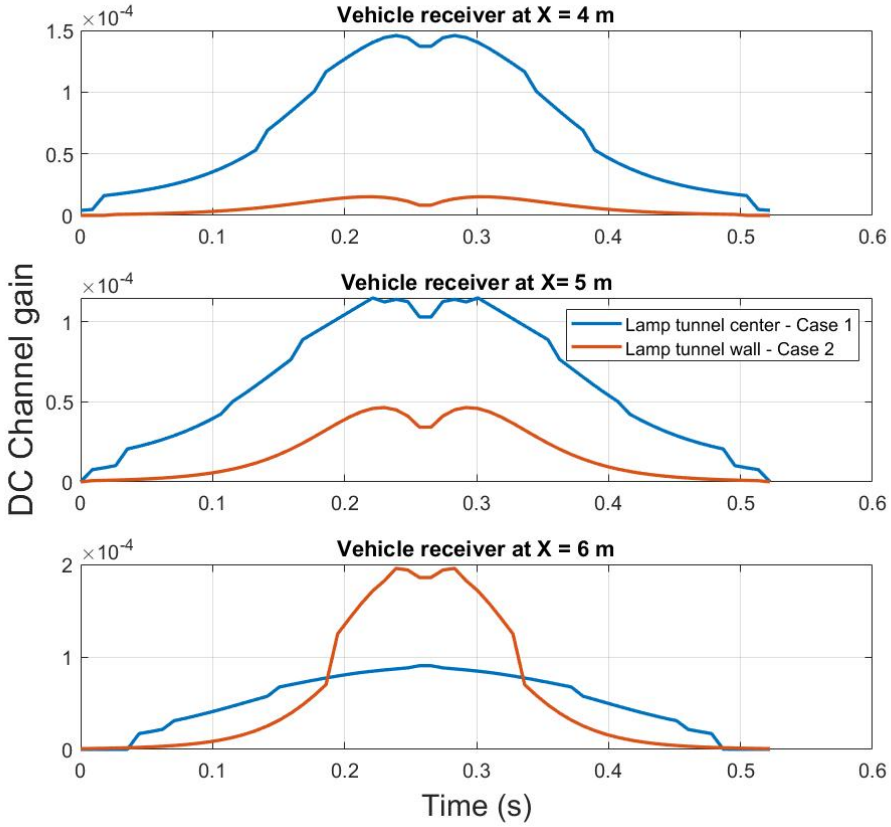

Figure 38: Downlik's DC channel gain of a VLC system in a vehicular scenario considering 2 lamps positions (cases). The receiver is place at x=4 m (top), x=5 m (middle) and x=6 m (bottom).

1 nanosecond in both cases, which provides a generous channel capacity beyond 100 MHz. Despite good value, the Case 2 channel capacity degrades fast when the vehicle leaves the AP. Figure 40 shows that the delay spread depends on vehicle lateral position. However, the results in the worst scenario does not represent a barrier for the communication.

6.4.2 Uplink Channel

Figure 41 shows the uplink CIR placing the sensors at a distance of {7.5, 11.2, 15} in the Y-axis. We see that the uplink is affected by the first-order reflections. It means that the bandwidth capabilities are not constant over time. Since the headlights emit a uniform light on the road, its power contribution does not decrease when the receiver is near the floor.

On the other hand, the same method used in the downlink channel analysis is also applied to study the uplink signal. Since the uplink's transmitter (car headlamp) has a narrow radiation pattern, the channel gain is strongly affected by the receiver's height. Figure 42 presents the uplink DC channel gain placing the photodiode

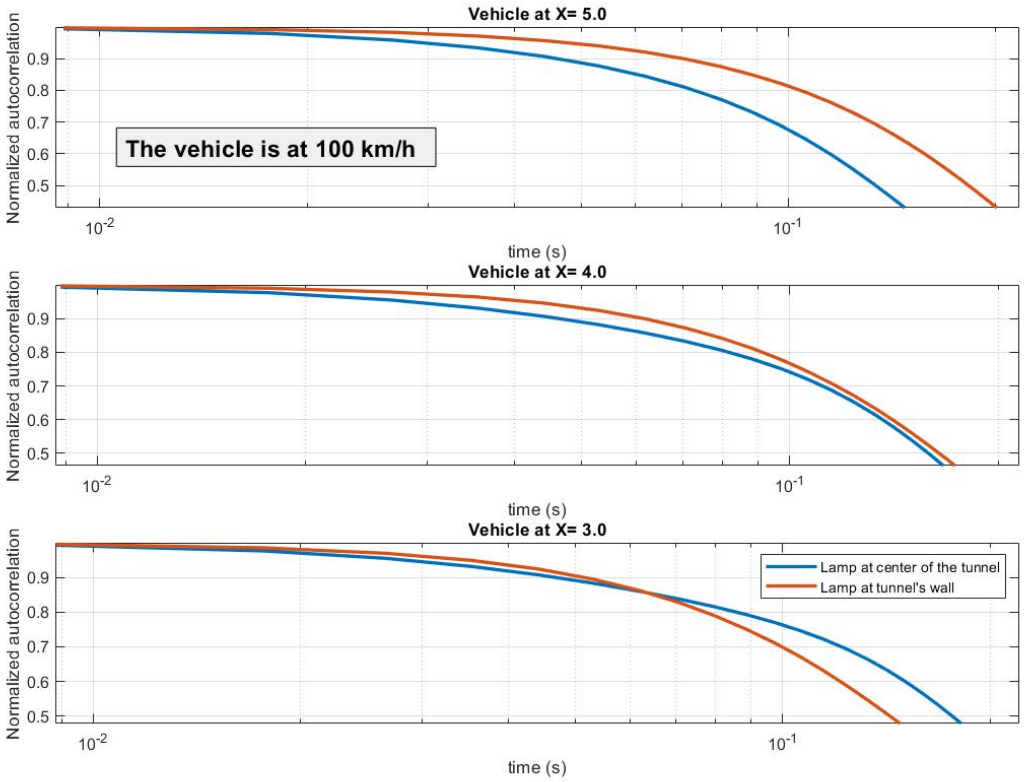

Figure 39: VLC downlink's CIR DC channel gain autocorrelation when the vehicular node is crossing the RSU coverage area.

receiver at three different heights { 0.8, 0.5, 0.2 } on the Z-axis. The evaluation starts when the vehicular node is at 15 meters from the receiver. Then, it approaches the receiver's position increasing the DC channel gain. Finally, the transmission is suddenly interrupted when the car is next to the sensor. When the receiver is placed at 0.8 height, its link duration is shorter. On the other hand, when the sensor is at 0.2 m, it has a good reception when the vehicle is near the sensor. But, the received power is low when the vehicle is in long distance. Finally, an intermediate option presents a good balance of the received power in short and long distances.

Figure 43 show the coherency time of the uplink for the three receiver's height. The three sensor position presents similar times from 140 to 170 ms. There is not a substantial performance difference between the configuration with 0.2 and 0.5 height.

Finally, uplink's RMS Delay Spread is shown in Figure 44. Firstly, the highest delay spread values are suffered when the car is at 12 meters of distance. They decrease when there is less distance between vehicle and receiver becoming zero. The values are shorter in comparison with the downlink's results and can be considered that virtually the channel can provide any bandwidth.

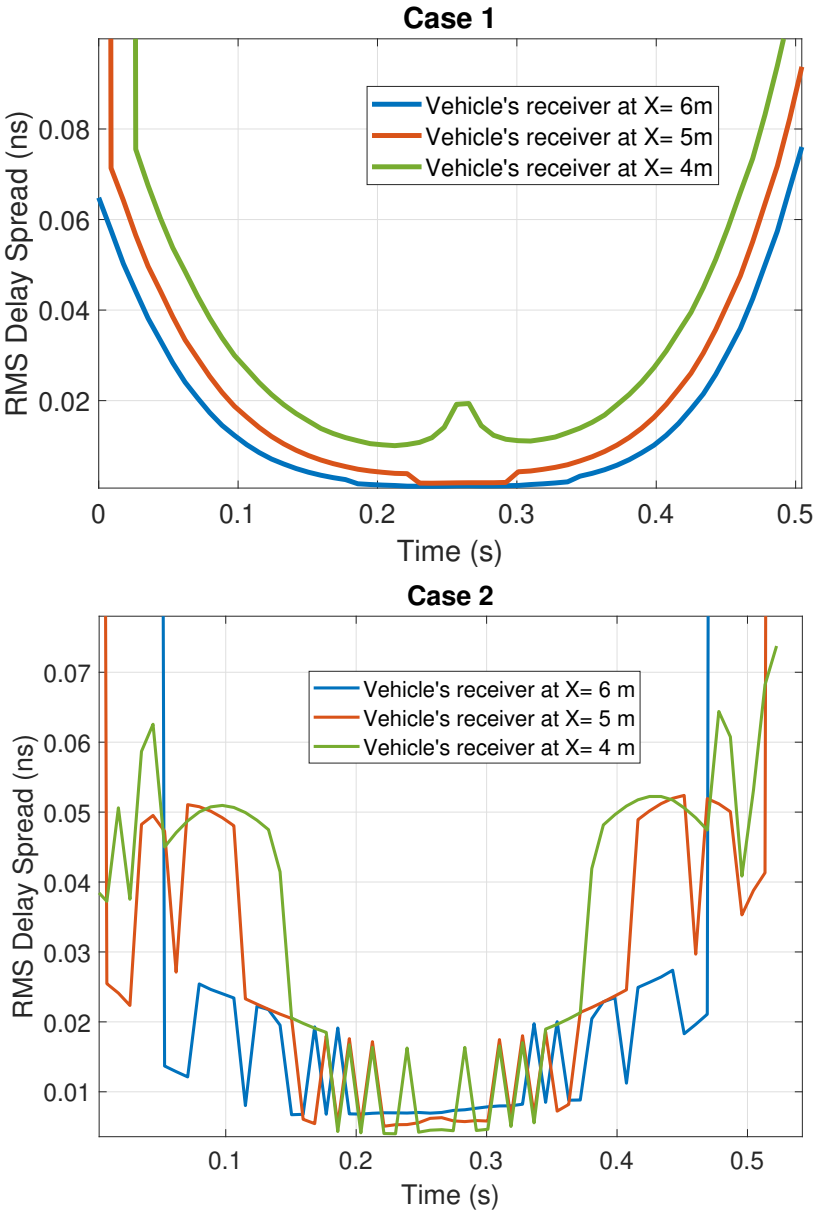

Figure 40: Downlink's delay spread evolution. In both case 1 (top) and case 2 (bottom) three different lateral positions are evaluated.

6.5 A vehicular VLC network framework for evaluating handover

This chapter shows a vehicular network architecture that provides VLC communication for a road tunnel environment. The previous studies demonstrate the feasibility of the proposed vehicular network architecture. These evaluations provided enough evidence to understand the mobility problems of this type of vehicular network. Therefore, this analysis helps to establish the settings of a realistic vehicular VLC network and looks for a handover solution that guarantees seamless communication.

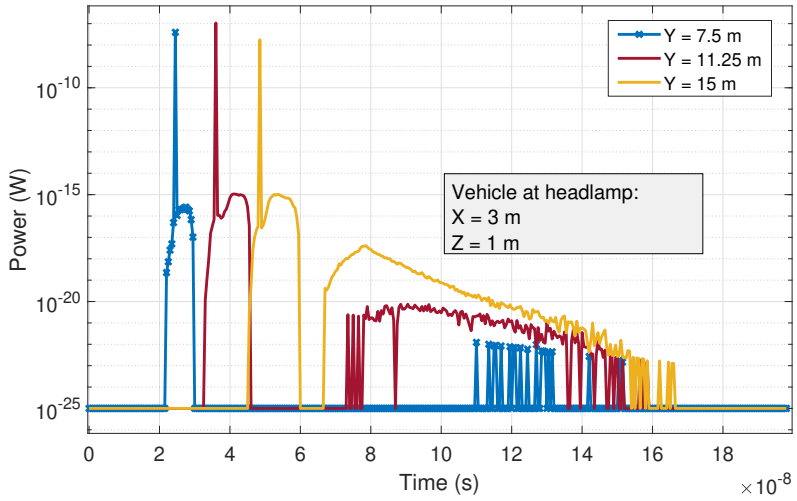

Figure 41: VLC uplink CIR $h(y,t)$ in a vehicular tunnel scenario for $y = \{7.5, 11.2, 15\}$

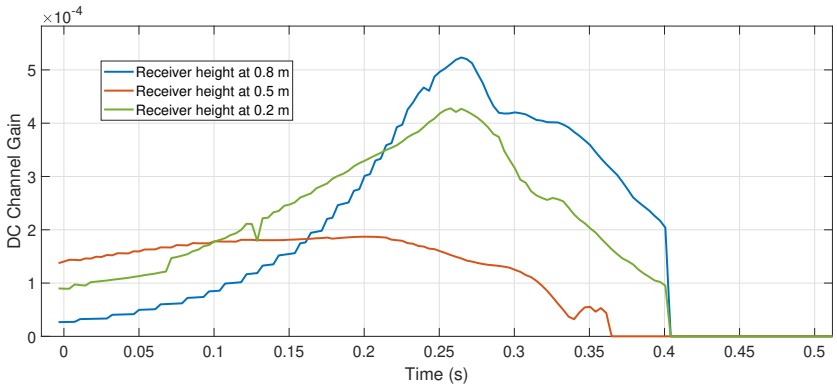

Figure 42: Uplink's DC channel gain of VLC vehicular system in a tunnel scenario.

The handover process constitutes a solution to the mobility problems in a vehicular network. It extends the reach of the access network and ensures uninterrupted communications. The evaluation of handover schemes is done using system level simulations. These simulations makes a detailed representation of the network including a emulation of its protocols. For this reason, it is necessary to elaborate a deep description of the framework parameters of MAC layer and PHY layer. Thanks to the chapter's results was possible to establish the network parameters that can be consulted in table 4. In addition, some modifications were done in the network architecture to improve the communication and deal with some problems. Shortly, we are going to discuss the most relevant parameter's.

The ideal conditions of both links make it possible to use the configuration with the highest capacity surpassing ITS requirements. This network operates using PHY II mode with an optical clock (60 MHz) and an OOK modulation scheme to provide a high data rate. Additionally, the proposal takes into account the suggestions from [49] which proposed avoid to use Reed-Salomon codification and the RLL codification

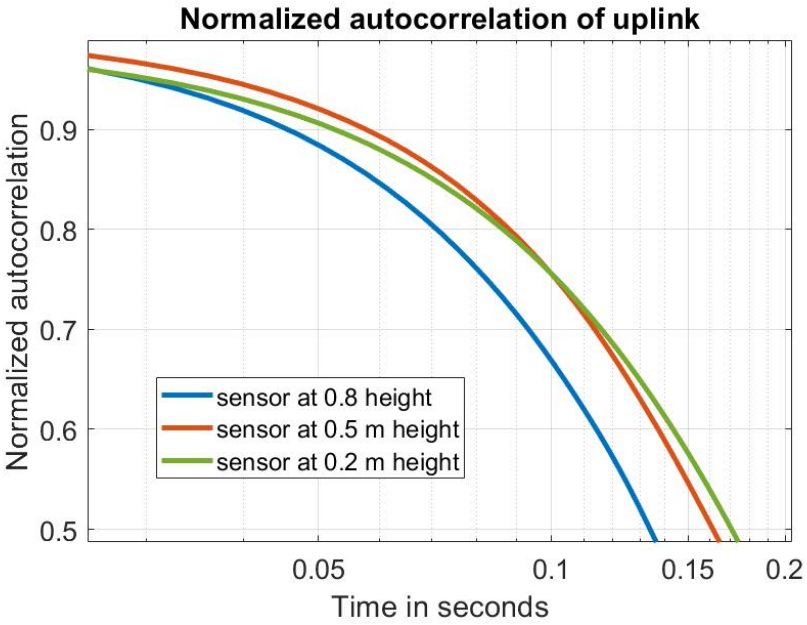

Figure 43: Normalized uplink's autocorrelation function.

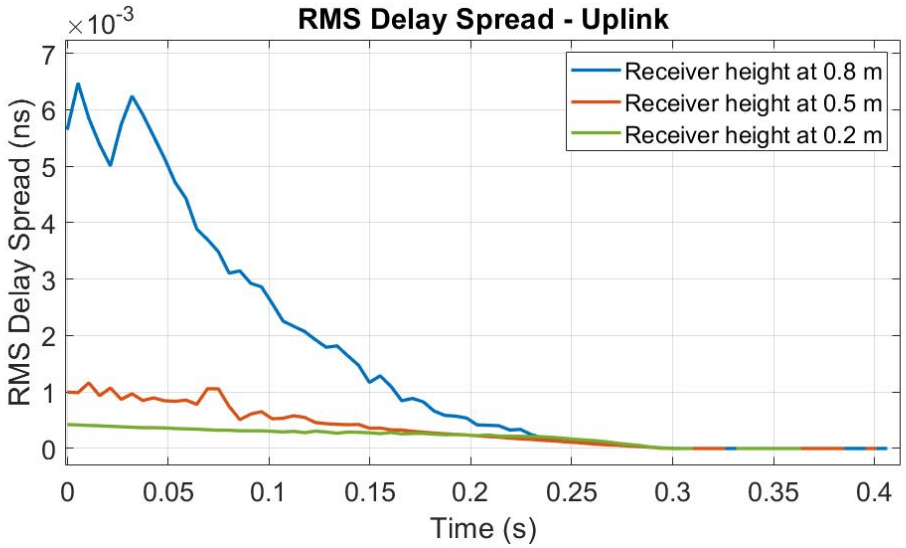

Figure 44: Evolution of the uplink's delay spread.

of 8b10b to minimize the transmission latency. Moreover, the frame's length was set to 1000 bits which is enough to contains any safety message. While, channel access scheme follows the typical specifications in the literature setting $aBackoffUnit$, number of backoff, etc.

It is importanto to comment, RSU receiver is placed 13 meters beyond the transmitter location. It allows the RSU uplink and downlink to have a similar range and cover almost the same area. This decision is underpinned by the uplink evaluation which also shows the ideal receiver's height is 0.5 meters. It presents a balanced performance with the coherence time, delay spread, and DC channel gain values.

Paramaters	Value	Parameters	Value
Phy Layer			
Optical Clock	60 MHz	Headlamp power	15 watts
AP Separation	8-15 m	Tunnel Lumminary power	50 watts
Vehicel speed	80 km/h	Receiver area	1 mm^2
Modulation	OOK	Run-length limited	8b10b
PHY mode	II	Forward Error Correction	none
Rx FOV	60^o	Lens	No
Radiation Pattern	See Fig 34	MMC number of ray	50,000
Reflection coefficient concrete	0.17	Bound per ray	3
Reflection coefficient asphalt	0.07	Channel update	1 ms
MAC layer			
Frame Header	207 bits	BO, SO	5,7
Signaling message size	500 bits	User Throughtput	450 Kbps
aBackoffUnit	200	Frame payload	1000 bits
aBaseSuperframeDuration	60	Number of backoff max	5
Handover			
THUL	.39 dBm	Recovery time	40 ms
THDL max	.54 dBm	Disconnection time	300 ms
THDL min	.65 dB	Association latency	200 ms
Time-to-Trigger	10 ms	Handover latency	2 ms

Table 6: Simulation parameters for handover validation in vehicular tunnels.

Finally, the network cells follow this organization. Each site network works with the classical superframe configuration for a single site. To allow the operation of different AP without interference with their neighbors, the BI is set to 2 ms long and four times longer than SD. This ratio is possible using a Beacon Order of 7 and SuperOrder of 5. Thus, each AP is active just a quarter of the time. The rest of the time is used in turns by neighbors APs. So, the SD shifts on the time to work as Time Division Multiple Access (TDMA), see Figure 45. These actions allow coexistence between contiguous APs and the user. The table includes also some handover parameter's that will be discussed after the handover solution has been introduced on the next chapter,.

The outcomes were not limited to setting the network's specifications. Furthermore, they reveal potential problems that the network needs to deal with. Its power signal increases gradually and suddenly it suffers a drastic power reduction. This signal comportment risk the communication because an untimely handover can break the uplink. For this reason, several modifications were done to the network architecture with a novel topology design named "2.5 layer network topology". The new topology extends the uplink range enabling the AP to obtain a VLC frame from any receiver It is possible by integrating all the infrastructure's receivers in a new sublayer named "2.5". The receivers work as standalone devices connected by fiber to a common switch, which acts as an intermediary between receivers and the APs. Each receiver is capable to demodulates and decoding the optical signal to a binary

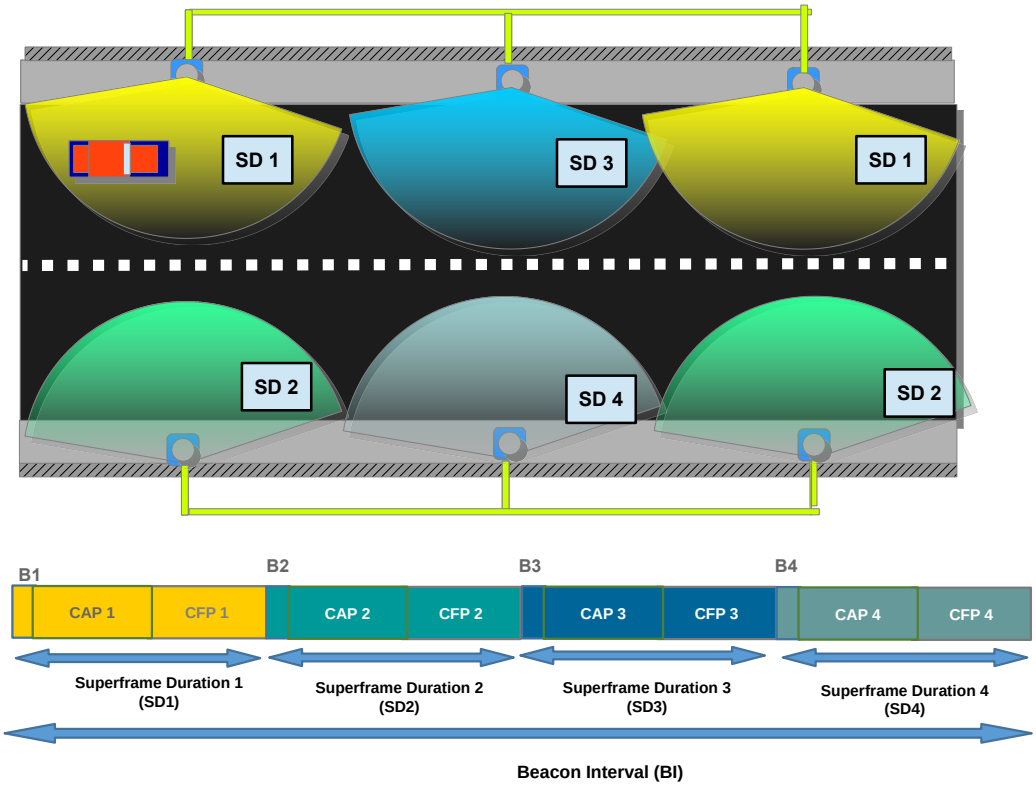

Figure 45: Cells distribution over the evaluation scenario (top), and cells distribution on the superframe structure (bottom).

frame. Then, they send the information to the switch that redirects the frame to the correct destination checking the OWPAN-ID address. Finally, the AP receives the frame information and manages the channel access. The APs are joined to the backbone network similarly as they were connected in a star topology. The described topology can be seen in Figure 46. There are some cases when two or more receivers can receive successfully the same frame. If this situation happens, the switch will eliminate the redundant frames of the network.

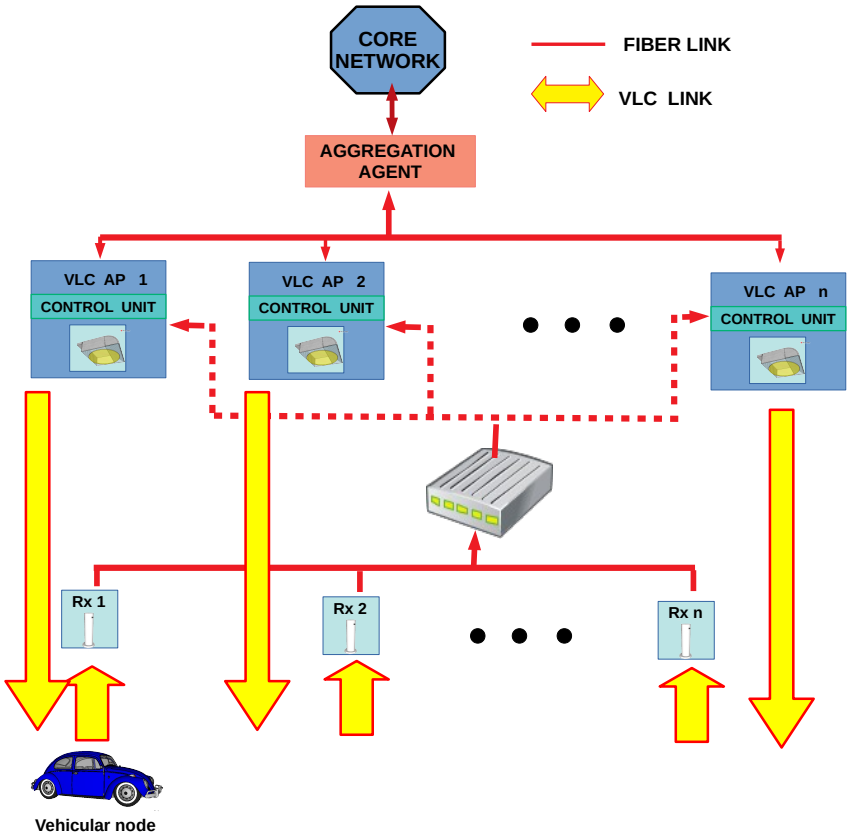

Figure 46: 2.5 Layer topology diagram.

Chapter 7

Handover strategy

Once the channel studies have concluded, and the network basic architecture and requirements are established, the next research step is the result analysis and sketching a comprehensive solution which provides seamless communication. In this thesis, the proposed solution consists on the integration of a novel network topology which operates jointly with an also novel handover scheme. The scheme proposal is composed of a detection algorithm and a handover protocol. The algorithm was designed considering the characteristics of both communication channels (Access Point downlinks and nodes uplinks). Moreover, the protocol solution permits low latency resolution. This chapter presents a detailed description of the handover strategy and introduces the validation process of the presented solution and the performance analysis.

The chapter structure is the following. The first section describes the handover scheme presented in this work. Then, the second section explains the methodology used on the validations and the experimental setup, including the metrics to measure the system performance. Finally, some results and conclusions are discussed.

7.1 Proposed Handover solution

In general the handover scheme consists of a three-stage process The first stage is the signal gathering process which is depicted in Figure 47. In this case, the handover decision is based on the RSS information, and thus it is necessary to measure the communication link periodically. Some minor modifications on the beacon frame format allow it to support the channel estimation function for the downlink RSS level, whose estimated value is storage to be consulted, and it updates every 2 ms. Otherwise, the uplink RSS level estimation requires to transmit a special frame known as "pilot frame" by the vehicular node. Additionally, it provides the infrastructure with the capabilities to estimate the uplink channel from multiple receivers. During this stage, the current site AP_n transmits a beacon frame to synchronize the users. When the vehicular nodes receives this signal, they estimate the instantaneous RSS of the downlink defined by $P_{DL}(t)$. Then, this node broadcasts a periodic pilot frame that includes the measured $P_{DL}(t)$. This pilot frame arrives at multiple AP

receivers, which individually estimate the instantaneous RSS of the uplink channel, *i.e.* $P_{UL}^{n}(t)$ for AP_n, $P_{UL}^{n+1}(t)$ for AP_{n+1}, etc. The links information are compiled to a single frame and shared to the network switch. After that, the information is sent to the HME to analyze if it is necessary to initiate a handover process. In the proposed scheme, the decision algorithm only considers the instantaneous RSS values from the current site, $P_{DL}(t)$, and next site, $P_{UL}^{n+1}(t)$.

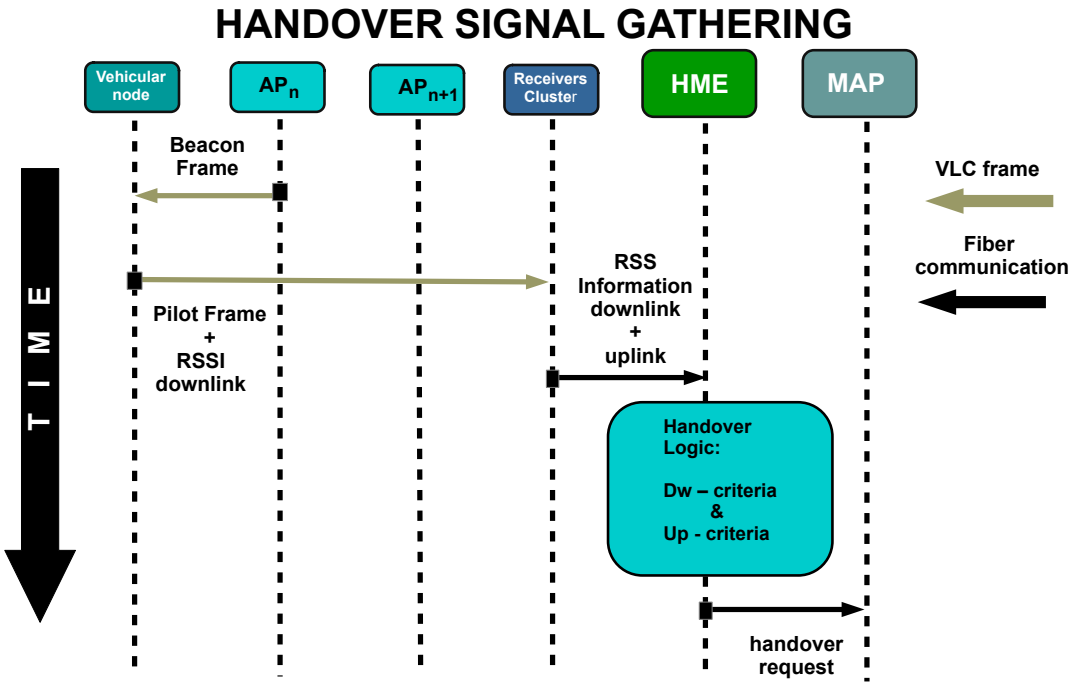

Figure 47: Signal gathering stage.

The second stage is the handover decision. Every time that the RSS information is updated, the system decides if the node's state enables the conditions to execute handover process successfully. The tunnel scenario predetermines a linear movement of the user with a steady speed which makes its movement predictable. As consequence, it is easy to calculated precise moment for a cell exchange, and bounds the possible destination to an unique AP. Thus, a simple logic can determine when the user is coming to the new station without the necessity to track the node's movement pattern. Due to the vehicular node's fast-moving this is a desirable condition because the algorithm resolves briefly.

There are many challenges to confront on the signal detection. Between the most common problems, there is the RSS reliance with receiver orientation. In V2I/I2V communication scheme the RSU receiver and transmitter are fixed, while vehicular nodes' receivers have 2D freedom degrees with almost null orientation changes

simplifying the task. For simplicity in a first approach the network triggered the handover process using only uplink information. However, this information is highly affected by the lateral displacements of the vehicle that contaminates the estimation. Despite the estimation has a good accuracy in controlled scenarios and the support of 2.5 layer topology, its performance decreases by slightly movement variations of vehicular node. As a consequence, the system does not perform the handover on time always, and the vehicular node loses the link. Once the initial test was completed with the low reliability results shown, a different decision scheme was chosen based on the RSS variations in both uplink and downlink channels.

Figure 48 shows the flowchart of the handover decision algorithm that consists of two independent loops. The first loop updates the downlink information at the vehicular node when a beacon frame arrives from its associated coordinator (or AP). Then, it calculates $P_{DL}(t)$, and after that, it registers the reference time, t_b, of the transmitted beacon frame in the last synchronization process that helps to detect an outage. In the second loop, the vehicular node creates a pilot frame every $t_{pilot} = 5$ ms, which includes the instantaneous measured downlink RSS $P_{DL}(t)$. Next, the vehicular node's checks if the current time does not exceed the value of $t_b + t_{dis}$ with t_{dis} as the threshold time of disconnection. Since the coverage area of two adjacent APs sometimes are not overlapped, it is not always possible to guarantee a soft handover. To consider this case, the system extends the disconnection time to allow the vehicle to cross this gap area by using the recovery time $t_{recovery}$. If the current time is greater than $t_b + t_{recovery}$ then the vehicular node forces the pilot transmission without using a CSMA/CA mechanism. The instantaneous RSS of the uplink channels are then calculated by those APs that receive the pilot frame, and only the value of $P_{UL}^{n+1}(t)$ is passed out to the HME entity.

To complete the handover decision stage, the HME entity checks the criteria of "condition 1". It implies that $P_{UL}^{n+1}(t) > Th_{UL}$ and $P_{DL}(t) < Th_{DLmax}$, where Th_{UL} is the instantaneous RSS threshold for the uplink channel, and Th_{DLmax} the maximum instantaneous RSS allowed at the downlink channel. If "condition 1" is not satisfied, then the rate of change of $P_{DL}(t)$ is evaluated as a second criterion, *i.e.*

$$\Delta P_{DL} = \frac{P_{DL}(t) - P_{DL}(t-\tau)}{\tau} \tag{7.1}$$

when the signal $P_{DL}(t)$ decreases below a certain threshold Th_{DLmin} with a negative slope during the time interval τ, then the system will initiate the handover process. Note that the threshold values were obtained experimentally after a series of simulations. These values were $Th_{UL} = 0.77$ dBm, $Th_{DLmax} = 0.54$ dBm, and $Th_{DLmin} = 0.39$ dBm.

The last stage is the handover execution stage in which HME makes the corresponding arrangements to move the user session. The proposed handover protocol uses Hierarchical Mobile IPv6 (HMIPv6) as a reference [122], but adapted to this network. HMIPv6 separates the mobility management into intra-domain and inter-domain to avoid updating the user's address every time. In other words, the user's movements inside this network are undetectable for external agents. This action

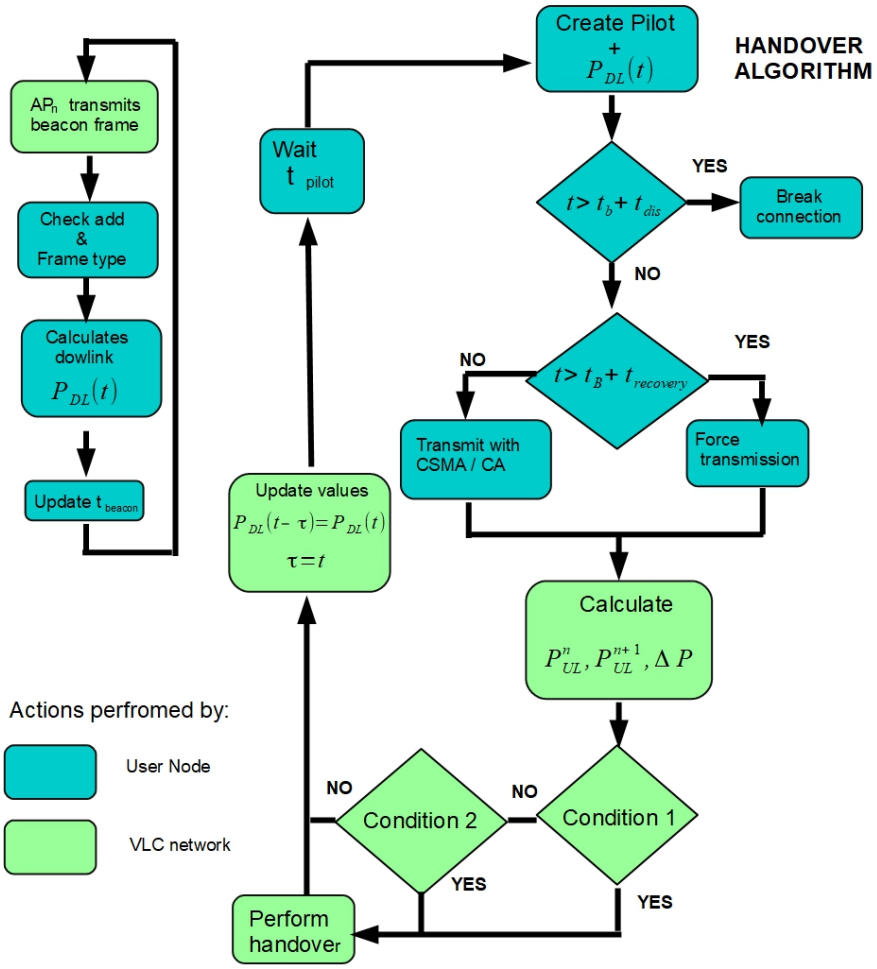

$$(1)\,\Delta P = \frac{P_{DL}(t) - P_{DL}(t-\tau)}{t-\tau}$$

$$Condition\,1.-\; P_{UL}^{n+1}(t) > Th_{UL} \wedge P_{DL}(t) < Th_{DL\,max}$$

$$Condition\,2.-\; P_{DL}(t) < Th_{DL\,min} \wedge \Delta P_{DL} < 0$$

Figure 48: Diagram of handover decision algorithm.

minimizes the time because it is unnecessary to perform security processes such as Duplicated Address Detection (DAD) that generates long waiting periods. Inside the inter-domain, the networks keep the IP address of each user in Mobility Anchor Point (MAP). Furthermore, it manages the internal user localization with a 16-bits short address. A supplementary function of MAP is to intercept all the packets and serves them to the destination. Another advantage is that HMIPv6 requires a low number of biding updates through the wireless channel optimizing the bandwidth

utilization.

Figure 49 shows the execution scheme. At the beginning of the protocol, there is the gathering stage where the receiver cluster estimates the SNR. The compiled RSS information is sent to HME. Then, HME executes the detection algorithms to determine if the user achieves the conditions to begin the mobility process. When the process starts, it sends a handover request to MAP which checks if AP_{n+1} has enough resources to receive an extra user. The request is delivered to AP_{n+1} that tries to establish direct communication with the vehicular node. So, it emits the petition using the VLC channel. If the user can reply successfully, the handover completes its process, and AP_{n+1} reports it to MAP. Finally, the AP_n receives a notification that the user does not belong anymore to the network.

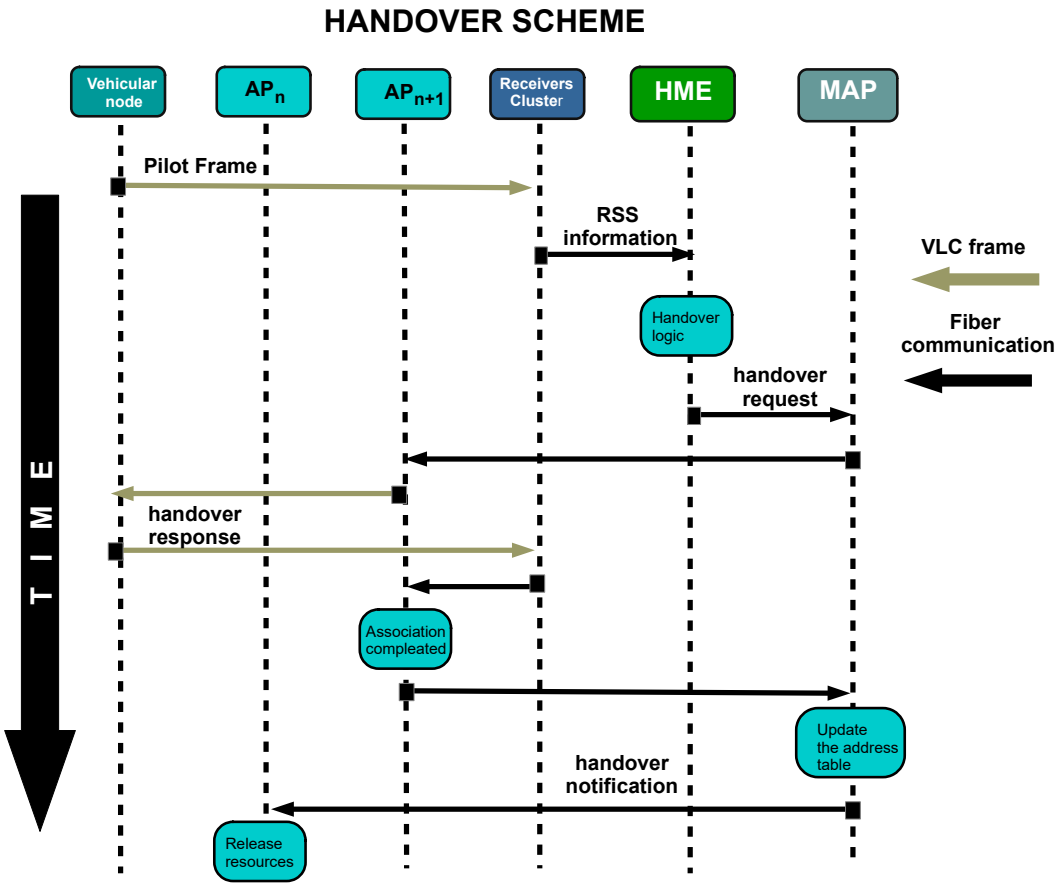

Figure 49: Handover execution protocol.

7.2 Evaluation Methodology

The validation process follows a evaluation methodology through system-level simulations with the simulator developed for this thesis, to which some additional mod-

ifications have been introduced to incorporate the new handover features. This approach simulates a representation of n vehicles moving with a steady speed inside the tunnel. Each vehicle is receiving information periodically via the VLC link. When the vehicle representation is getting close to the edges of the AP coverage area, the system needs to trigger the handover process. Otherwise, it loses connection. The simulator evaluates jointly the vehicle reallocation which changes link conditions, the channel access in each transmission, and protocols in the MAC layer. The goal is to compare the performance of different system configurations sensing indicators such as the packet latency, number of errors in the network, and the outage period.

7.2.1 Performance Analysis

To measure the performance of the proposed vehicular VLC networks different metrics have been considered covering the main aspects of the network behavior. The first metric is the service availability which is calculated by using the following equation:

$$\text{Ratio} = \frac{(\text{service time} - \text{interrupted time})}{\text{service time}} \tag{7.2}$$

Availability is calculated as the ratio of the time that the vehicular node's communication service is available regarding the total time (the sum of service time and the period wituout connection). The node must successfully receive and transmit data to be considered as having communication service. This state is monitored every 5 ms, and the requirement is that the user needs to receives at least one frame during this interval. Otherwise, the simulator assumes that the node has lost connection during this period. Repeated frames are ignored because it means that the node is not able to reply to the communication.

The second metric is the End-to-End Frame Error Rate (EFER) measurement. It represents the reliability of the system after the re-transmission and failure detection mechanism of the MAC layer. A frame can be lost if the re-transmission limit time is exceeded and the AP is not able to reach the node. Therefore, the data packet transmission performance can be characterized as the ratio of the incoming data frames from upper layers in a particular AP, referred to as "total frames", and the transmitted frames which have been received correctly in the MAC layer of the vehicular node, referred as "delivered frames", *i.e.*

$$\text{EFER} = 1 - \frac{\text{delivered frames}}{\text{total frames}} \tag{7.3}$$

The third metric is the Frame Error Rate on the PHY layer (PFER). This measure considers all the AP transmission attempts, referred to as "the number of transmissions", including the transmitted frames which were not correctly delivered. This will reflect the total spent resources during the communication. In a similar fashion to EFER, PFER uses the complement of the ratio between delivered frames and the total number of transmission frames,

$$\text{PFER} = 1 - \frac{\text{delivered frames}}{\text{number of transmissions}}. \tag{7.4}$$

PFER and EFER require a bidirectional communication to increase the number of "delivered frames", including the successful transmission of an acknowledgment frame.

Finally, the average data rate of the vehicular node is also measured to evaluate the performance of the network service quality. The instantaneous data rate metric, R_{ins}, is defined as

$$R_{ins} = \frac{\sum_{i=1}^{rf} P_{load}(i)}{t_m} \tag{7.5}$$

where R_{ins} is the data rate measured during the time window $t_m = 5$ ms with $P_{load}(i)$ as the payload of the i-th received frame. Then, the average data rate, R_{avg}, during the total simulation time, t_{sim}, is given as

$$R_{avg} = \sum_{j=1}^{t_s/t_m} \frac{t_m R_{ins}^j}{t_s} \tag{7.6}$$

7.2.2 Handover in the Simulation Tool

This section describes the process for the integration of the proposed handover schemes and the 2.5 layer network topology into the developed simulator. Figure 50 displays the simulator organization to study the vehicular network considering the topology 2.5 layer network. It is composed by the user nodes, a single infrastructure module and a new node type, the Network Controller module. This "Network Controller" module performs some Layer 3 (Network Layer) functions associated with the HME and MAP, including the handover protocols. As was commented before, these protocols are based on HMPIV6 which split the address control by means of an inner and outer address based structure. So, this module manage the address resolution with its corresponding delay. For example, when the user is requiring a new address because it has just ingress, the module gives a longer response interval than a handover request. Additionally, this new module manages some of the network metrics such as $EFER$ or R_{ins}.

Another relevant change in the simulator, is the network infrastructure representation to include the new topology. Previously, the network was shaped by multiple independent coordinator modules to represent each AP. Instead, in the new network architecture there is a single infrastructure module. The infrastructure node is a complex module composed of an array of PHY submodules, an intermediate switch submodule, and an array of MAC submodules. The MAC and PHY submodules are still operating as was described in Chapter 4, but the connections between them are different. Its organization can be seen in Figure 51. The PHY submodule input and output from the VLC channel remain equally, as well as the input and output of the MAC layer submodule with the elements in Layer 3. Otherwise, the internal

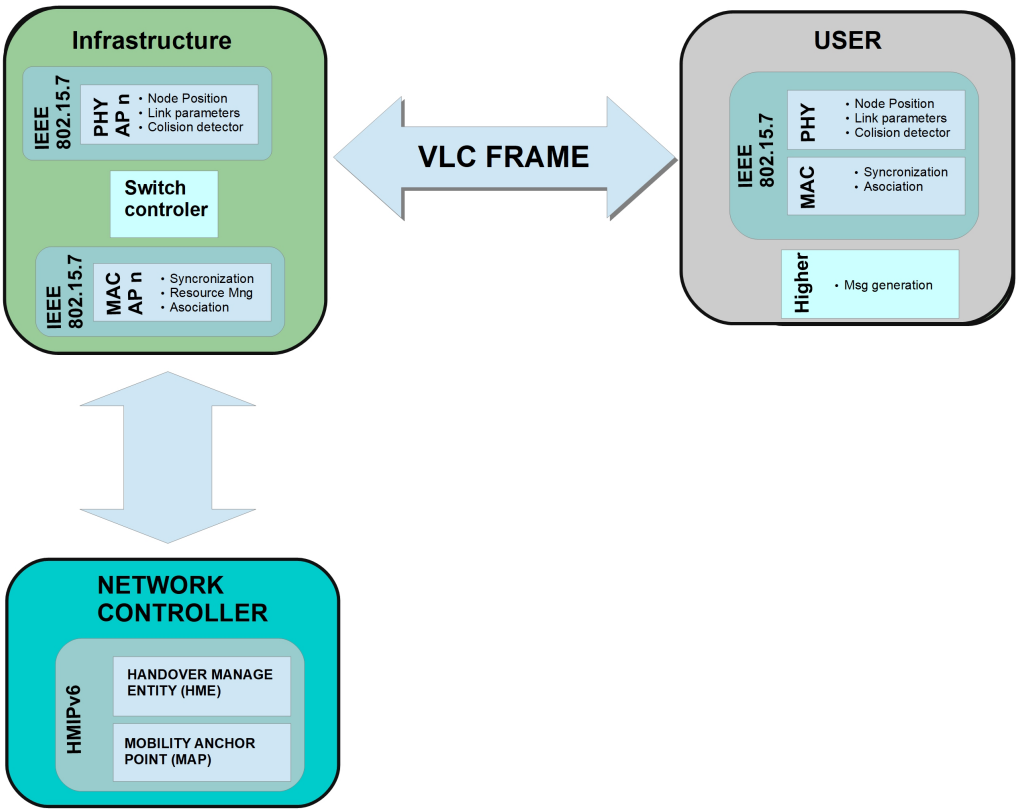

Figure 50: OMNet++ framework for handover simulation in VLC networks.

output from the PHY submodule is connected to the switch representation. The switch submodule output is connected to each MAC submodule's internal input. This switch submodule checks the messages' destination information each time it receives a "message" (that represents a VLC frame in the simulation environment), to forward it to the correct destination. At the same time, it starts a time window to eliminate redundant packets. Finally, the connection between the MAC module internal output and the PHY module internal input remains as was originally.

The PHY module from the user node incorporates some mobility patterns to emulate the vehicle track. It establishes a new node's location every 1 ms, and updates the channel information. One of the strongest limitations was the time spent on the MCRT simulation when there is a vast number of link updates in a single simulation. Subsequently, the simulation time can be extensive. To reduce it, the simulator takes advantage of the mobility restrictions and the scenario geometry to generate a database of precalculated bandwidth and DC channel gain values on a grid of points distributed on the plane of possible node locations. Each time the channel need to be evaluated, the simulator finds the 4 closest grid points to the actual node position and approximates the corresponding bandwidth and DC channel gain values by an averaging estimation. The grill resolution is 20 cm in both axes (Y-axis and X-axis) representing the vehicle motion on the track and lateral displacement respectively. These are the most relevant modifications in the simulator.

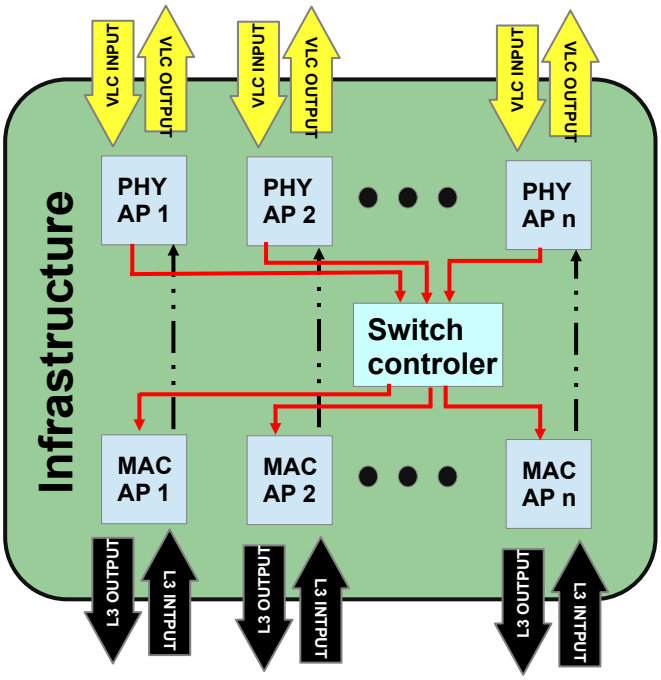

Figure 51: Infrastructure module organization.

7.2.3 Experimental Setup

The proposed VLC network topology and handover protocol for high mobility will be evaluated by simulations an comparison of two different scenarios. The first scenario is intended to measure and compare the performance of the network operating with a single user with some configurations with different network topology and detection scheme. While the second scenario selects the configuration with the best performance, and quantify the impact when the number of vehicular nodes increases.

Figure 52 shows the graphical representation of the first scenario. It considers a single-vehicle moving at 80 km/hr through a two-lane tunnel with a lighting system that contains a set of luminaries (APs) in the tunned model described in 6.1 On each AP, the VLC receiver is 13 m forward of the luminary mounted on the wall and 50 cm above the road, opposite to the traffic direction with a 90^0 elevation, to ensure a good signal reception over an adequate period. On the other hand, the vehicular node has a built-in VLC system, which uses its headlamps as the transmitter and adds a receiver near to the left headlamp (on the hood), pointing to the tunnel ceiling with an elevation of 180^o. The vehicular node is assumed to be transiting on the lane closest to the tunnel wall with the transmitter (headlamps) at 1 m above the ground level and its receiver at 2.4 meters from the tunnel wall. This is the longest distance between the lane edge and the closest wall in a two-lane tunnel. Consequently, this setup determines the critical scenario for the uplink. Since the natural driving of a person makes the car moves from side to side into the lane, it loses its alignment with the road lane and consequently with the tunnel wall.

Therefore, the handover process may be affected by these displacements, an also by the narrow radiation pattern of the headlamps. For these reasons, we include an error margin of 0.225 m to the vehicle's position from the tunnel wall to simulate these types of behaviors. For the simulations, the initial position of the vehicular node starts from 10 to 13 m behind the first tunnel luminary. This configuration evaluates the vehicle's communication with a receiver placed in the closest wall. Additionally, this simulation setup assumes that the vehicles keep a safe separation distance, providing Line-of-Sight communications at any time.

This first scenario is evaluated considering three hypothetical network configurations to validate the proposed handover solution:

- **Configuration 1:** Perform the handover process using only uplink information, i.e., satisfy the "Condition 1" criterion, in a conventional network topology.
- **Configuration 2:** Perform the handover process with the "Condition 1" criterion in the 2.5 layer network topology.
- **Configuration 3:** Perform the handover process using both uplink and downlink information, i.e., satisfy "Condition 1" and "Condition 2" criteria, in the 2.5 layer network topology, see Figure 48.

The simulation process is performed as follows. First, the vehicular node moves straight forward with a steady speed while the APs are transmitting beacon frames. When the vehicular node receives one of these frames, it starts the discovery process to find the best possible connection. Then, it waits for a random period to send an association request. After the association process is resolved, the AP transmits data frames with a constant throughput. When the vehicle is leaving the AP coverage area, the network needs to detect its departure using the handover decision algorithm described before. If the estimation is correct, the handover protocol is executed to start a new session in the next AP and continue the communication. In other cases, the handover process fails, the AP will continue transmitting the data frames until the disconnection time expired. At the same time, the vehicular node detects a failure if it stops receiving the beacons. Then, the vehicular node needs to keep sensing the channel looking for an available AP to start the association process again.

The second scenario considers vehicles in a convoy that commute in a tunnel, see Figure 53. With this scenario, we extend the experimental evaluation of the handover process which can be depleted by vehicles sharing the same channel. In this setup, there are m vehicles moving at the same speed as a caravan. The infrastructure configuration is the same as the single-vehicle evaluation case. Besides, the vehicles are positioned in a line forming a caravan. The first vehicle is placed in a random point following the same distribution and limits regarding the user in scenario 1. The other vehicles are lined behind the position of this car with a random distance

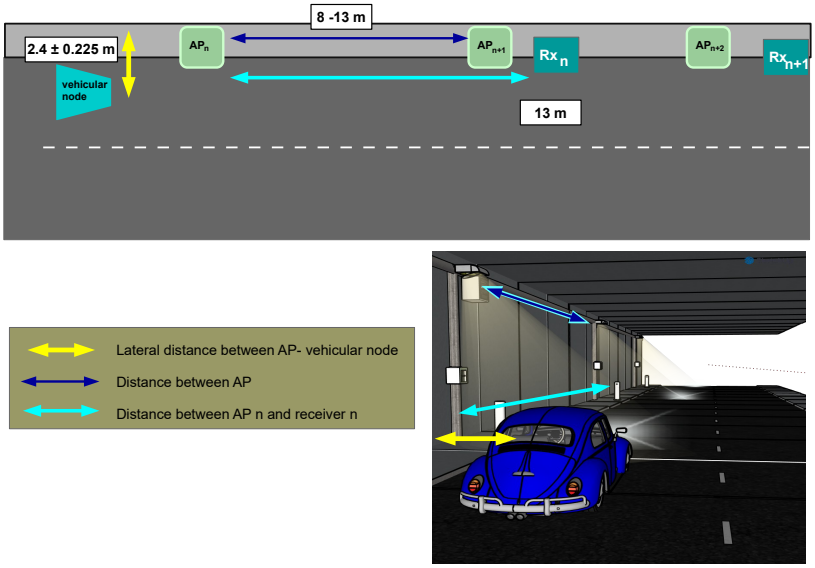

Figure 52: Scenario 1: Graphical representation of the VLC network with one vehicular node.

between 7 and 10 m. This scenario does not accomplish the suggested safety separation distance between vehicles, but it is done to evaluate the possible case when a vehicle ingresses an occupied cell. Under this situation, the vehicular nodes need to share the AP available resources. Therefore, there is a possibility that one of the handover messages may collide with another vehicle's communication. The simulation process of this second scenario follows the same process as described in the single vehicular node case.

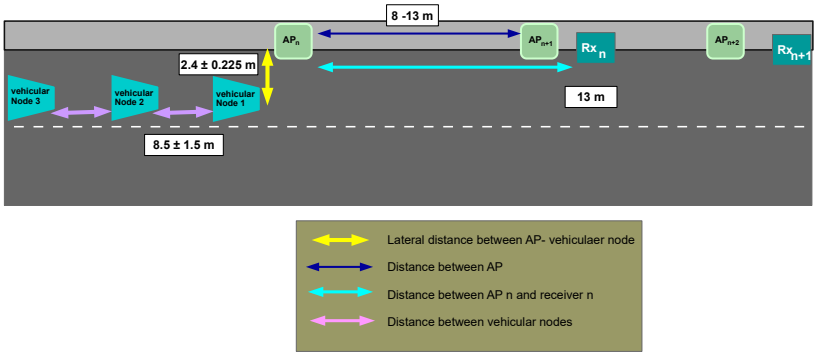

Figure 53: Scenario 2: Graphical representation of the VLC network with multiple vehicular nodes.

Table 6 in chapter 6.5 summarizes the more relevant simulation parameters for the experimental scenarios. Each experiment was evaluated 100 times under the same parameters. The parameters considered has been 8 different distances between AP, 3 system configuration (1 start topology, and 2 proposed topology), and 2 scenarios

(single-user and multiples users). There is a total of 2400 simulations for the first scenario, and 3200 simulations for the second scenario. Each simulation recreates 18 seconds of communication where the vehicle needs to perform between 27 to 50 handovers to have seamless communication. The decision algorithm is executed when a vehicle sends a pilot every $5ms$, it implies that the detection algorithm is executed around 3600 times in a single simulation. Additionally, the nodes update their channel every $1ms$ to have smooth changes and have an accurate model.

Finally, the following parameters were established for the handover process: the disconnection time t_{dis}, recovery time $t_{recovery}$, association latency t_a, and the handover latency t_h. They determine the latency of the handover and the outage duration when this process fails. A vehicular node will lose synchronization when it has not received a beacon frame after $t_{recovery} = 40$ ms, then it will be disconnected after $t_{dis} = 300$ ms. This tolerance period allows the vehicle to do the handover process when the network has a gap area between two APs.

7.3 Results and discussion

This section presents and analyzes the results of the network performance for the different setups. Firstly, we study the single-user case scenario. Then, it explores the network with multiple users. Finally, we discuss if the expectations of the system performance have been accomplished.

7.3.1 Single vehicle

This evaluation contemplates a single vehicular node under a controlled environment. Figure 54 shows and compares the service availability, defined in equation (7.2), as a function of the APs separation under the three different scenario configurations described in Section 7.2.3. We observe that configurations 2 and 3 keep a high availability when the separation between the APs is less than 14m. For a higher separation, the service availability begins to decay. With configuration 1, this service declines below 85% at a distance of 8m and gets worse for larger distances. It is clear that the proposed 2.5 layer topology yields a significant improvement in the link reliability as compared with the conventional topology. The main reason for this behavior is that in a conventional topology the link can be broken before the handover starts, which causes to stop gathering information to execute the handover.

Figure 55 presents the service time ratio using a logarithmic scale. The best overall performance is achieved with Configuration 3. We see that the interruptions in Configuration 2, using only the uplink information, are ten times longer than the interruptions in Configuration 3, where the service is interrupted averagely 1% of the time while it only uses the uplink information. Otherwise, this interruption time decreases until 0.1% in Configuration 3. It is not always possible to carry out the handover when the distance that separates the APs is more than 12m, therefore, the performance decreases. We highlight that the 2.5 layer topology can support communication even when the link has been broken, as a result, it provides a supplementary communication time to detect the movement. And consequently,

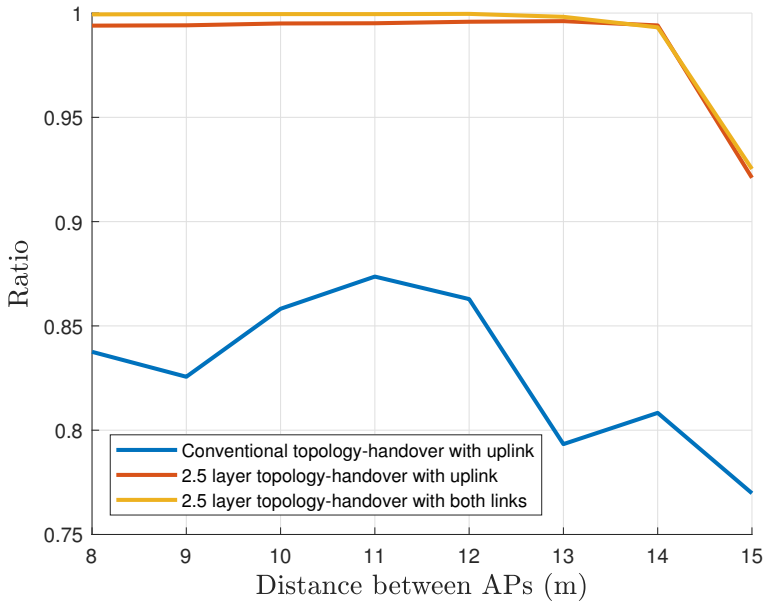

Figure 54: Service availability comparison with single user for three network configuration.

there is seamless communication without severe interruptions. This improvement guarantees that the vehicle will stay connected almost all the time.

The measured EFER of the VLC network with a single vehicular node is now shown in Figure 56. Here, we observe that Configuration 1 delivers EFER rates of about 10^{-1} which are considered too high for vehicle safety messages. Configuration 2 achieves a performance of EFER rates lower than 3×10^{-3} when the separation between APs is under 13m, then it increases up to 7×10^{-2} for separation of 15m. Finally, Configuration 3 shows the most favorable performance with an EFER of 5×10^{-4}, almost one order of magnitude higher than Configuration 2. From a separation of 12m between APs, the performance begins to decline, and eventually, Configurations 3 and Configuration 2 obtain the same results.

Similarly, in Figure 57 the compared PFER is presented concerning the position of the AP. From these results, the maximum errors for Configuration 2 and 3 do not exceed 15 % in the case where the separation between the APs is below 14m. Configuration 3 shows the minimum PFER of about 12% up to a distance of 13m. On the contrary, the successful transmissions with the conventional topology reach a PFER of about 0.65 for distances below 12m, and for longer distances between APs, the received frames are reduced to half of them.

Finally, we plot the behavior of the data rate service in Figure 58. The network is set to transmit a steady data rate of 450 kbps per vehicular node that proves to be enough to hold message-based safety applications as suggested in [17]. These results reflect that there is not a substantial throughput difference between Configurations 2 and 3. The system can handle the maximum requirements for both configurations thanks to the redundancy of the uplink channel. On the other hand, Configuration

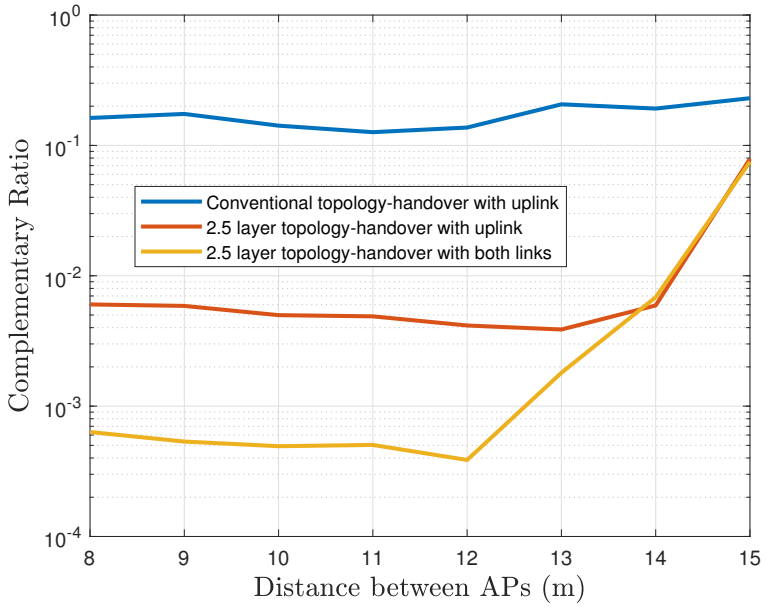

Figure 55: The outage ratio comparison (logarithmic scale) for three network configuration considering a single user.

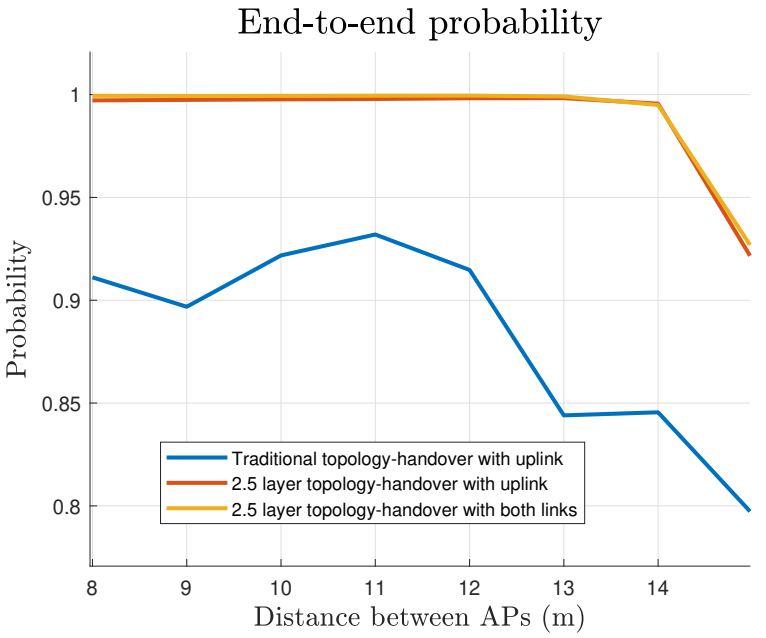

Figure 56: End-to-end frame error rate considering the backoff mechanism (logarithmic scale)for three network configuration considering a single user.

1 suffers from throughput degradation problems because of the lack of redundancy.

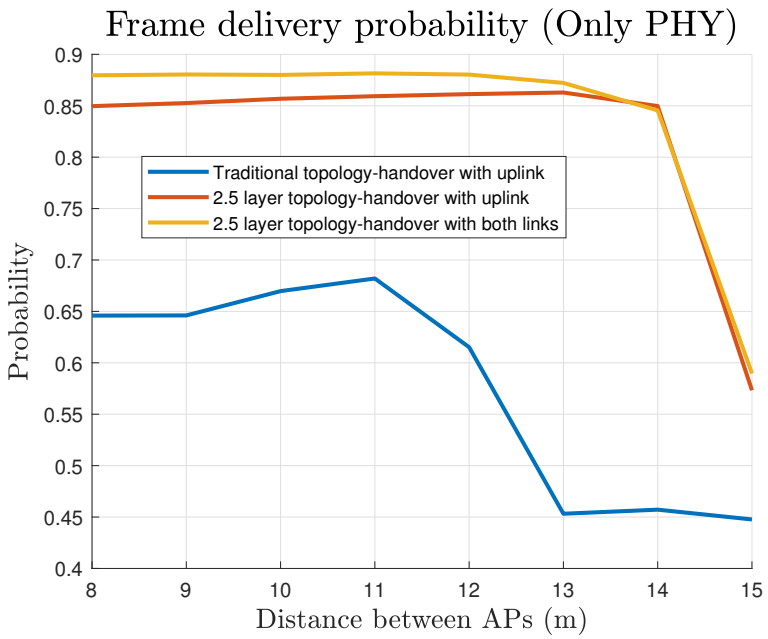

Figure 57: Physical layer Frame Error Rate (logarithmic scale) for three network configuration considering a single user.

7.3.2 Multiple vehicles

One of the goals of a handover algorithm is to prevent a handover failure due to insufficient resources in the target cell. To measure this influence, we evaluate the performance of the network considering a scenario with multiple vehicles as described in Section 7.2.3. For these evaluations, we consider only configuration 3 since it is the best performance one. And as quality metrics related to the cells' available resources when the number of vehicular nodes increases, we will focused on the service availability, PFER, and EFER.

It is important to note that, due to the limited cell coverage, the individual user performance is not impacted deeply by scaling the network with more users. It means that we do not have to scale up the simulation with a large number of vehicular nodes to determine the performance limit. Furthermore, the coverage area of each AP helps to delimit to a maximum of 3 vehicles per cell, minimizing the need of serving a large number of vehicles.

From Figure 59, it is evident how the service availability decreases with the number of vehicular nodes. For this scenario, the service time is affected because multiple vehicles join the same AP. Therefore, the AP does not transmit any information to a new vehicle until the previous frames in the buffer of the AP have been delivered. Thus, the service is more likely to be interrupted during the handovers. As expected, the results depicted in Figure 59 corroborate that the service time is reduced on average. Moreover, the operation of multiple vehicles in a close area makes the blackout time to increase up to 20 ms when the AP separation distance is less than 13 m. Furthermore, when the separation of the APs is shorter, the handover occurs

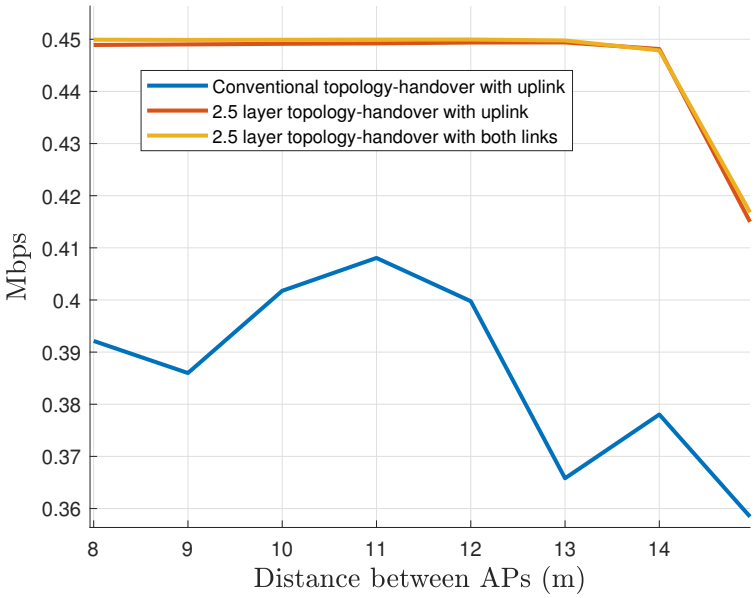

Figure 58: Average User's datarate during the entire simulation for three network configuration considering a single user.

much more frequently.

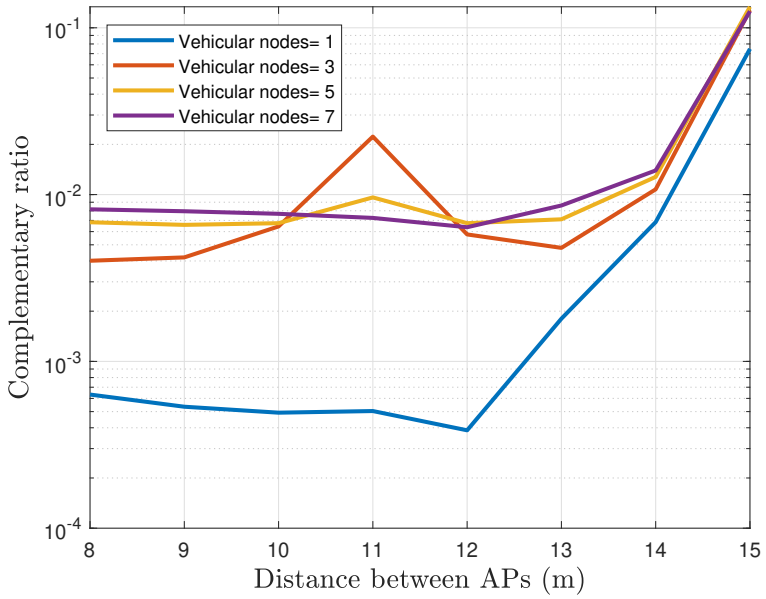

Figure 59: The complement of the service availability for different number of vehicular nodes operating in the network (Outage ratio).

Figure 60 plots the comparison of the EFER for a different number of vehicular nodes. The results exhibit a considerable drawback when more than one user is associated with an AP. We observe that the EFER converges to 3×10^{-2} at distances

under 13 meters, which is a substantial rise in comparison with 5×10^{-4} from the single-vehicle scenario. On the other hand, Figure 61 shows that the PFER performance has a similar tendency to EFER. As expected, a single-vehicle crossing the tunnel achieves superior performance with an error rate of 12% when the distances between lamps are less than 12m, which is regulatory. However, PFER does not exceed a maximum value of 19% regardless of the number of vehicles in the same scenario. Indeed, the PFER performance value for three or more vehicles does not change notably.

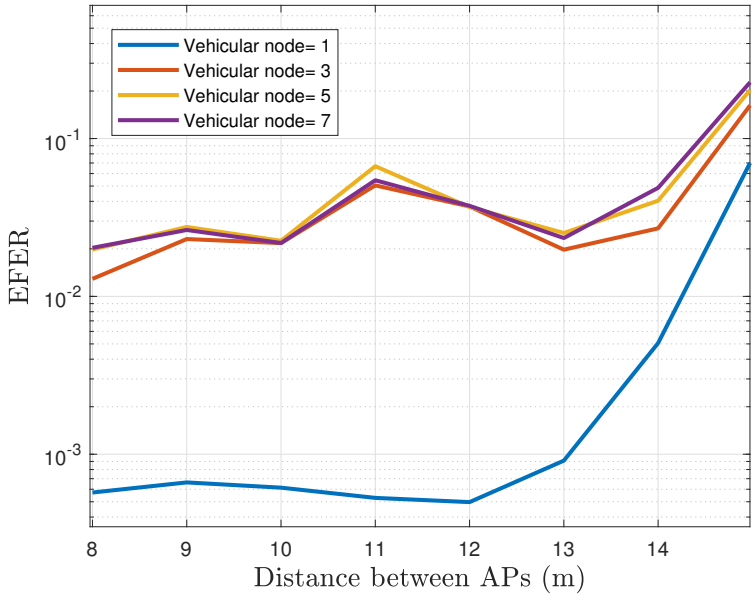

Figure 60: The EFER for different number of vehicular nodes operating in the network.

Finally, Figure 62 depicts the measured data rate with respect to the separation of the AP and the number of active vehicular nodes. Here, the data rate is reduced to 420 Kbps with $m = 3, 5$, and 7 vehicular nodes in the network. More interesting, it is worth noting how quickly the data rate of convergence is obtained when the separation between APs is under 14m. It means that the solution is scalable without significant penalties.

7.3.3 Results conclusions

The presented experimental simulations evaluate the performance of a vehicular VLC network in a tunnel scenario for single and multiple vehicles where different handover schemes were considered, including the novel proposal introduced in this thesis. The results provide further knowledge about the behavior of the VLC network in realistic use-case scenarios for vehicular users showing for example, how the network's performance can be affected by the number of users due to the shared medium. This is not an exclusive issue for VLC networks, other technologies as DSRC have also to deal with it. It is demonstrated in [123] that DSRC suffers similar drawbacks when the vehicle density grows. The packet delivery ratio diminishes

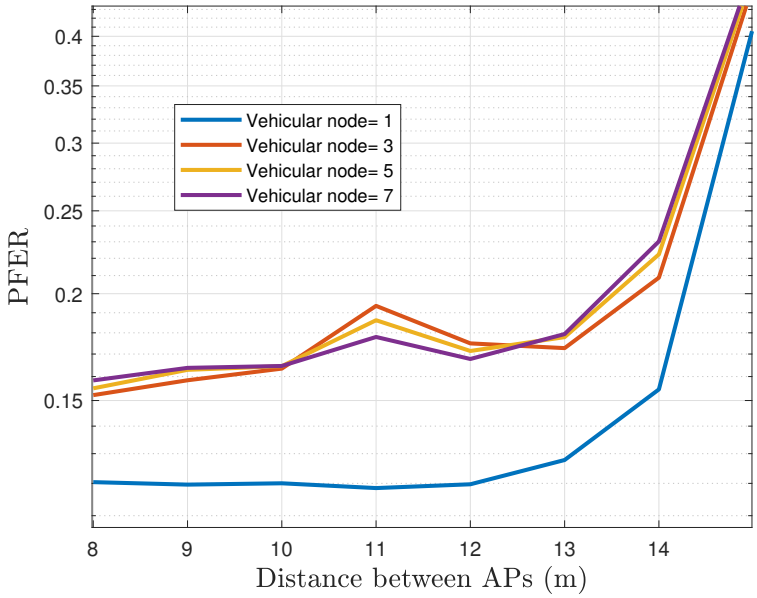

Figure 61: The PFER for different number of vehicular nodes operating in the network.

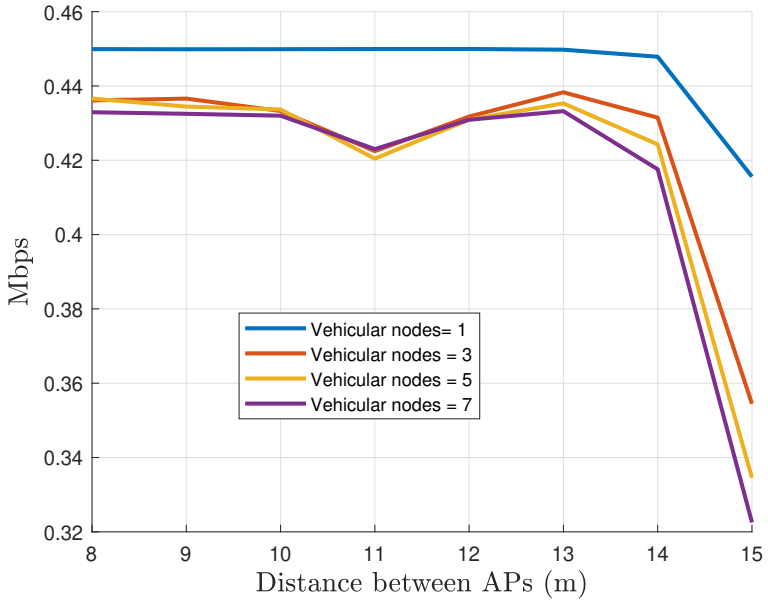

Figure 62: The data rate per vehicular node for different number of vehicular nodes operating in the network.

in DSCR under these conditions. Moreover, a fair comparison of the performance degradation for these two technologies is difficult due to their remarkable differences. On the one hand, VLC cell does not require sharing resources with multiple vehicular nodes, while DSRC cell provides service to a wide area. Thus, it has a channel used by a large number of nodes. On the other hand, a VLC network will require

more frequent handovers to provide service. This action will also limit the service quality.

Despite its disadvantages, the proposed VLC handover strategy appears as a promising scheme to support communication for some vehicular scenarios and provides an alternative for alternative networks supporting the conventional DSRC infraestructures.

Chapter 8

Conclusion and Future work

The scope of this thesis has focused on the mobility problem in VLC networks. The study has involved the handover problems of a potential application of VLC and proposing a solution to support a steady connection. This research work bonded to vehicular communications, which present peculiar restrictions such as a low latency tolerance to restore the communication when an outage occurs. Several aspects have been considered, such as the accuracy of the network performance simulation or the proposal of handover strategies specially adapted to this kind of system. Further, the design of the proposed scheme required the unique characteristics of the VLC technology of the vehicular surroundings. There is very little literature regarding the mobility issues in a VLC network, making the need to address many open to developing a functional solution. Therefore, the presented study provides valuable knowledge to sustain future work in this research area. This chapter presents the conclusions of the work described in this thesis, followed by suggestions for further research in this area.

8.1 Conclusions

In Chapter 2, the literature review shows that there is an interest from the scientific community and a need to include VLC in safety applications for ITS. This technology has followed the natural integration process, first studying the technology's theoretical limits through channel studies. Then, several works perform proof of concept and experimental validations to demonstrate its feasibility in vehicular scenarios. Naturally, the next step is to consider the interoperability and the integration of the technology to function as a network.

Some important conclusions can be obtained from the literature review. First, the application of VLC systems to vehicular networks considers OFDM modulation since it is resilient to adversary channel conditions. However, the utilization of the IEEE standard 802.15.7-2018 with OOK modulation has not been discarded, and some works studied its performance considering vehicular environments [51, 50, 49]. Second, there are some benefits that VLC technology presents in ITS applications. For

example, the channel is not affected by Doppler effects, and it possesses a long coherence time permitting the transmission of a long frame. Additionally, the average VLC links span some seconds in the V2V scheme, which is enough to exchange vital information [40, 39]. Moreover, the proof of concepts of this technology demonstrates its potential as a serious candidate to serve as a backup of DSRC [53].

The integration of VLC in ITS safety applications requires that vehicular nodes are always available in an emergency. It becomes a complicated goal because of the user's high-speed movement and the limited range of a VLC AP. Therefore, it creates the necessity to develop a low latency mobility support mechanism. According to the literature review, the handover solutions for VLC networks are still in the early stages. Most of the existing works focus on solutions for heterogeneous networks and indoor scenarios [85, 92, 89]. However, the significant differences with vehicular scenarios make them unfeasible without proper modifications, as *Murat et al.* with CoMP in [94] to mention an example. A third conclusion is that few recently published papers about the topic reflect that "Handover for vehicular VLC network" is an open issue with great potential.

After analyzing the literature outside VLC in technology such as RF, we can conclude that the longest delay during a handover is caused in the execution phase. Hence, the low latency requirements can only be achieved by a solution that considers jointly the detection process and resolution protocols. The works [124, 72, 74, 82] presents different alternatives to be explored such as PMIPv6, FMIPv6, among others. But, it is necessary to evaluate them together with wireless technology. Unfortunately, only [4] has studied end-to-end this problem.

Chapter 3 presents a description of the framework analyzing the standard IEEE 802.15.7-2018 [9]. After checking it meticulously, the main conclusion is that the standard does not provide a concrete solution to ensure a steady connection. Some minor mechanisms are helping to locate the AP with the strongest signal. Although, it needs to be requested by the user and expenses network resources. It is not ideal because the user needs a methodology to sense the link-state looking the best moment for a request. Neither the standard brings a protocol to speed up the ingress of the user to a new AP or prevent communication outage.

Chapter 4 introduces the methodology used in this work which has a simulation approach through system-level simulations. This approach was selected since analytical procedures such as Markov Chain [106] are complex and limited to exploring predefined scenarios. The simulation tool developed for VLC Networks is an accomplished milestone that covers Objective 2. The simulator meets the specifications of IEEE 802.15.7-2018 standard with a detailed description of the MAC layer. It highlights similar platforms because it evaluates PHY and MAC layers considering a realistic channel model. This approach can appraise an indirect optical link reflected in a scenario's surface through a Monte-Carlo ray-tracing simulator. Most of the works in the literature ignore the non-LOS contributions while they assess the channel access scheme [125, 126]. In chapter 5, some simulation tests were carried out to evaluate the effects of non-LOS components. These experiments have a node distribution that provides identical LOS components but different non-LOS

contributions. The outcomes demonstrate the importance of including multi-path contributions to evaluate MAC layer protocols for VLC systems. In particular, the CDMA/CA mechanism does not always collapse when the nodes do not get a direct signal contribution. We can conclude that an accurate evaluation of a VLC network requires precise channel models. Due to the high directionality and reflectance of the optical signal, the VLC channel depends highly on the scenario conditions.

There are several vehicular scenarios, each one with its peculiarities. The analysis of this study was centered on vehicular tunnels because it represents a controlled environment where DSRC performance is compromised. Chapter 6 presents the analysis of the proposed VLC Network from a physical layer perspective. The evaluation considers the characteristics and restrictions of a two-lane vehicular tunnel. MCRT simulations were employed to get the uplink and downlink CIR of different vehicle positions. This evaluation proceeds according to Objective 1. The results demonstrate that the system can support communication in this scenario by providing a high bandwidth. In addition, the collected data aimed to plan a handover solution. This chapter covers a relevant part of the thesis' work. Thus, there are several conclusions to discuss.

The illumination system in tunnel and streets follows strict normative [127, 117, 117]. We can conclude that the studies of VLC networks deployed in these scenarios need to consider such restrictions. Moreover, the singular radiations profile of the tunnel lamp and headlight needs to be considered, instead of using a typical Lambertian pattern, to estimate the VLC network capacity.

On the initial network proposal used to evaluate the channel, the RSU receiver location was separated from the other elements' position (Transmitter and Controller Unit), placing this sensor near the vehicular road. This novel configuration permits the RSU to get the LOS component from a vehicular node transmitter, instead of the typical channel model for V2I communication[38], where the receiver is always placed beside the transmitter. Although this action can be considered a minor contribution, it is relevant to mention that this alternative has not been explored to improve communication on VLC systems. The results revealed that the receiver's location empowers the system to work full-duplex VLC operation mode in vehicular scenarios. Furthermore, it guarantees a low delay spread in both links (V2I and I2V). Moreover, the link is enough sturdy to support communication over 15 meters. These desirable specs guarantee the improved performance of both VLC links validating Hypothesis 1.

As part of the analysis, the channel of multiple node locations was connected to study the temporal nature of the communication link. In this evaluation, we suppose the vehicle moves in rectilinear movement at a steady speed of 100 km/h. After processing the results, both the V2I and I2V links present long coherence-time over tens milliseconds. It means that the channel can hold large frames without interruption or channel degradation. In the literature, there is a similar analysis for the V2V case in [40, 39]. In spite, this is the only work that considers the vehicle movements. The remainder literature takes care of the spatial distribution of the BER using the vehicle as reference [41, 42] but ignoring the vehicle movement. The main conclusion

of this point is that the channel conditions are stable to support the communication in both links.

Furthermore, the uplink presents a continuous increment tendency reflected in its DC channel gain, followed by an abrupt disruption. This channel pattern puts at risk the link-state because the detection algorithms have a reduced error margin. Hence, it is necessary to provide communication redundancy for the uplink. Considering this point, chapter 6.5 introduces modifications to the network topology to solve this problem. This new system architecture is a novel solution defined as "2.5 Layer". The new network topology deals with one of the fundamental problems in the VLC system is the transmitter's narrow radiation pattern, which forces the user nodes to point to the AP. This solution enables all network receivers to acquire the optical information jointly, and then it is redirected to the destination AP. This action increases the communication range of an AP. Chapter 7 evaluates a fair comparison between the classical start topology and this proposal, where the latter demonstrates superior performance and soft transition. We conclude that the smart network design can expand the VLC network capabilities. The proposed solution can adapt to enhance home and office networks, but it is necessary to do extensive studies.

Finally, both link signals present drawbacks to be used as an indicator to estimate the initialization of the mobility process. On the one hand, the downlink signal depends on the tunnel lamp position of the two possible configurations (center and lateral placed), where the channel behavior changes drastically in both cases. On the other hand, the uplink signal is modified by the lateral displacement of the vehicle. It means that both optical signals suffer variations that can compromise the detection. Hence, the best option to detect the user movement is using both links' information. Additionally, the process needs to be sensitive to prioritize the cell exchange. For this reason, the algorithm will trigger when at least one of the conditions is completed. The obtained detection algorithm achieves Objective 4.

Chapter 7 show the developed handover solution composed of a modified HMIPv6 protocol and a detection algorithm. The sum of both strategies completes Objective 3. The test reveals an efficient operation of the proposed scheme providing a steady connection when the vehicle transit in the tunnel. Several conclusions were obtained in this chapter, but possibly the most relevant are described next.

We observe that the sum of both strategies plus the handover protocol, the vehicular nodes are connected 99.9% of the time, which allows them to receive an emergency message. In addition, the frame error rate of $5e^{-4}$ shown in EFER, for a single user, can be considered as error-free. These results illustrate the potential of the solution to support a VLC network deployed in this scenario. The outcomes reveal that the vehicle possesses seamless communication validating Hypothesis 2. Besides, the validation test considered the hypothetical case of a vehicle that demands 450 kbps without a service impact. These conditions are more demanding than the requirement of safety ITS application. Moreover, the number of retransmissions is low, guaranteeing almost null latency. Following the specs presented in [45], the

VLC system with the handover strategies can overstep its fulfillments validating Hypothesis 3.

The handover strategy developed for this particular scenario can be used as an initial point to develop solutions for a range of urban environments. However, the user presents complex mobility patterns with more degrees of freedom, complicating the handover estimation, and requiring more complex detection algorithms. Also, several data frames were lost during the handover resolution, indicating the need to develop instruments to recover the packets lost and queued in the AP during the handover process.

While the network works with multiple vehicular nodes, it exposes a slight operation downgrade. Even so, the system remains operative when the number of nodes continues growing. It means that the network size can scale up without significant repercussions. In conclusion, we can infer that the VLC can support the communication of a moderate number of vehicles without compromising its connectivity. Finally, the evidence reveals the presented strategy as a potential solution that needs refining. The tests corroborate the functionality of handover to conclude with Objective 5.

8.2 Future work

This thesis represents an introductory study of handover solutions for VLC networks in a vehicular environment. Consequently, there are still a lot of open issues to solve, and in the next years, more people will be working in this research area. This section summarizes the lines of research derived from this thesis work.

The first point to discuss is the execute phase, based on the HMIPv6 protocol, which splits the network into inter-domain and intra-domain. The presented examination covers the situations where the user performs a handover to an AP inside the inter-domain. However, a single MAP has limitations of the maximum number of users and APs that can provide service. As a consequence, a long tunnel scenario needs multiple networks operating to provide service. Thus, it will be cases when a moving user needs to connect to an RSU that belongs to another domain requiring an intra-domain handover. For this reason, it is necessary the inclusion of extra mechanisms to solve these cases. It is a similar situation when a vehicular node ingress/egress the tunnel, and so there is necessary to do a handover from/to a DSRC network. One possible solution is the use of PMIPv6 [124] as complementary scheme. As well as, there is necessary to do a formal study about the size limits of the HMIPv6.

The second point to debate is the presented scheme based on a hard handover where the low latency makes it imperceptible for the users. Unfortunately, there are some packets lost during the handover resolution. Thus, it is necessary to explore alternatives to soft these transitions. Between the options to study is the integration of the JT-CoMP scheme [94] in our handover solution. Another possibility is to elaborate on a new mechanism to support the handshake. For example, an early proposal draft could be the following. The RSU can store the unsuccessfully transmitted frames

for a determinate period. Then, when the handover has been completed the queued frames and a copy of these undelivered frames could be sent to the next user's AP. Although, this is a brief preliminary description to cite an example. This kind of protocol requires additional mechanisms to avoid problems such as storing expired information or lost essential frames.

The detection algorithm in this work shows a good estimation to prevent failures in this scenario. As part of the future works, the validation process could be extended comparing the performance with other proposals from literature, such as skippi or flight. There is a special interest to contrast its operation with Flight because both solutions were planned to cover vehicular scenarios. To do this, we need the specifications and understand in detail its procedure to elaborate an accurate simulation model.

Furthermore, the 2.5 layer topology is a solution that has the potential to solve the communication issues in the VLC network for diverse environments such as homes and offices. This solution can deal with one of the biggest obstacles to developing a full-duplex VLC system that is the uplink range limitations. In a typical VLC network, the user node's transmitter must beam the AP's receiver. Oppositely, in the proposed network it is not necessary. For example, in a hypothetical scenario where there is a " 2.5 layer topology" network deployed in an office, and its receivers are spread in many points of the room. This network design could support the communication of the VLC gadget when it is doing short distance moves and changing its direction. Moreover, this network proposal can be used jointly with handover schemes to ensure a seamless connection.

Finally, we are interested to explore alternatives for the detection process. The handover detection can be empowered by the implementation of a Neural Network (NN) to find the best parameters configuration in a handover scheme. In particular, NN with a Reinforcement Learning scheme (NN-RL) presents desirable characteristics over supervised methods. Because it does not require a labeled dataset to train the network. This means that there is not necessary to measure the optical signal of a vast number of positions inside the room to have enough data. Instead, the NN-RL generates this dataset while the network is operating using the communication frames to generate the inputs signals for NN. Then, it classifies the information based on its experience. This NN does handover estimations using this data and monitoring the result of its decision checking the user connection after a while. Then, NN-RL classify it if was right or wrong to be accounted for in the next estimations. As consequence, its predictions gradually will be more accurate improving the network performance. This approach allows flexible adaption of the handover scheme to scenarios with different node distributions. This future line can be studied using the different evaluation tools developed in this thesis work. The NN methods can be included inside the VLC network simulator doing minor changes in its structure.

Bibliography

[1] Tseng, H.-Y. *et al.* Characterizing link asymmetry in vehicle-to-vehicle visible light communications. In *2015 IEEE Vehicular Networking Conference (VNC)*, 88–95 (2015).

[2] Demir, M. S., Miramirkhani, F. & Uysal, M. Handover in vlc networks with coordinated multipoint transmission. In *2017 IEEE International Black Sea Conference on Communications and Networking (BlackSeaCom)*, 1–5 (2017).

[3] Saud, M. S., Chowdhury, H. & Katz, M. Heterogeneous software-defined networks: Implementation of a hybrid radio-optical wireless network. In *2017 IEEE Wireless Communications and Networking Conference (WCNC)*, 1–6 (2017).

[4] Alizadeh Jarchlo, E. *et al.* Li-wi: An upper layer hybrid vlc-wifi network handover solution. *Ad Hoc Networks* **124**, 102705 (2022). URL `https://www.sciencedirect.com/science/article/pii/S157087052100202X`.

[5] Cisco Annual Internet Report (2018–2023) White Paper. Tech. Rep., CISCO (2020).

[6] (GSA), G. M. S. A. Lte ecosystem july 2020 – global status report.

[7] Pathak, P. H., Feng, X., Hu, P. & Mohapatra, P. Visible light communication, networking, and sensing: A survey, potential and challenges. *IEEE Communications Surveys Tutorials* **17**, 2047–2077 (2015).

[8] Komine, T. & Nakagawa, M. Performance evaluation of visible-light wireless communication system using white led lightings. In *Proceedings. ISCC 2004. Ninth International Symposium on Computers And Communications (IEEE Cat. No.04TH8769)*, vol. 1, 258–263 Vol.1 (2004).

[9] Ieee standard for local and metropolitan area networks–part 15.7: Short-range optical wireless communications. *IEEE Std 802.15.7-2018 (Revision of IEEE Std 802.15.7-2011)* 1–407 (2019).

[10] System architecture, physical layer and data link layer specification. *G.9991 : High-speed indoor visible light communication transceiver* 1–88 (2019).

[11] Signify. High performance secure data connectivity where you need it. `https://www.signify.com/global/innovation/trulifi` (2020). [Online; accessed 04-November-2021].

[12] Lee, C. *et al.* 26 gbit/s lifi system with laser-based white light transmitter. *Journal of Lightwave Technology* 1–1 (2021).

[13] Miramirkhani, F. & Uysal, M. Channel modeling and characterization for visible light communications. *IEEE Photonics Journal* **7**, 1–16 (2015).

[14] Lopez-Hernandez, F. J., Perez-Jimenez, R. & Santamaria, A. Monte carlo calculation of impulse response on diffuse ir wireless indoor channels. *Electronics Letters* **34**, 1260–1262 (1998).

[15] Kenney, J. B. Dedicated short-range communications (dsrc) standards in the united states. *Proceedings of the IEEE* **99**, 1162–1182 (2011).

[16] Ahmed-Zaid, F. *et al.* Vehicle safety communications – applications (vsc-a) final report: Appendix volume 3 security (2011).

[17] Cailean, A.-M., Cagneau, B., Chassagne, L., Popa, V. & Dimian, M. A survey on the usage of dsrc and vlc in communication-based vehicle safety applications. In *2014 IEEE 21st Symposium on Communications and Vehicular Technology in the Benelux (SCVT)*, 69–74 (2014).

[18] Enhance lighting for the internet of things(eliot). `https://www.eliot-h2020.eu`. Accessed: 2021-11-26.

[19] European network on future generation optical wireless communication technologies - newfocus. `https://www.newfocus-cost.eu`. Accessed: 2021-11-26.

[20] Visible light based interoperability and networking (vision). `https://www.vision-itn.eu`. Accessed: 2021-11-26.

[21] Burchardt, H., Serafimovski, N., Tsonev, D., Videv, S. & Haas, H. Vlc: Beyond point-to-point communication. *IEEE Communications Magazine* **52**, 98–105 (2014).

[22] Ieee standard for local and metropolitan area networks–part 15.7: Short-range wireless optical communication using visible light. *IEEE Std 802.15.7-2011* 1–309 (2011).

[23] Dissanayake, S. D. & Armstrong, J. Comparison of aco-ofdm, dco-ofdm and ado-ofdm in im/dd systems. *Journal of Lightwave Technology* **31**, 1063–1072 (2013).

[24] Gfeller, F. & Bapst, U. Wireless in-house data communication via diffuse infrared radiation. *Proceedings of the IEEE* **67**, 1474–1486 (1979).

[25] Barry, J., Kahn, J., Krause, W., Lee, E. & Messerschmitt, D. Simulation of multipath impulse response for indoor wireless optical channels. *IEEE Journal on Selected Areas in Communications* **11**, 367–379 (1993).

[26] Lopez-Hernandez, F. J., Perez-Jimenez, R. & Santamaria, A. Ray-tracing algorithms for fast calculation of the channel impulse response on diffuse IR wireless indoor channels. *Optical Engineering* **39**, 2775 – 2780 (2000). URL `https://doi.org/10.1117/1.1287397`.

[27] Nguyen, H. *et al.* A matlab-based simulation program for indoor visible light communication system. In *2010 7th International Symposium on Communication Systems, Networks Digital Signal Processing (CSNDSP 2010)*, 537–541 (2010).

[28] Mana, S. M. *et al.* Lifi experiments in a hospital. In *2020 Optical Fiber Communications Conference and Exhibition (OFC)*, 1–3 (2020).

[29] Hasan, M. J., Khalighi, M. A., García-Márquez, J. & Béchadergue, B. Performance analysis of optical-cdma for uplink transmission in medical extra-wbans. *IEEE Access* **8**, 171672–171685 (2020).

[30] Haddad, O., Khalighi, M.-A., Zvanovec, S. & Adel, M. Channel characterization and modeling for optical wireless body-area networks. *IEEE Open Journal of the Communications Society* **1**, 760–776 (2020).

[31] Jungnickel, V. *et al.* Lifi for industrial wireless applications. In *2020 Optical Fiber Communications Conference and Exhibition (OFC)*, 1–3 (2020).

[32] Bober, K. L. *et al.* Distributed multiuser mimo for lifi in industrial wireless applications. *Journal of Lightwave Technology* **39**, 3420–3433 (2021).

[33] Igboanusi, I. S., Nwakanma, C. I., Lee, J. M. & Kim, D.-S. Vlc-uwb hybrid (vuh) network for indoor industrial robots at military warehouses / distribution centers. In *2019 International Conference on Information and Communication Technology Convergence (ICTC)*, 762–766 (2019).

[34] Matus, V., Guerra, V., Zvanovec, S., Rabadan, J. & Perez-Jimenez, R. Sandstorm effect on experimental optical camera communication. *Appl. Opt.* **60**, 75–82 (2021). URL `http://www.osapublishing.org/ao/abstract.cfm?URI=ao-60-1-75`.

[35] Chavez-Burbano, P. *et al.* Optical camera communication system for internet of things based on organic light emitting diodes. *Electronics Letters* **55**, 334–336 (2019). URL `https://ietresearch.onlinelibrary.wiley.com/doi/abs/10.1049/el.2018.8037`. `https://ietresearch.onlinelibrary.wiley.com/doi/pdf/10.1049/el.2018.8037`.

[36] Wada, M., Yendo, T., Fujii, T. & Tanimoto, M. Road-to-vehicle communication using led traffic light. In *IEEE Proceedings. Intelligent Vehicles Symposium, 2005.*, 601–606 (2005).

[37] Kumar, N., Alves, L. N. & Aguiar, R. L. Design and analysis of the basic parameters for traffic information transmission using vlc. In *2009 1st International Conference on Wireless Communication, Vehicular Technology, Information Theory and Aerospace Electronic Systems Technology*, 798–802 (2009).

[38] Lee, S. J., Kwon, J. K., Jung, S. Y. & Kwon, Y. H. Simulation modeling of visible light communication channel for automotive applications. In *2012 15th International IEEE Conference on Intelligent Transportation Systems*, 463–468 (2012).

[39] Wu, L. & Tsai, H. Modeling vehicle-to-vehicle visible light communication link duration with empirical data. In *2013 IEEE Globecom Workshops (GC Wkshps)*, 1103–1109 (2013).

[40] Cui, Z., Wang, C. & Tsai, H. Characterizing channel fading in vehicular visible light communications with video data. In *2014 IEEE Vehicular Networking Conference (VNC)*, 226–229 (2014).

[41] Luo, P. *et al.* Fundamental analysis of a car to car visible light communication system. In *2014 9th International Symposium on Communication Systems, Networks Digital Sign (CSNDSP)*, 1011–1016 (2014).

[42] Uysal, M., Ghassemlooy, Z., Bekkali, A., Kadri, A. & Menouar, H. Visible light communication for vehicular networking: Performance study of a v2v system using a measured headlamp beam pattern model. *IEEE Vehicular Technology Magazine* **10**, 45–53 (2015).

[43] Kim, Y. H., Cahyadi, W. A. & Chung, Y. H. Experimental demonstration of vlc-based vehicle-to-vehicle communications under fog conditions. *IEEE Photonics Journal* **7**, 1–9 (2015).

[44] Kim, Y.-H., Cahyadi, W. A. & Chung, Y. H. Experimental demonstration of led-based vehicle to vehicle communication under atmospheric turbulence. In *2015 International Conference on Information and Communication Technology Convergence (ICTC)*, 1143–1145 (2015).

[45] Căilean, A. & Dimian, M. Current challenges for visible light communications usage in vehicle applications: A survey. *IEEE Communications Surveys Tutorials* **19**, 2681–2703 (2017).

[46] Cailean, A.-M. *et al.* Visible light communications cooperative architecture for the intelligent transportation system. In *2013 IEEE 20th Symposium on Communications and Vehicular Technology in the Benelux (SCVT)*, 1–5 (2013).

[47] Yoo, J.-H. *et al.* Demonstration of vehicular visible light communication based on led headlamp. In *2013 Fifth International Conference on Ubiquitous and Future Networks (ICUFN)*, 465–467 (2013).

[48] Yu, S., Shih, O., Tsai, H., Wisitpongphan, N. & Roberts, R. D. Smart automotive lighting for vehicle safety. *IEEE Communications Magazine* **51**, 50–59 (2013).

[49] Bellè, A., Falcitelli, M., Petracca, M. & Pagano, P. Development of ieee802.15.7 based its services using low cost embedded systems. In *2013 13th International Conference on ITS Telecommunications (ITST)*, 419–425 (2013).

[50] Turan, B., Narmanlioglu, O., Ergen, S. C. & Uysal, M. Physical layer implementation of standard compliant vehicular vlc. In *2016 IEEE 84th Vehicular Technology Conference (VTC-Fall)*, 1–5 (2016).

[51] Cailean, A.-M. & Dimian, M. Impact of ieee 802.15.7 standard on visible light communications usage in automotive applications. *IEEE Communications Magazine* **55**, 169–175 (2017).

[52] Aly, B., Elamassie, M. & Uysal, M. Experimental characterization of multi-hop vehicular vlc systems. In *2021 IEEE 32nd Annual International Symposium on Personal, Indoor and Mobile Radio Communications (PIMRC)*, 1–6 (2021).

[53] Fraunhofer Institute for Telecommunications, H., Heinrich Hertz Institute. Lifi-technology enables driverless platooning of trucks for the first time on japanese highway.

[54] Paasch, C., Detal, G., Duchene, F., Raiciu, C. & Bonaventure, O. Exploring mobile/wifi handover with multipath tcp. In *Proceedings of the 2012 ACM SIGCOMM Workshop on Cellular Networks: Operations, Challenges, and Future Design*, CellNet '12, 31–36 (Association for Computing Machinery, New York, NY, USA, 2012). URL `https://doi.org/10.1145/2342468.2342476`.

[55] Stevens-Navarro, E. & Wong, V. Comparison between vertical handoff decision algorithms for heterogeneous wireless networks. In *2006 IEEE 63rd Vehicular Technology Conference*, vol. 2, 947–951 (2006).

[56] Du, Z., Wang, C., Sun, Y. & Wu, G. Context-aware indoor vlc/rf heterogeneous network selection: Reinforcement learning with knowledge transfer. *IEEE Access* **6**, 33275–33284 (2018).

[57] Chen, L. & Li, H. An mdp-based vertical handoff decision algorithm for heterogeneous wireless networks. In *2016 IEEE Wireless Communications and Networking Conference*, 1–6 (2016).

[58] Kassab, M., Bonnin, J. M. & Belghith, A. Fast and secure handover in wlans: An evaluation of the signaling overhead. In *2008 5th IEEE Consumer Communications and Networking Conference*, 770–775 (2008).

[59] Hamza, E. B. & Kimura, S. A scalable sdn-epc architecture based on openflow-enabled switches to support inter-domain handover. In *2016 10th International Conference on Innovative Mobile and Internet Services in Ubiquitous Computing (IMIS)*, 272–277 (2016).

[60] Wang, Y., Videv, S. & Haas, H. Dynamic load balancing with handover in hybrid li-fi and wi-fi networks. In *2014 IEEE 25th Annual International Symposium on Personal, Indoor, and Mobile Radio Communication (PIMRC)*, 575–579 (2014).

[61] Sur, A. & Sicker, D. Multi layer rules based framework for vertical handoff. In *2nd International Conference on Broadband Networks, 2005.*, 571–580 Vol. 1 (2005).

[62] Bui, T.-C., Kiravittaya, S., Nguyen, N.-H., Nguyen, N.-T. & Spirinmanwat, K. Leds configuration method for supporting handover in visible light communication. In *TENCON 2014 - 2014 IEEE Region 10 Conference*, 1–6 (2014).

[63] Da Costa Silva, K., Becvar, Z. & Frances, C. R. L. Adaptive hysteresis margin based on fuzzy logic for handover in mobile networks with dense small cells. *IEEE Access* **6**, 17178–17189 (2018).

[64] Inzerilli, T., Vegni, A. M., Neri, A. & Cusani, R. A location-based vertical handover algorithm for limitation of the ping-pong effect. In *2008 IEEE International Conference on Wireless and Mobile Computing, Networking and Communications*, 385–389 (2008).

[65] Choi, H.-H., Lim, J. B., Hwang, H. & Jang, K. Optimal handover decision algorithm for throughput enhancement in cooperative cellular networks. In *2010 IEEE 72nd Vehicular Technology Conference - Fall*, 1–5 (2010).

[66] Becvar, Z., Cheng, R.-G. & Charvat, M. Mobility management for d2d communication combining radio frequency and visible light communications bands. *Wireless Networks* **62**, 5473–5484 (2020).

[67] Liu, R. & Zhang, C. Dynamic dwell timer for vertical handover in vlc-wlan heterogeneous networks. In *2017 13th International Wireless Communications and Mobile Computing Conference (IWCMC)*, 1256–1260 (2017).

[68] Wu, X. & Haas, H. Handover skipping for lifi. *IEEE Access* **7**, 38369–38378 (2019).

[69] Perkins, C. E. & Johnson, D. B. Mobility support in ipv6. In *Proceedings of the 2nd Annual International Conference on Mobile Computing and Networking*, MobiCom '96, 27–37 (Association for Computing Machinery, New York, NY, USA, 1996). URL `https://doi.org/10.1145/236387.236400`.

[70] Osborne, L., Abdel-Hamid, A. & Ramadugu, R. A performance comparison of mobile ipv6, hierarchical mobile ipv6, and mobile ipv6 regional registrations. In *2005 International Conference on Wireless Networks, Communications and Mobile Computing*, vol. 2, 1545–1550 vol.2 (2005).

[71] Perkins, C. E. & Johnson, D. B. Mobility support in ipv6. In *Proceedings of the 2nd Annual International Conference on Mobile Computing and Networking*, MobiCom '96, 27–37 (Association for Computing Machinery, New York, NY, USA, 1996). URL `https://doi.org/10.1145/236387.236400`.

[72] Kempf, J., Wood, J. & Fu, G. Fast mobile ipv6 handover packet loss performance: measurement for emulated real time traffic. In *2003 IEEE Wireless Communications and Networking, 2003. WCNC 2003.*, vol. 2, 1230–1235 vol.2 (2003).

[73] Chiang, M.-S. & Kuo, Y.-L. An improved fast handover control scheme over the wireless networks. In *2015 Third International Conference on Robot, Vision and Signal Processing (RVSP)*, 306–309 (2015).

[74] Castelluccia, C. Hmipv6: A hierarchical mobile ipv6 proposal. *SIGMOBILE Mob. Comput. Commun. Rev.* **4**, 48–59 (2000). URL `https://doi.org/10.1145/360449.360474`.

[75] Hasan, S. F. A discussion on software-defined handovers in hierarchical mipv6 networks. In *2015 IEEE 10th Conference on Industrial Electronics and Applications (ICIEA)*, 140–144 (2015).

[76] Kang, J.-E., Kum, D.-W., Li, Y. & Cho, Y.-Z. Seamless handover scheme for proxy mobile ipv6. In *2008 IEEE International Conference on Wireless and Mobile Computing, Networking and Communications*, 410–414 (2008).

[77] Prados-Garzon, J. *et al.* Handover implementation in a 5g sdn-based mobile network architecture. In *2016 IEEE 27th Annual International Symposium on Personal, Indoor, and Mobile Radio Communications (PIMRC)*, 1–6 (2016).

[78] Lee, J. & Yoo, Y. Handover cell selection using user mobility information in a 5g sdn-based network. In *2017 Ninth International Conference on Ubiquitous and Future Networks (ICUFN)*, 697–702 (2017).

[79] Lee, J. M., Yu, M. J., Yoo, Y. H. & Choi, S. G. A new scheme of global mobility management for inter-vanets handover of vehicles in v2v/v2i network environments. In *2008 Fourth International Conference on Networked Computing and Advanced Information Management*, vol. 2, 114–119 (2008).

[80] Tsourdos, S., Michalas, A., Sgora, A. & Vergados, D. D. Enhanced fast handovers for pmipv6 in vehicular environments. In *IISA 2014, The 5th International Conference on Information, Intelligence, Systems and Applications*, 420–425 (2014).

[81] Farahbakhsh, R. & Sorooshi, M. Cross layering design of ipv6 fast handover in mobile wimax. In *2010 17th International Conference on Telecommunications*, 304–308 (2010).

[82] Ryu, S., Kim, M. & Mun, Y. Enhanced fast handovers for proxy mobile ipv6. In *2009 International Conference on Computational Science and Its Applications*, 39–43 (2009).

[83] Boutabia, M. & Afifi, H. Mih-based fmipv6 optimization for fast-moving mobiles. In *2008 Third International Conference on Pervasive Computing and Applications*, vol. 2, 616–620 (2008).

[84] Yun, L., Ying, W., Zhao, W. & You, X. A fast handover scheme in ieee802.16 relay networks. In *2010 Second International Conference on Future Networks*, 243–247 (2010).

[85] Kizilirmak, R. C., Narmanlioglu, O. & Uysal, M. Centralized light access network (c-lian): A novel paradigm for next generation indoor vlc networks. *IEEE Access* **5**, 19703–19710 (2017).

[86] Tran, C.-N., Hoang, T.-M. & Nguyen, N.-H. Proactive link handover deploying coordinated transmission for indoor visible light communications (vlc) networks. *Journal of Optical Communications* (2020). URL `https://doi.org/10.1515/joc-2019-0282`.

[87] Liang, S., Tian, H., Fan, B. & Bai, R. A novel vertical handover algorithm in a hybrid visible light communication and lte system. In *2015 IEEE 82nd Vehicular Technology Conference (VTC2015-Fall)*, 1–5 (2015).

[88] Liu, R. & Zhang, C. Dynamic dwell timer for vertical handover in vlc-wlan heterogeneous networks. In *2017 13th International Wireless Communications and Mobile Computing Conference (IWCMC)*, 1256–1260 (2017).

[89] Dinc, E., Ergul, O. & Akan, O. B. Soft handover in ofdma based visible light communication networks. In *2015 IEEE 82nd Vehicular Technology Conference (VTC2015-Fall)*, 1–5 (2015).

[90] Younus, S. H., Al-Hameed, A. A. & Hussein, A. T. Novel handover scheme for indoor vlc systems. *IET Communications* **15**, 1053–1059 (2021). URL `https://ietresearch.onlinelibrary.wiley.com/doi/abs/10.1049/cmu2.12141`. `https://ietresearch.onlinelibrary.wiley.com/doi/pdf/10.1049/cmu2.12141`.

[91] Chowdhury, H. & Katz, M. Cooperative data download on the move in indoor hybrid (radio-optical) wlan-vlc hotspot coverage. *Transactions on Emerging Telecommunications Technologies* **25**, 666–677 (2014). URL `https://onlinelibrary.wiley.com/doi/abs/10.1002/ett.2841`. `https://onlinelibrary.wiley.com/doi/pdf/10.1002/ett.2841`.

[92] Saud, M. S. & Katz, M. Implementation of a hybrid optical-rf wireless network with fast network handover. In *European Wireless 2017; 23th European Wireless Conference*, 1–6 (2017).

[93] Narmanlioglu, O. & Uysal, M. Event-triggered adaptive handover for centralized hybrid vlc/mmw networks. *IEEE Transactions on Communications* 1–1 (2021).

[94] Demir, M. S., Eldeeb, H. B. & Uysal, M. Comp-based dynamic handover for vehicular vlc networks. *IEEE Communications Letters* **24**, 2024–2028 (2020).

[95] Shao, S. *et al.* Optimizing handover parameters by q-learning for heterogeneous radio-optical networks. *IEEE Photonics Journal* **12**, 1–15 (2020).

[96] Dang, Q.-H. & Yoo, M. Handover procedure and algorithm in vehicle to infrastructure visible light communication. *IEEE Access* **5**, 26466–26475 (2017).

[97] Jarchlo, E. A. *et al.* Flight: A flexible light communications network architecture for indoor environments. In *2019 15th International Conference on Telecommunications (ConTEL)*, 1–6 (2019).

[98] Jarchlo, E. A. *et al.* Fdla: A novel frequency diversity and link aggregation solution for handover in an indoor vehicular vlc network. *IEEE Transactions on Network and Service Management* 1–1 (2021).

[99] Abualhoul, M., Al-Bado, M., Shagdar, O. & Nashashibi, F. A Proposal for VLC-Assisting IEEE802.11p Communication for Vehicular Environment Using a Prediction-based Handover. In *ITSC 2018 – 21st IEEE International Conference on Intelligent Transportation Systems* (Maui, Hawaii, U.S. Outlying Islands, 2018). URL `https://hal.inria.fr/hal-01888576`.

[100] Pfefferkorn, D., Helmholdt, K. & Blume, H. Performance estimation of indoor optical wireless communication systems using omnet++. In *2017 IEEE 22nd International Workshop on Computer Aided Modeling and Design of Communication Links and Networks (CAMAD)*, 1–5 (2017).

[101] Junho Hwang, Tronghop Do & Myungsik Yoo. Performance analysis on mac protocol based on beacon-enabled visible personal area networks. In *2013 Fifth International Conference on Ubiquitous and Future Networks (ICUFN)*, 384–388 (2013).

[102] Wang, Z., Liu, Y., Lin, Y. & Huang, S. Full-duplex mac protocol based on adaptive contention window for visible light communication. *IEEE/OSA Journal of Optical Communications and Networking* **7**, 164–171 (2015).

[103] Ley-Bosch, C., Alonso-González, I., Sanchez-Rodriguez, D. & Ramírez-Casañas, C. *Evaluation of the effects of hidden node problems in IEEE 802.15.7 uplink performance.* (2016). URL `http://bibproxy.ulpgc.es/login?url=https://search.ebscohost.com/login.aspx?direct=true&db=ir01603a&AN=ulpgc.10553.52545&lang=es&site=eds-live&scope=site`.

[104] Jiang, Z., Zhou, X., She, Y. & Huang, L. An enhanced slotted csma/ca algorithm based on data aggregation for ieee802.15.4 in wireless sensor network. In *2014 4th IEEE International Conference on Information Science and Technology*, 635–639 (2014).

[105] Mehr, K. A., Nobar, S. K. & Niya, J. M. Ieee 802.15.7 mac under unsaturated traffic: Performance analysis and queue modeling. *IEEE/OSA Journal of Optical Communications and Networking* **7**, 875–884 (2015).

[106] Dang, N. T. & Mai, V. V. A phy/mac cross-layer analysis for ieee 802.15.7 uplink visible local area network. *IEEE Photonics Journal* **11**, 1–17 (2019).

[107] Aldalbahi, A., Rahaim, M., Khreishah, A., Ayyash, M. & Little, T. D. C. Visible light communication module: An open source extension to the ns3 network simulator with real system validation. *IEEE Access* **5**, 22144–22158 (2017).

[108] Rodríguez, S. P., Jiménez, R. P., Mendoza, B. R., Hernández, F. J. L. & Alfonso, A. J. A. Simulation of impulse response for indoor visible light communications using 3d cad models. *EURASIP Journal on Wireless Communications and Networking* **2013**, 1–7 (2013).

[109] FJ Lopez-Hermandez, M. B. Dustin: algorithm for calculation of impulse response on ir wireless indoor channels. In *Electronics Letters*, vol. 33, 1804–1806 (1997).

[110] Lopez-Hernandez, F. J., Perez-Jimenez, R. & Santamaria, A. Ray-tracing algorithms for fast calculation of the channel impulse response on diffuse IR wireless indoor channels. *Optical Engineering* **39**, 2775 – 2780 (2000). URL `https://doi.org/10.1117/1.1287397`.

[111] Torres-Zapata, E., Guerra, V., Rabadan, J., Luna-Rivera, M. & Perez-Jimenez, R. Mac/phy comprehensive visible light communication networks simulation. *Sensors* **20** (2020). URL `https://www.mdpi.com/1424-8220/20/21/6014`.

[112] Nobar, S. K., Mehr, K. A. & Niya, J. M. Comprehensive performance analysis of ieee 802.15.7 csma/ca mechanism for saturated traffic. *IEEE/OSA Journal of Optical Communications and Networking* **7**, 62–73 (2015).

[113] Meng, F. & Han, Y. A new association scheme of ieee 802.15.4 for real-time applications. In *2009 5th International Conference on Wireless Communications, Networking and Mobile Computing*, 1–5 (2009).

[114] Javed, M., Zen, K., Lenando, H. B. & Zen, H. Fast association process (fap) of beacon enabled for ieee 802.15.4 in strong mobility. In *2013 8th International Conference on Information Technology in Asia (CITA)*, 1–8 (2013).

[115] Hrovat, A., Guan, K. & Javornik, T. Traffic impact on radio wave propagation at millimeter-wave band in tunnels for 5g communications. In *2017 11th European Conference on Antennas and Propagation (EUCAP)*, 2903–2906 (2017).

[116] Viittala, H., Soderi, S., Saloranta, J., Hamalainen, M. & Iinatti, J. An experimental evaluation of wifi-based vehicle-to-vehicle (v2v) communication in a tunnel. In *2013 IEEE 77th Vehicular Technology Conference (VTC Spring)*, 1–5 (2013).

[117] C. Jeremy Hung, J. M. P. P. N. M. P., PE & John Wisniewski, P. Technical manual for design and construction of road tunnels — civil elements. Standard, U.S. Department of Transportation Publication Federal Highway Administration (FHWA), Madrid, Spain (2009).

[118] Dirección General de Industria, Energía y Minas de Madrid. Guia de iluminación en tuneles e infraestructuras subterraneas. Standard, Consejería de Economía y Hacienda de Madrid, Madrid, Spain (2015). URL `https://www.fenercom.com/pdf/publicaciones/`

Guia-de-iluminacion-en-tuneles-e-infraestructuras-subterraneas-fenercom-2015.pdf.

[119] Adrian, W. & Jobanputra, R. Influence of pavement reflectance on lighting for parking lots (2005).

[120] Herold, M. *Spectral Characteristics of Asphalt Road Surfaces* (2007).

[121] Kim, C.-M., Choi, S.-I. & Koh, S.-J. Idmp-vlc: Iot device management protocol in visible light communication networks. In *2017 19th International Conference on Advanced Communication Technology (ICACT)*, 578–583 (2017).

[122] Aljeri, N. & Boukerche, A. A dynamic map discovery and selection scheme for predictive hierarchical mipv6 in vehicular networks. *IEEE Transactions on Vehicular Technology* **69**, 793–806 (2020).

[123] Bin Ali Wael, C. *et al.* Analysis of ieee 802.11p mac protocol for safety message broadcast in v2v communication. In *2020 International Conference on Radar, Antenna, Microwave, Electronics, and Telecommunications (ICRAMET)*, 320–324 (2020).

[124] Chowdhury, K., Leung, K., Patil, B., Devarapalli, V. & Gundavelli, S. Proxy Mobile IPv6. RFC 5213 (2008). URL https://rfc-editor.org/rfc/rfc5213.txt.

[125] Lain-Jinn Hwang, Shiann-Tsong Sheu, Yun-Yen Shih & Yen-Chieh Cheng. Grouping strategy for solving hidden node problem in ieee 802.15.4 lr-wpan. In *First International Conference on Wireless Internet (WICON'05)*, 26–32 (2005).

[126] Musa, A., Baba, M. D. & Haji Mansor, H. M. A. The design and implementation of ieee 802.15.7 module with ns-2 simulator. In *2014 International Conference on Computer, Communications, and Control Technology (I4CT)*, 111–115 (2014).

[127] Road tunnel ligthing. common nordic guideline. Standard, Comitte 61:Bridges and tunnels, Denmark, Norway, Filand (1995).